

Phenomenology of the charm decays

By

Aritra Biswas

PHYS10201005005

The Institute of Mathematical Sciences, Chennai

A thesis submitted to the

Board of Studies in Physical Sciences

In partial fulfillment of requirements

For the Degree of

DOCTOR OF PHILOSOPHY

of

HOMI BHABHA NATIONAL INSTITUTE



November 3, 2017

Homi Bhabha National Institute

Recommendations of the Viva Voce Board

As members of the Viva Voce Board, we certify that we have read the dissertation prepared by Aritra Biswas entitled “Phenomenology of the charm decays” and recommend that it maybe accepted as fulfilling the dissertation requirement for the Degree of Doctor of Philosophy.

_____ Date:
Chairman - Ghanashyam Date

_____ Date:
Guide/Convener - Nita Sinha

_____ Date:
Examiner -

_____ Date:
Member 1 - Jim Libby

_____ Date:
Member 2 - Balachandran Sathiapalan

Final approval and acceptance of this dissertation is contingent upon the candidate’s submission of the final copies of the dissertation to HBNI.

I hereby certify that I have read this dissertation prepared under my direction and recommend that it may be accepted as fulfilling the dissertation requirement.

Date:

Place:

Guide: _____

STATEMENT BY AUTHOR

This dissertation has been submitted in partial fulfilment of requirements for an advanced degree at Homi Bhabha National Institute (HBNI) and is deposited in the Library to be made available to borrowers under rules of the HBNI.

Brief quotations from this dissertation are allowable without special permission, provided that accurate acknowledgement of source is made. Requests for permission for extended quotation from or reproduction of this manuscript in whole or in part may be granted by the Competent Authority of HBNI when in his or her judgement the proposed use of the material is in the interests of scholarship. In all other instances, however, permission must be obtained from the author.

Aritra Biswas

DECLARATION

I, hereby declare that the investigation presented in this thesis has been carried out by me. The work is original and has not been submitted earlier as a whole or in part for a degree/ diploma at this or any other Institution/University.

Aritra Biswas

LIST OF PUBLICATIONS ARISING FROM THE THESIS

Journal

1. “Nonleptonic decays of charmed mesons into two pseudoscalars”, Aritra Biswas, Nita Sinha, Gauhar Abbas, Phys.Rev.D92 (2015) no.1, 014032, DOI: 10.1103/PhysRevD.92.014032 .

Arxived

1. “Searching for New physics in Charm Radiative decays”, Aritra Biswas, Sanjoy Mandal, Nita Sinha, arXiv:1702.05059.

Aritra Biswas

DEDICATIONS

I dedicate this thesis to my parents, for being my constant source of inspiration, my guiding light, for being the shining examples whom I have tried to follow, for being the most charismatic and influential people in my life, for being who they are.

ACKNOWLEDGEMENTS

I am not sufficiently gifted with a vocabulary that allows me to pen-down the numerous people who've had a major influence on my life in the last seven-years. However, I will try my best.

The first name that comes to my mind has to be that of my convener, Prof. Nita Sinha. She believed in me and agreed to guide me at a very crucial and difficult time in my career. Without her patience and constant support, I honestly would not have been able to arrive at this stage of my career. I fondly remember our discussions and debates over various matters, both academic and non-academic. I will forever be grateful to her.

The very next mention is Prof. M.V.N. Murthy, whom I regard as my unofficial co-guide. He has been instrumental in clearing various doubts throughout my academic career and is one of the most accessible and respectable senior professors that I have had the good fortune of interacting with. Apart from academics, he is also my jamming partner. One of the things I will miss most are our weekly hindustani classical music sessions.

My seniors and senior collaborators Tanumoy Mandal, Sunando Patra and Gauhar Abbas deserve special mention for going out of their way in many cases to help me improve my problem solving techniques and thinking abilities. They played a big part in developing my confidence as a researcher. I would also like to mention my dear friends Jahanur Hoque,

Trisha Nath, Upayan Baul and Anish Mallick (the last four were my office mates too), who provided me mental support during my lows and highs. The various trips that we went to and the amazing moments that we've shared together will forever be etched in my memory. People like Bose, Kaju da, Abhra da, Tuhin Da, Shilpa, Niranka, Suman da, Diganta da, Sarbeswar da and numerous others have made my time at matscience one of the most cherished in my life so far. Last but not the least, I want to mention my parents, the two most important people of my life, who have believed in me at every single stage. Whatever I have achieved, is mostly due to them.

Finally, I would like to thank the entire faculty and office fraternity of Matscience for being so cooperative and gentle. No doubt the amazing environment of this place has deemed it as one of the premier research institutes in India. I will miss this place, in all its entirety.

Aritra Biswas

Contents

| | |
|--|-------------|
| Contents | viii |
| List of Figures | 1 |
| List of Tables | 3 |
| 1 Introduction | 7 |
| 1.1 The Standard Model | 7 |
| 1.1.1 History | 8 |
| 1.1.2 Mathematical Structure and Particle content | 13 |
| 1.2 Weak interactions, CKM mechanism and the charm quark . | 16 |
| 2 Two-body pseudoscalar charm decays | 29 |
| 2.1 Introduction | 29 |
| 2.2 The Un-unitarized Amplitudes | 34 |
| 2.2.1 Weak Hamiltonian and Wilson coefficients | 34 |
| 2.2.2 Weak Annihilation Contributions | 39 |
| 2.2.3 Non-perturbative Inputs: Form Factors and Decay Constants | 41 |
| 2.3 Final State Interactions | 51 |

| | | |
|----------|---|------------|
| 2.4 | Numerical Analysis and Results | 56 |
| 2.5 | Conclusions | 61 |
| 2.A | The Wilson Coefficients | 67 |
| 2.B | Series Expansion Method for Form Factors | 69 |
| 3 | Searching for New physics in Charm Radiative decays | 71 |
| 3.1 | Introduction | 71 |
| 3.2 | Amplitudes within the Standard Model | 74 |
| 3.2.1 | Long distance contributions | 74 |
| 3.2.2 | Short distance contribution | 81 |
| 3.3 | New Physics models | 90 |
| 3.3.1 | Down type isosinglet vector-like quark | 90 |
| 3.3.2 | Left-right symmetric model | 94 |
| 3.4 | Results and discussions | 98 |
| 3.4.1 | Branching ratios in the SM and for the NP models | 98 |
| 3.4.2 | Photon polarization as a probe for new physics | 101 |
| 3.5 | Conclusions | 106 |
| 3.A | Additional Information regarding the long distance contri- butions | 107 |
| 3.B | The LO and NLO anomalous dimension matrices | 111 |
| 3.C | The functions \mathbf{G}_p | 112 |
| 4 | Conclusion and future directions | 115 |
| | Bibliography | 119 |

List of Figures

| | | |
|-----|--|----|
| 1.1 | The Standard Model of Particle Physics. The diagram shows the elementary particles of the Standard Model (the Higgs boson, the three generations of quarks and leptons, and the gauge bosons), including their names, masses, spins, charges, chiralities, and interactions with the strong, weak and electromagnetic forces. It also depicts the crucial role of the Higgs boson in electroweak symmetry breaking, and shows how the properties of the various particles differ in the (high-energy) symmetric phase (top) and the (low-energy) broken-symmetry phase (bottom). | 15 |
| 1.2 | The one-loop contribution to $K^0 \rightarrow \mu^+\mu^-$ in a three quark theory. | 25 |
| 1.3 | The charm quark contribution. | 25 |
| 2.1 | The dominant quark diagram amplitudes | 37 |
| 2.2 | The q^2 dependence of the scalar form factors. The plot on the left displays $F_0(q^2)$ for $D \rightarrow \pi$ transition, while that on the right is for $D \rightarrow K$ transition. . . | 44 |
| 3.1 | The two types of pole contribution effects. Type-I (left) and type II (right). . . | 74 |
| 3.2 | The vector meson dominance (VMD) contribution | 79 |
| 3.3 | The Feynman diagrams for the process $c \rightarrow u\gamma$ | 81 |

3.4 Contour plots showing the variation of the polarization λ_γ as a function of ζ and ζ_g for LRSM with no LD contribution on left and LRSM with LD amplitude of $2 \times 10^{-9} \text{ GeV}^{-1}$ on right. For both the cases, the right-handed CKM elements are set for maximum deviation of the polarization function from its SM value. The bar-legends for the different contours of λ_γ are displayed along with the respective figures. Here $0 < \zeta < 10^{-3}$ and $0 < \zeta_g < 2$ 103

3.5 Contour plots showing the variation of the polarization λ_γ as a function of ζ and ζ_g . The left panels show the plots for LRSM with a VLQ of mass 800 GeV, while the right panels display the plots for LRSM with a VLQ of mass 1200 GeV. The LD amplitudes(in units of GeV^{-1}) are 2×10^{-9} , 1×10^{-8} , and 8×10^{-8} , for the top, middle and bottom rows respectively. For all the cases, the right-handed CKM elements are set for maximum deviation of the polarization function from its SM value. The bar-legends for the different contours of λ_γ are displayed along with the respective figures. Here $0 < \zeta < 10^{-3}$ and $0 < \zeta_g < 2$. 104

List of Tables

| | | |
|-----|--|----|
| 2.1 | Best fit values of BK parameters for the scalar form factors . | 45 |
| 2.2 | z-expansion coefficients obtained after using the BK parameters in Table 2.1 | 46 |
| 2.3 | Parameter best fit values | 61 |
| 2.4 | $D \rightarrow PP$ SCS B.R.'s, Columns 2 and 3 show our results with annihilation included, for the with and without FSI cases respectively, while column 4 which displays results without annihilation, includes FSI. All the numbers are in units of 10^{-3} | 61 |
| 2.5 | $D \rightarrow PP$ CF B.R.'s, inclusion of Annihilation/FSI in our branching ratio estimates shown in various columns is the same as specified for Table 2.4. All the numbers are in units of 10^{-2} | 62 |
| 2.6 | $D \rightarrow PP$ DCS B.R.'s, inclusion of Annihilation/FSI in our branching ratio estimates shown in various columns is the same as specified for Table 2.4. All the numbers are in units of 10^{-4} | 62 |

| | | |
|-----|---|-----|
| 3.1 | Central values of CKM matrix elements in SM and in SM+VLQ. | 92 |
| 3.2 | The values of the Wilson coefficients at the charm scale in SM and a heavy vector-like quark(VLQ) model with the benchmark values of 800 GeV and 1200 GeV for the heavy-quark mass. We take the mass of the charm quark $m_c = 1.275$ GeV, the $\overline{\text{MS}}$ mass of the bottom quark $m_b = 4.18$ and the mass of the W boson $M_W = 80.385$. The four-loop expression for the strong constant α_s has been used. | 94 |
| 3.3 | LRSM, LRSM+VLQ parameter and their allowed range . . | 97 |
| 3.4 | The values for $ A $ and the inclusive $c \rightarrow u\gamma$ BR in the SM and vector-like quark(VLQ) model. For the vector-like quark model, the values have been calculated for the benchmark values $m'_b = 800$ GeV and 1200 GeV. | 99 |
| 3.5 | Branching ratios for the LRSM model without and with contribution from heavy vector-like quark(VLQ). The Branching ratio is expressed as a function of ζ , ζ_g and θ_{12} (for LRSM) and of ζ , ζ_g , θ_{12} , θ_{14} , θ_{24} and θ_{34} (for LRSM+VLQ). The corresponding parameters are varied to determine the maximum and minimum values. | 100 |
| 3.6 | Decay width and poles masses used in Type I and Type II pole amplitude analysis. | 108 |
| 3.7 | Pole masses, electromagnetic coupling and form factors used in VMD amplitude analysis. | 108 |

| | |
|--|-----|
| 3.8 The pole-I, pole-II and VMD amplitudes and the exclusive radiative branching ratios. | 109 |
|--|-----|

Chapter 1

Introduction

1.1 The Standard Model

The Standard model (SM) of elementary particle physics is essentially the mathematical compactification of everything we know about the fundamental particles and their interactions until now. It is till date one of the most successful models in theoretical physics. Over the last sixty years, it has been put to rigorous experimental tests and all its predictions and parameters have been verified and measured to an appreciable degree of accuracy. Although believed to be theoretically self consistent, it does however leave some experimentally observed phenomena unexplained and hence cannot be regarded as a complete theory of fundamental interactions. For example, it does not incorporate gravity or account for the neutrino masses. It also does not account for the accelerating expansion of the universe (as possibly described by dark energy), does not contain a possible dark matter

candidate which is consistent with cosmological observations or provide a solution to the problem of baryon asymmetry (the imbalance of baryonic and antibaryonic matter in the observable universe). However, owing to its brilliant success, it is often used as the basis for the development of more exotic theories, such as extra dimensions, supersymmetry etc. which are believed to be able to answer the questions that SM cannot, and can be experimentally verified in future. In what follows, I will briefly discuss the history of the development of the SM, and its structure (i.e. its particle contents, interactions and mediators).

1.1.1 History

At the start of the twentieth century, scientists believed that they understood the fundamental principles of nature completely. Atoms were considered to be the building blocks of matter, and Newton's laws of motion were believed to be the dynamical explanation governing the behaviour of matter. However, Max Planck's idea of quantized radiation and the subsequent proposal of a quantum theory of light by Albert Einstein in 1905 were to be the primary steps in the development of the Quantum theory of matter which shattered the then existing deterministic picture of theoretical physics. Einstein also proposed his famous Theory of Relativity, which showed that Newtonian mechanics was an approximation of the same for low velocities. In 1909, Hans Geiger and Ernest Marsden, under

the guidance of Ernest Rutherford performed the famous gold foil scattering experiment which established that atoms have a small, dense and positively charged nucleus. This was followed by the discovery of the proton by Ernest Rutherford in 1919. All this and the subsequent discovery of the quantum nature of X-rays by Arthur Compton(1923), the proposal of wave-particle duality by Louis De Broglie(1924) and the formulation of the exclusion principle by Wolfgang Pauli(1925), finally paved the way for Erwin Schrodinger to formulate his famous theory of Quantum mechanics in 1926. In 1927, Werner Heiseberg formulated the famous Uncertainty principle and in 1928 Paul Dirac combined special relativity and quantum mechanics to explain the electron. By 1930, quantum mechanics and special relativity became well established.

In 1931, with the discovery of the neutron by James Chadwick, the mechanisms of nuclear binding and decay become problems of primary interest. By 1933-34, Enrico Fermi put forward the theory of beta decay and thus introduced the idea of weak interactions. This was the first theory to use neutrinos and particle flavour changes. During the same time, Hideki Yukawa combined relativity and quantum theory to describe nuclear interactions by an exchange of new particles (mesons called "pions") between protons and neutrons. This marked the beginning of the meson theory of nuclear forces. From the size of the nucleus he concluded that the mass of these particles would be about 200 electron masses. In 1937, a sim-

ilar particle was discovered in cosmic ray experiments, which was first thought to be the pion, but later understood to be the muon. The pion was finally discovered in 1947. This is the same year in which physicists developed procedures to calculate electromagnetic properties of electrons, positrons, and photons and the Feynman diagrams were introduced. The following years witnessed the discovery a number of new particles such as the K^+ (1949), the π^0 (1950), the Λ^0 and K^0 (1951) and the Δ (1952). With the discovery of the Bubble Chamber by Donald Glaser and the advent of the Brookhaven Cosmotron (a 1.3 GeV particle accelerator) in 1952, a plethora of new particles were discovered.

In 1954, C.N. Yang and Robert Mills developed a new class of theories called Gauge theories [1, 2]. Although not realized at that time, these now form the basis of the SM at present. The following years would witness the first steps towards the unification of the weak, strong and electromagnetic forces into the SM as we know it now. In 1957, Julian Schwinger [3] proposed the idea of the unification of weak and electromagnetic interactions. During the period 1957-59, Schwinger [3], Sidney Bludman and Sheldon Glashow suggested in separate papers that all weak interactions are mediated by charged heavy bosons, which were later called the W^+ and the W^- bosons. In 1961, physicists for the first time used the idea of group theory (in particular the $SU(3)$ group) as a scheme to mathematically classify the then increasing number of particles. In 1964, Murray

Guell-Mann [4] tentatively put forward the idea of quarks. He suggested that the mesons and baryons are composites of three quarks or antiquarks called up(u), down(d) and strange(s) with spin $\frac{1}{2}$ and charge $2/3$, $-1/3$ and $-1/3$ respectively. In the same year, Sheldon Glashow and James Bjorken [5] coined the term ‘charm’ for a fourth quark which had been suggested in several contemporary papers. However very few physicists took this idea seriously at that time. This was also the year that witnessed the discovery of CP-violation by James Cronin and Val Fitch in Kaon decays [6], for which they were awarded the Nobel Prize in 1980. The next year, O.W. Greenberg, M.Y. Han, and Yoichiro Nambu introduced the quark property of colour charge (all observed hadrons are colour neutral) [7, 8]. In 1967 Steven Weinberg [9] and Abdus Salam [10] separately proposed a theory that unified the weak and the electromagnetic interactions. During the two years that followed, an experiment was conducted at the Stanford Linear Accelerator(SLAC), in which electrons, scattered off protons, appeared to be bouncing off small hard cores inside the proton. James Bjorken and Richard Feynman analyzed this data in terms of a model of constituent particles inside the proton (they didn’t use the name "quark" for the constituents, even though this experiment provided evidence for quarks). In 1970 Sheldon Glashow, John Iliopoulos, and Luciano Maiani recognized the critical importance of a fourth type of quark in the context of the Standard Model [11]. A fourth quark allowed a theory that had flavour-conserving Z^0 -mediated weak interactions but no flavour-

changing ones. In 1973, Harald Fritzsch and Murray Gell-Mann formulated a quantum theory of strong interactions involving the quarks and gluons [12]. This theory (called Quantum Chromodynamics (QCD)) is now a part of the SM. In the same year David Gross, Frank Wilczek and David Politzer discover that QCD has a special property called the ‘asymptotic freedom’ [13, 14]. In 1974, John Iliopoulos presented, for the first time in a single report, the view of physics now called the SM. The following years gradually witnessed the experimental discoveries of the complete particle spectrum predicted by the SM. The J/ψ particle (which is a charm-anticharm bound state) was discovered independently by Samuel Ting [15] and Burton Richter [16](1974). Gerson Goldhaber and Francois Pierre discovered the D^0 meson (anti-up and charm quarks) in 1976 [17]. The theoretical predictions agreed dramatically with the experimental results, offering support for the Standard Model. Martin Perl discovered the τ lepton in the previous year [18]. The bottom quark was discovered the very next year by Leon Lederman and his collaborators at Fermilab [19]. In 1978 Charles Prescott and Richard Taylor observed a Z^0 mediated weak interaction in the scattering of polarized electrons from deuterium which showed a violation of parity conservation [20], as predicted by the Standard Model.¹ Strong evidence for a gluon radiated by the initial quark or antiquark was found at PETRA, a colliding beam facility at the DESY laboratory in Hamburg, the following year [22]. In 1983 The W^\pm [23] and

¹However, it is to be noted that the discovery of parity violation was due to C.S. Wu and his team [21] long back in 1957 in the beta-decay of Cobalt-50.

Z^0 [24] intermediate bosons demanded by the electroweak theory were observed by two experiments using the CERN synchrotron using techniques developed by Carlo Rubbia and Simon Van der Meer to collide protons and antiprotons. In 1989 experiments carried out in SLAC and CERN strongly suggested that there were three and only three generations of fundamental particles. This was inferred by showing that the consistency of the Z^0 -boson lifetime only with the existence of exactly three very light (or massless) neutrinos.

In 1995, after eighteen years of searching at many accelerators, the CDF [25] and D0 [26] experiments at Fermilab finally discovered the top quark at the unexpected mass of 175 GeV. And in 2012, almost half a century after Peter Higgs predicted a Higgs boson as part of a mechanism (invented by a number of theorists) by which fundamental particles gain mass, the ATLAS [27] and CMS [28] experiments at the CERN lab discovered the Higgs boson. With the discovery of the Higgs Boson, the experimental verification and confirmation of the SM was complete.

1.1.2 Mathematical Structure and Particle content

The SM of particle physics is a theory concerning the electromagnetic, weak, and strong nuclear interactions, as well as classifying all the subatomic particles known. In mathematical terms, it is essentially a gauge quantum field theory containing the internal symmetries of the unitary

gauge group $SU(3)_c \times SU(2)_L \times U(1)_Y$. In terms of particle content, it contains a total of twenty five fundamental particles. Three generations of six quarks and three generations of six leptons with two quarks/leptons in each generation. All of these quarks and leptons are fermions, meaning that they have half integral spins. Each lepton generation contains one lepton (e, μ, τ) and its corresponding neutrino (ν_e, ν_μ and ν_τ). Each quark generation contains one up-type (u, c and t) and one down type (d, s and b) quark. Barring these, there are twelve gauge bosons. They are the charged W^+, W^- and the neutral Z^0 , which act as the mediator of weak interactions, the photon(γ) which is the mediator of the electromagnetic interactions and eight gluons which are the mediators of strong interactions. Last but not the least, there is the Higgs Boson, which is responsible for the masses of the fundamental particles. A schematic diagram of the particle content of the standard model can be found in fig.1.1.²

The form of the interactions among the fermions (the quarks and leptons) on one side and the bosons (which are the carriers of the interactions) on the other arises by imposing invariance under space time dependent symmetry group. The gauge structure of the SM specified previously is based on the $U(1)_Y$ transformations according to the hypercharge of the particle, $SU(2)_L$ transformations of weak isospin left-handed doublets and $SU(3)_c$ transformations in the quark colour space. The leptons, quarks and the gauge bosons get their masses due to the spontaneous breaking of sym-

²The figure is taken from [29].

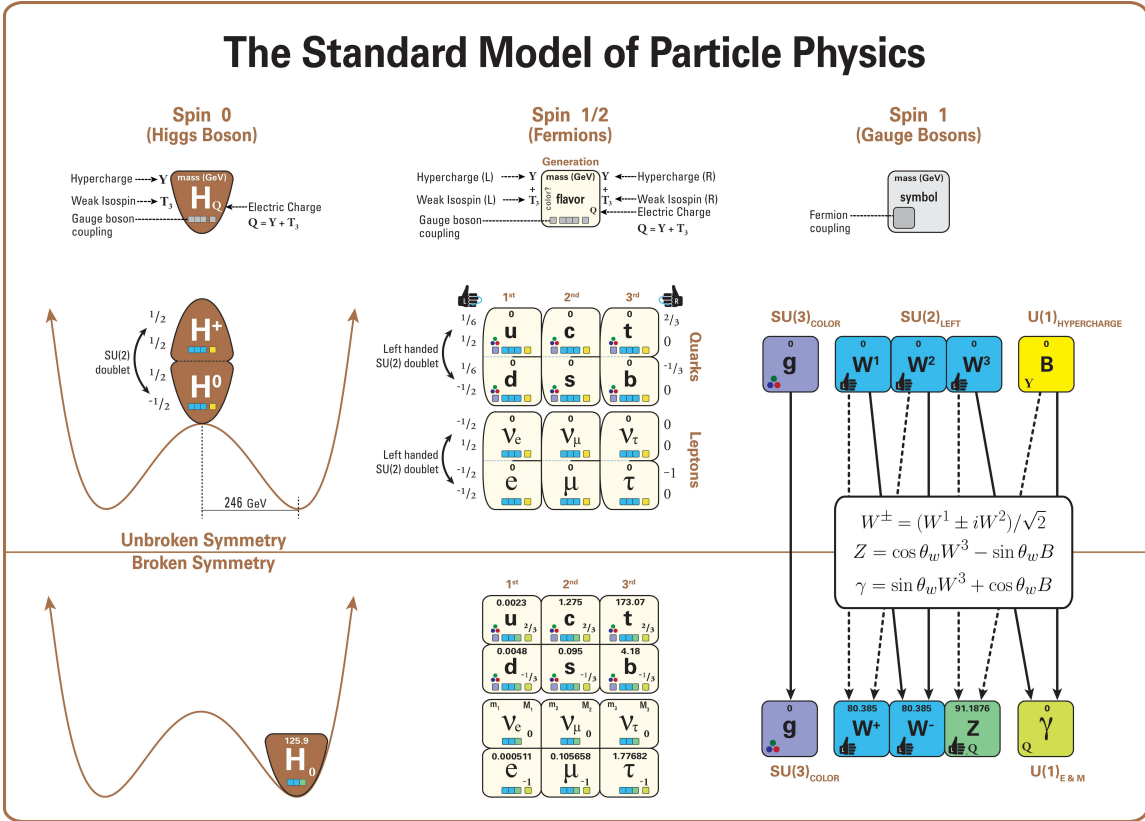


Figure 1.1: The Standard Model of Particle Physics. The diagram shows the elementary particles of the Standard Model (the Higgs boson, the three generations of quarks and leptons, and the gauge bosons), including their names, masses, spins, charges, chiralities, and interactions with the strong, weak and electromagnetic forces. It also depicts the crucial role of the Higgs boson in electroweak symmetry breaking, and shows how the properties of the various particles differ in the (high-energy) symmetric phase (top) and the (low-energy) broken-symmetry phase (bottom).

metry which keeps the equations of motion, but not the vacuum, invariant under the symmetry group. The mechanism for this spontaneous symmetry breaking, known as the Higgs mechanism, introduces an additional scalar weak doublet with a non-zero vacuum expectation value, invariant only under the subgroup $U(1)_{EM}$ but not under the whole $SU(2)_L \times U(1)_Y$ symmetry. The physical fluctuations around this vacuum are represented by the Higgs boson. The SM so constructed is mathematically self consistent and renormalizable. The renormalizability essentially means that the infinities

arising from the theory can be removed in a physically sensible way by redefining the free parameters of the theory.

The $SU(2)_L$ quark fields are not the mass eigenstates in general. For a quark of a given charge, the rotation from the mass basis to the weak basis is achieved via the unitary Cabibbo Kobayashi Maskawa (CKM) matrix. The elements of this matrix give the coupling between a down-type (charge $-\frac{1}{3}$), an up-type (charge $\frac{2}{3}$) and a W boson. The matrix can be parametrized in terms of three real and one imaginary parameter. The imaginary parameter is the only source of CP violation within the SM. There are no flavour changing neutral currents within the SM at tree level, since the electromagnetic and neutral weak currents are rendered flavour diagonal.

1.2 Weak interactions, CKM mechanism and the charm quark

Having discussed about the SM in brief, we will now focus our attention on the physics of the electroweak ($SU(2)_L \times U(1)_Y$) sector. In particular we will discuss briefly the physics and salient characteristics of the weak interactions. We will end this section with a brief discussion on the charm quark.

In the SM, the weak interaction occurs by the emission or absorption of the W and the Z bosons (hence these bosons are called the 'mediators' of the

weak interaction). All known fermions interact via the weak interactions. The masses of the mediators are much greater than those of the interacting particles, which is consistent with the short range of the weak force. Owing to their large masses, the W and Z bosons have a short lifetime of under 10^{-24} seconds. The force is termed 'weak' since its field strength is several orders of magnitude less than that of the corresponding strong or electromagnetic force. The weak interaction coupling constant is $O(10^{-6})$ to (10^{-7}) compared to the strong interaction coupling constant of 1 and the electromagnetic coupling constant of about 10^{-2} [30]. The weak interaction has a very short range ($O(10^{-16})$ to $O(10^{-17})$ meters) [30, 31]. At a distance $\sim O(10^{-18})$ meters, the weak interaction has a strength similar in magnitude to that of the electromagnetic force, but this suffers an exponential decrease with increasing distance. At distances of around 3×10^{-17} meters, the weak interaction is 10,000 times weaker than its electromagnetic counterpart [32].

The weak interaction is unique with reference to a number of aspects:

- It is the only interaction capable of changing the flavour of quarks.
- It is the only interaction that violates both P(parity) and CP(charge conjugate-parity) symmetries.
- It is propagated by force carrier particles that have significant masses.

These particles obtain their masses by the Higgs mechanism.

The SM describes the electromagnetic and weak interactions as different aspects of a unified electroweak theory. According to the electroweak theory, at very high energies there are four massless gauge boson fields similar to the photon and a complex scalar doublet which is the Higgs field. However, at low energies, due to the spontaneous breaking of the gauge symmetry (which amounts to one of the Higgs' doublet fields acquiring a vacuum expectation value) the $SU(2)_L \times U(1)_Y$ gauge symmetry of the electroweak theory is spontaneously broken into the $U(1)$ symmetry of electromagnetism. This symmetry breaking produces three massless fields which interact with the Higgs field to acquire mass. These are the W^+ , W^- and Z bosons, while the fourth field that remains massless is the photon.

All particles have a property called weak-isospin, denoted by T_3 . It is a quantum number that governs how the particle will behave under weak interactions. The role of weak isospin in weak interactions is similar to that of the electric charge in electromagnetic interactions or the colour charge in strong interactions. All fermions have a weak isospin value of either $+\frac{1}{2}$ or $-\frac{1}{2}$. For example, all up type quarks have a weak isospin of $+\frac{1}{2}$ and all down-type quarks have a weak isospin of $-\frac{1}{2}$. A quark with a given T_3 can never decay to another quark of similar T_3 via weak interactions. Any given interaction conserves weak isospin. For example, a π^+ meson normally decays into a μ^+ and a ν_μ , both of which have weak isospin values of $+\frac{1}{2}$. There are two types of weak interactions. They are called the

‘charged-current interaction’ and the ‘neutral-current interaction’ depending on whether they are mediated by a charged boson or a neutral boson respectively. Examples of charged current interactions is the conversion of a charged lepton into its corresponding neutrino, or the conversion of down-type quark into an up-type quark by the absorption of a W^+ boson. Flavour changing neutral current interactions, as mentioned before, do not occur in the SM at the tree level.

I will now discuss briefly about the CKM(Cabibbo, Kobayashi and Maskawa) matrix³. It is essentially a unitary matrix whose elements specify the coupling strengths of flavour changing weak decays. Let us call the left handed quark doublets

$$\psi_{jL} = \begin{pmatrix} U_j \\ D_j \end{pmatrix}_L \quad (1.1)$$

where U_j are the charge $+\frac{2}{3}$ fields and D_j are the charge $-\frac{1}{3}$ fields. The corresponding right-handed fields (U_{jR} and D_{jR}) are singlets. The Yukawa coupling responsible for the mass of the charge $-\frac{1}{3}$ element is

$$- g_{jk} \bar{D}_{jR} \phi^\dagger \psi_{kL} + h.c. \quad (1.2)$$

When ϕ develops a vacuum expectation value (VEV), we have the mass

³I closely follow [33] for this discussion

term

$$- M_{jk}^D \bar{D}_{jR} D_{kL} + h.c. \quad (1.3)$$

where

$$M_{jk}^D = g_{jk} v / \sqrt{2} \quad (1.4)$$

where v is the VEV of ϕ . It can easily be verified that eqn.(1.2) is invariant under $SU(2) \times U(1)$. To construct a Yukawa coupling for the U_{jR} field, one defines

$$\tilde{\phi} = i\tau_2 \phi^*. \quad (1.5)$$

The Yukawa coupling can then be written as

$$- h_{jk} \bar{U}_{jR} \tilde{\phi}^\dagger \psi_{kL} + h.c. \quad (1.6)$$

where

$$\tilde{\phi} = \begin{pmatrix} \phi^{0*} \\ \phi^- \end{pmatrix} \quad (1.7)$$

with

$$\phi^- = -\phi^{+*}. \quad (1.8)$$

The mass of the U term is then produced by the corresponding VEV

$$- M_{jk}^U \bar{U}_{jR} U_{kL} + h.c. \quad (1.9)$$

$$M_{jk}^U = h_{jk} v / \sqrt{2}. \quad (1.10)$$

One can redefine the mass fields so that the M^U mass term is diagonal:

$$-M_{jk}^U \bar{U}_{jR} U_{kL} + h.c. \quad (1.11)$$

$$M^U = \begin{pmatrix} m_u & 0 & 0 \\ 0 & m_c & 0 \\ 0 & 0 & m_t \end{pmatrix}. \quad (1.12)$$

But then, M^D cannot be diagonalized because the ψ_L field is already fixed.

However, one can redefine the D_R fields so that the mass term for D can be written as

$$-M_{jl}^D V_{lk}^\dagger \bar{D}_{jR} D_{kL} + h.c. M^D = \begin{pmatrix} m_d & 0 & 0 \\ 0 & m_s & 0 \\ 0 & 0 & m_b \end{pmatrix}. \quad (1.13)$$

where V^\dagger is a unitary matrix. The D_{jR} are simply the mass eigenstates fields now, but V^\dagger relates D_{kL} to the mass eigenstates as

$$\begin{pmatrix} d \\ s \\ b \end{pmatrix}_L = V^\dagger D_L. \quad (1.14)$$

Therefore

$$D_L = V \begin{pmatrix} d \\ s \\ b \end{pmatrix}_L. \quad (1.15)$$

In terms of the mass eigenstates, the quark charged current is

$$\left(\bar{u} \quad \bar{c} \quad \bar{t}\right)\gamma^\mu(1 + \gamma^5)V\begin{pmatrix} d \\ s \\ b \end{pmatrix}. \quad (1.16)$$

The unitary matrix V contains all the information of the general mass matrices that was the starting point of this analysis.

A general $n \times n$ unitary matrix has $2n^2$ real parameters in total. However, there are n constraints from the normalization of each column and $n(n - 1)$ constraints from the orthogonality between each pair of columns (the conditions on the rows do not add extra constraints). Hence, a general $n \times n$ unitary matrix has n^2 independent real parameters. Not all of these parameters are physically meaningful in the CKM matrix. This is because, for n quark generations, $2n - 1$ phases can be absorbed by the freedom to select the phases of the quark fields. Therefore, the number of physical real parameters is $n^2 - (2n - 1) = (n - 1)^2$. Of these, the number of real rotation parameters are $\frac{1}{2}n(n - 1)$. The number of independent phase factors is therefore $n^2 - (2n - 1) - \frac{1}{2}n(n - 1) = \frac{1}{2}(n - 1)(n - 2)$. The 3×3 CKM matrix describing the mixing of the three quark generations in the SM therefore has four independent real parameters, of which three are rotation parameters leaving one phase. This phase is solely responsible for the violation of the CP symmetry within the SM. It is to be noted that with two quark generations, a CP violating phase cannot be accommodated in the corre-

sponding mixing matrix. Hence, it is mandatory for a theory to have at least three quark generations in order to accommodate CP violation. In the basis of eqn.(1.16), the CKM matrix (V) has the form [34]

$$\begin{pmatrix} V_{ud} & V_{us} & V_{ub} \\ V_{cd} & V_{cs} & V_{cb} \\ V_{td} & V_{ts} & V_{tb} \end{pmatrix}. \quad (1.17)$$

The Standard parametrization for the CKM matrix is [35]

$$\begin{pmatrix} c_{12}c_{13} & s_{12}c_{13} & s_{13}e^{-i\delta_{13}} \\ -s_{12}c_{23} - c_{12}s_{23}s_{13}e^{i\delta_{13}} & c_{12}c_{23} - s_{12}s_{23}s_{13}e^{i\delta_{13}} & s_{23}c_{13} \\ s_{12}s_{23} - c_{12}c_{23}s_{13}e^{i\delta_{13}} & -c_{12}s_{23} - s_{12}c_{23}s_{13}e^{i\delta_{13}} & c_{23}c_{13} \end{pmatrix}. \quad (1.18)$$

where $c_{ij} = \cos \theta_{ij}$ and $s_{ij} = \sin \theta_{ij}$. The phase δ_{13} is the SM CP violating phase.

In 1963 Nicola Cabibbo introduced the Cabibbo angle (θ) to preserve the universality of the weak interactions [36]. The main motivation behind this was the need to explain the observation that the strangeness changing hadronic weak currents appeared to be suppressed relative to the strangeness conserving ones. With three quark flavours (u , d and s) the charged weak current as postulated by Cabibbo is given by

$$J_{\mu}(x) = \bar{u}(x)\gamma_{\mu}(1 + \gamma_5)(\cos \theta d(x) + \sin \theta s(x)). \quad (1.19)$$

Here θ denotes the mismatch between the flavour symmetry breaking directions chosen by the strong and the weak interactions, known as the Cabibbo angle. Eqn.(1.19) can be viewed as the u quark being coupled to a certain specific linear combination of the d and the s quark ($d_c(x) = \cos \theta d(x) + \sin \theta s(x)$). The orthogonal combination ($s_c(x) = -\sin \theta d(x) + \cos \theta s(x)$) however remains uncoupled. One would expect that decays like $K_L \rightarrow \mu^+ \mu^-$ would proceed via a weak neutral current mediated by the Z boson. However, it was found that $K_L \rightarrow \mu^+ \mu^-$ does not occur at the tree level. In fact, no flavour changing neutral current (FCNC) processes are allowed at the tree level in SM. Glashow, Illiopoulos and Miani (GIM) [11] conjectured that with the addition of a fourth up-type (charge $+\frac{2}{3}$) quark, the full charged weak current is given by

$$J_\mu(x) = \bar{u}(x)\gamma_\mu(1 + \gamma_5)d_c(x) + \bar{c}(x)\gamma_\mu(1 + \gamma_5)s_c(x). \quad (1.20)$$

In matrix notation, eqn.(1.20) reads

$$J_\mu(x) = \bar{U}(x)\gamma_\mu(1 + \gamma_5)CD(x) \quad (1.21)$$

where,

$$U = \begin{pmatrix} u \\ c \end{pmatrix}; \quad D = \begin{pmatrix} d \\ s \end{pmatrix}; \quad C = \begin{pmatrix} \cos \theta & \sin \theta \\ -\sin \theta & \cos \theta \end{pmatrix} \quad (1.22)$$

With this, the current $J_3 = [J, J^\dagger]$ is diagonal in flavour space. Therefore, the neutral current in a gauge theory, which is a linear superposition of

J_3 and the electromagnetic current will also be diagonal. Hence, FCNC processes do not occur at the tree level in the SM.

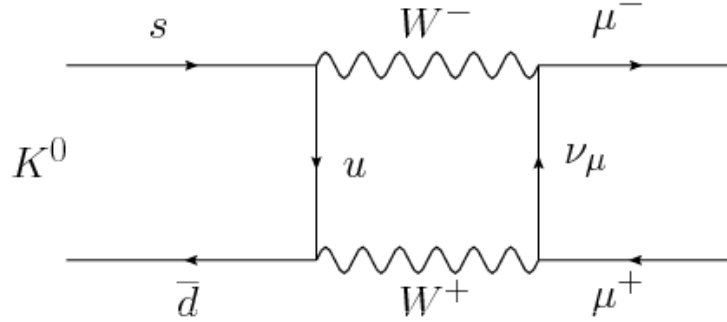


Figure 1.2: The one-loop contribution to $K^0 \rightarrow \mu^+ \mu^-$ in a three quark theory.

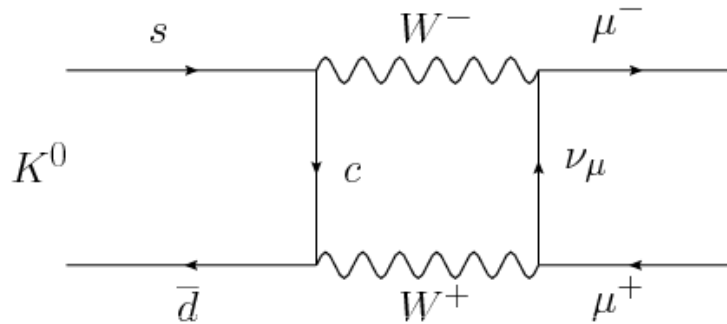


Figure 1.3: The charm quark contribution.

This however, does not explain the observed rate. For example, the $K_L \rightarrow \mu^+ \mu^-$ decay can be generated by 1.2. In a renormalizable gauge theory 1.2 is expected to give a branching ratio $g^4 \sim \alpha \sim \mathcal{O}(10^{-4})$, where α is the fine structure constant.

Here comes the second ingredient of the GIM mechanism. Glashow, Iliopoulos and Miami observed that with the inclusion of a fourth quark, a second diagram (fig.1.3) contributes to the process, with the u quark replaced by the c quark. In the limit of exact flavour symmetry, these two diagrams cancel each other. Flavour symmetry breaking induces a

mass difference between the quarks, so the sum of the two diagrams is of the order of $g^4(m_c^2 - m_u^2)/m_W^2 \sim \alpha^2 m_c^2/m_W^2$. Prior to the discovery of the charm quark, this predicted its mass. The mass of the charm quark (1.275 GeV [35]) was found to satisfy the observed rates within errors. The same mechanism applies to the present theory with six quark flavours with the CKM matrix.

As mentioned at the beginning of this chapter, the SM is not the complete picture. We believe that new physics (NP) exists at scales higher than the electroweak symmetry breaking scale of 1 TeV. However, among the numerous models for NP, the correct candidate (if any) can only be identified by experiments. It is in this regard that flavour physics has assumed an important role over the last three decades. With no NP particles being discovered at the LHC, and their masses in various models being pushed higher, it appears that precision measurements in the flavour sector may be the only way for constraining and looking for NP.

Charm physics can be instrumental in this respect. This is because, CP violation in charm within the SM is expected to be negligible. Any CP violation in the charm sector would hence be an unambiguous signal for the presence of NP. This CP violating effect could be manifested in $D^0 - \bar{D}^0$ mixing or in the decays of the D mesons. However, before looking for NP scenarios in charm decays, it is mandatory to first have a better understanding of the observed branching ratios. NP can also manifest itself as

new particles contributing to loops in rare charm decays. The difficulty in extracting information on NP in these cases are the dominant long distance contributions that plague such decays.

In the course of my PhD, I have tried to look into some of these issues. The second chapter is on two-body pseudoscalar charm decays. We attempt to parametrize the annihilation and exchange contributions to these decays. The non-factorizable corrections which are known to be important while applying the method of factorization to charm decays have been considered and parametrized. We take extreme care in the treatment of the form factors. Finally, final-state interactions, which have previously been shown to play a significant role in explaining $D \rightarrow PP$ decays, have also been incorporated via a K-matrix formalism. The elements of this matrix, which are the decay widths of a particular resonance going to the concerned two-body final state pseudoscalars, have been taken from Ref. [35]. The ones that are not reported or are ill-measured have been treated as parameters. We estimate all these parameters from a fit to the existing data for the $D \rightarrow PP$ branching ratios from Ref. [35]. The third chapter is on radiative charm decays, where we explore the possibility of a heavy vector-like down type isosinglet quark in presence of an additional left-right symmetry enhancing the corresponding inclusive branching ratio as compared to the SM, as well as provide a possible method for the detection of such NP in presence of the dominant long-distance contributions. We provide detailed

discussions regarding the renormalization group evolution of the short distance Wilson coefficients, both in the SM and the heavy vector-like quark model. We also discuss the possibility of using the photon polarization as a probe for identifying NP in the presence of a left-right symmetric model with a heavy vector-like quark.

Chapter 2

Two-body pseudoscalar charm decays

2.1 Introduction

The discovery of charm mixing and hints of CP violation in the charm sector resulted in non-leptonic charm meson decays being a focus of attention in the last few years [37, 38]. CP violation in charm, direct as well as in mixing, is expected to be negligible. Hence any hint of CP violation in charmed mesons is expected to be from physics beyond the standard model. Charm may therefore be instrumental in providing insights into new physics [39–47]. Earlier FOCUS [48], CLEO [49] and various other collaborations had produced many interesting results in the charm sector. The 3.2σ hint [50, 51] of a difference of CP asymmetries between the singly suppressed K^+K^- and $\pi^+\pi^-$ charmed decay modes resulted in a large volume of work [52–68]. These works mostly used different models of New Physics, to explain the result. The hint has since then been slowly

moving towards zero and currently there seems to be no evidence for any direct CP violation in charm in any mode [69]. In spite of that, all the recent work done on $D \rightarrow PP$ decays motivated by this hint clearly show that it is critical to first understand the observed branching ratios of all the charmed hadronic decay modes well, within the Standard Model, before any observation of an anomalous rate or any new CP asymmetry can be claimed to be due to the presence of New Physics.

This however, is not an easy task. The mass of the charm quark (1.275 GeV) makes it very difficult to come up with a proper theoretical technique for calculation of hadronic charmed meson decays. Unlike the bottom quark, the charm is not sufficiently heavy to allow realization of the infinitely heavy quark limit. The well-known theoretical approaches based on QCD, for example, heavy quark effective theory [70], QCD factorization [71,72], the perturbative QCD approach [73–76] and the soft-collinear effective theory [77], which lead to very satisfactory predictions for B decays, cannot hence be used to explain data in the case of charmed mesons. Furthermore, the charm quark is also not light enough for a chiral expansion to be applicable.

The factorization approach is still one of the most successful ways to study two-body charm meson decays in the absence of any other reliable and effective theoretical method [78, 79]. However, calculation of Wilson coefficients of effective operators is known to suffer from the problem of γ_5 -

and renormalization scheme dependence in the naive factorization scheme. These difficulties can be overcome in the framework of the ‘generalized factorization approach’ where Wilson coefficients are effective and include important non-factorizable (NF) corrections [80, 81].

There was another attempt to explain hadronic D decays previously using the so called large $1/N_c$ (where N_c is number of colour degrees of freedom) approach [82]. It was observed that dropping Fierz transformed terms characterized by $1/N_c$ can narrow the gap between predictions and observations up to a satisfactory level. QCD sum rule calculations showed that Fierz terms were certainly compensated by the NF corrections [83–85].

One should mention another model independent so called ‘quark diagram’ or ‘topological diagram’ approach in the literature [86–94]. In this approach, all two-body non-leptonic weak decays of heavy mesons are expressed in terms of distinct quark diagrams, depending on the topologies of weak interactions, including all strong interaction effects. Based on $SU(3)$ symmetry, it allows extraction of the quark diagram amplitudes by fitting against experimental data. However $SU(3)$ breaking effects in charmed meson decays have been shown to be important and need to be carefully incorporated [95, 96].

The importance of final state interactions (FSI) in nonleptonic charm decays had been realized and discussed in several papers [97–100] in the early 80’s, where the authors had been intrigued by the anomalies in the

observed branching ratios of the Cabibbo favoured (CF), neutral versus the charged $K\pi$ modes, the differing rates of the singly Cabibbo suppressed (SCS) K^+K^- and $\pi^+\pi^-$ modes, followed by measurements of rates of few other modes that had unexpected suppression/enhancement. Many of these were conjectured to be due to FSI. Surprisingly, even in the last couple of years, in many of the papers that worried about the charm CP asymmetry problem, these old puzzles were still considered unresolved.

Even for the case of hadronic B meson decays, the role of FSI's is being examined rather carefully in the last few years [101, 102]. The mass of the charmed meson lying right in the heart of the resonance region, resonant final state rescattering is bound to play a bigger role in the $D \rightarrow PP$ and needs to be evaluated. However, dynamical calculations of these long distance effects are not possible and hence they can only be determined phenomenologically after comparison of the theoretical estimates with experimental data. Unitarity constraints play an important role in providing the theoretical estimates.

Another contribution in hadronic two body decays that has been debated for a long period is that of the weak annihilation and exchange diagrams. Rosen proposed [103] that the W exchange diagrams may be large and since this appears only in D^0 and not in D^+ decays, it could account for the difference in the lifetimes of these two mesons. Bigi and Fukugita [104] had then put forward several D and B meson decay modes that could be

the smoking gun signals of the W-exchange contributions. Yet, when the mode $D^0 \rightarrow \phi \bar{K}^0$ was observed, it was argued [105] that it could have been generated from the decay mode $D^0 \rightarrow K^* \eta$, with this final state rescattering to the $\phi \bar{K}^0$ mode. Annihilation type contributions along with FSI's were incorporated in the hadronic two body vector-pseudoscalar modes of charmed meson decays in Ref. [106]. Studies using the quark diagram approach of Ref. [107] had also indicated that annihilation type contributions are needed to explain the observed data.

This chapter is about the role of FSI in the two body D (D here can be any of the D^0 , D^+ , or D_s^+) meson decays. The assumption is that FSI effects are dominated by resonance states close to the mass of D mesons. In fact, there exist isospin 0, 1 and 1/2 resonances near the D mass, that may contribute to rescatterings among different channels in these respective isospin states and enhance/suppress some of the decay rates. In the next section, the formalism for the calculation of the un-unitarized amplitudes, using a modified factorization approach, where the effective Wilson coefficients include NF corrections is described. This is in analogy with the QCD factorization approach of Beneke-Neubert for hadronic B meson decays [108], where using the hard scattering approach, the NF corrections are calculable in heavy quark approximation. However, for charm, since this approximation fails, these NF corrections are not calculable and are left as parameters. I also indicate our parametrization of the annihilation

contributions and discuss our inputs: the decay constants, and the form factors, for which we used a z-series expansion approach. In Sec. 2.3, the need to incorporate additional long distance FSI effects is discussed. I also show this can be achieved with a K matrix formalism for coupled channels. Using the observed widths, masses and known decay rates of the resonances to the various channels to evaluate the diagonal elements and leaving the unknown elements of the K matrix as parameters, the unitarized amplitudes are calculated (as discussed in [106]) to estimate the branching ratios of all the SCS, CF and doubly Cabibbo suppressed (DCS) $D \rightarrow PP$ decay modes. In Sec. 2.4, I list the isospin decomposition of all the decay modes, the parameters that need to be determined from our fits as well as the errors in theoretical inputs used. I list all the branching ratios after our numerical χ^2 fits as well as the values of the fitted parameters.

2.2 The Un-unitarized Amplitudes

2.2.1 Weak Hamiltonian and Wilson coefficients

The study of weak decays of charmed mesons to two body hadronic modes necessarily requires a careful evaluation of the strong interaction corrections. The weak effective Hamiltonian may be expressed in terms of coefficient functions, which incorporate the strong interaction effects above

the scale $\mu \sim m_c$ and the current-current operators as:

$$\mathcal{H}_w = \frac{G_F}{\sqrt{2}} [C_1(\mu)O_1(\mu) + C_2(\mu)O_2(\mu)] + h.c. . \quad (2.1)$$

where, G_F is the Fermi coupling constant, C_1 and C_2 are the Wilson coefficients and the operators are,

$$\begin{aligned} O_1 &= (\bar{u}_\alpha q_{2\alpha})_{V-A} (\bar{q}_{1\beta} c_\beta)_{V-A} \\ O_2 &= (\bar{u}_\alpha q_{2\beta})_{V-A} (\bar{q}_{1\beta} c_\alpha)_{V-A} . \end{aligned}$$

α and β in the above are colour indices, while q_1, q_2 can be either the d or the s quark. The quark diagrams dominantly contributing to the branching ratios of $D \rightarrow P_1 P_2$ [94] are the colour-favoured Tree amplitude T , the Colour-suppressed amplitude C , the W-exchange amplitude E and the W annihilation amplitude A , shown in Fig. 2.1.

Penguin contributions in charmed meson decays are highly suppressed as the dominant down type quark contribution to the flavour changing neutral current $c \rightarrow u$ transition is from the b quark which is accompanied by the presence of the tiny product, $V_{cb}^* V_{ub}$ of the CKM matrix elements. Hence, the two operators in Eq. (2.1) are sufficient for calculating the amplitudes and branching ratios of the $D \rightarrow PP$ modes.

In the naive factorization approach, the matrix element of the four-fermion operator in the heavy quark decay is replaced by a product of two cur-

rents. The amplitudes for the non-leptonic 2 body decay modes are then the product of a transition form factor and a decay constant. However, NF corrections must exist; while such corrections for scales larger than μ are taken into consideration in the effective weak Hamiltonian, those below this scale also need to be carefully incorporated. In the QCD factorization approach for B meson decays [71, 72, 109], these NF corrections are handled using the hard scattering approach, where the vertex corrections and the hard spectator interactions are added at the next to leading order in α_s and its accuracy is limited only by the corrections to the heavy quark limit. But, in the case of charm decays, where the heavy quark expansion is not a very good approximation, it is best to parametrize these NF corrections and then determine them by fitting the theoretical branching ratios with the experimental data. In the diagrammatic approach of Ref. [94] also, either the Wilson coefficients themselves or the NF corrections appearing in the Wilson coefficients are determined from fits to data.

Hence, we write the scale dependent Wilson coefficients, modified to include the NF corrections which are parametrized by χ_1 and χ_2 with their respective phases ϕ_1 and ϕ_2 as,

$$a_1(\mu) = C_1(\mu) + C_2(\mu) \left(\frac{1}{N_c} + \alpha(\mu)\chi_1 e^{i\phi_1} \right) \quad (2.2)$$

$$a_2(\mu) = C_2(\mu) + C_1(\mu) \left(\frac{1}{N_c} + \alpha(\mu)\chi_2 e^{i\phi_2} \right). \quad (2.3)$$

The dominant Tree and Colour amplitudes for $D \rightarrow P_1 P_2$, where P_1 is

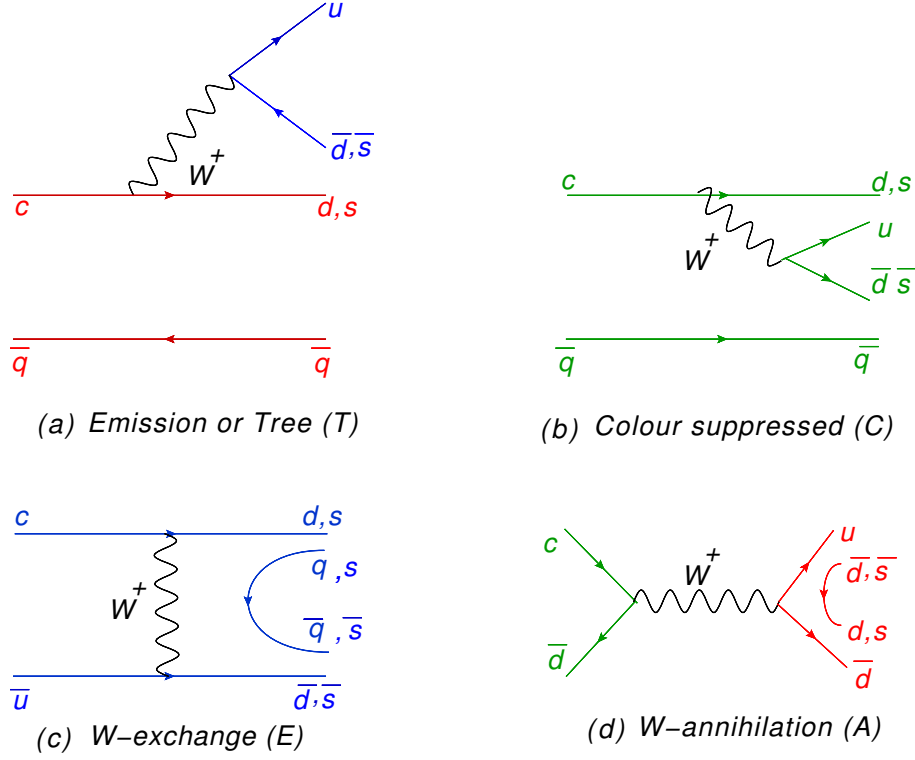


Figure 2.1: The dominant quark diagram amplitudes

the final meson which carries the spectator quark, while P_2 represents the meson emitted from the weak vertex (as depicted in Fig. 2.1), are then written as:

$$T(C) = \frac{G_F}{\sqrt{2}} V_{CKM} a_1(\mu) (a_2(\mu)) f_{P_2} (m_D^2 - m_{P_1}^2) F_0^{DP_1}(m_{P_2}^2), \quad (2.4)$$

where, f_{P_2} is the P_2 meson decay constant and $F_0^{DP_1}(m_{P_2}^2)$ denotes the transition form factor for $D \rightarrow P_1$ evaluated at $m_{P_2}^2$. We follow the prescription of Ref. [110] and choose the scale μ to be the energy release in individual decay processes rather than fixed at m_c . This scale which is dependent on the final state masses, allows for SU(3) breaking, additional to that coming from different decay constants and form factors. This scale is taken to be,

$\mu = \sqrt{\Lambda m_D(1 - r_2^2)}$, where, $r_2^2 = m_{P_2}^2/m_D^2$ and Λ is another free parameter. $\Lambda, \chi_1, \chi_2, \phi_1$ and ϕ_2 are taken to be universal for all the decay modes and are fitted from experimental data.

A comment is in order at this point. While [110] includes NF corrections only in the color suppressed amplitudes, we have included these in the tree amplitudes as well. Of course NF corrections in the color suppressed contributions are well motivated, however, vertex corrections etc. will be present even in the tree contributions and hence these need to be added. Even in B decays, in the QCD factorization approach of Beneke-Neubert [108], these corrections are evaluated for both the Wilson coefficients C_1 and C_2 (and hence are present in tree and color suppressed amplitudes). For D decays, since the non-factorizable corrections are expected to be even more important due to the $1/m_c$ corrections being non-negligible, perhaps incorporating them in tree and color suppressed contributions results in better fits to data. In fact, such corrections were incorporated both in tree and color suppressed amplitudes in ref. [107] and several other papers. In case of charmed meson decays, since these corrections are not calculable, they are parametrized, with the parameters to be determined from fits to data.

2.2.2 Weak Annihilation Contributions

For a long time, W-exchange and W-annihilation contributions used to be neglected due to the so-called helicity suppression. However, observation of many decay modes of charmed and bottom mesons, which are possible only via the annihilation or exchange diagrams have indicated that these contributions could be substantial. These short distance weak annihilation effects were hence included in the diagrammatic approach. In principle these could result from rescattering, even in the absence of annihilation and exchange processes. In fact, weak annihilation topologies were assumed to be induced by nearby resonances through FSI's in Ref. [107]. The authors in [107] as well as Ref. [111] use SU(3) to relate the couplings of the final state mesons with the resonances. This leads to the result that the long distance W-exchange contribution can be induced by a tree amplitude, while W-annihilation can be induced by a color suppressed internal W-emission. The resonant FSI modify the W-exchange and W-annihilation amplitudes but the T and C amplitudes are unaffected. We emphasize that the assumption of SU(3), plays an important role in these results. In a most general coupled channel formalism, all contributions in the various channels will be affected by the resonant FSI, as will be shown in Sec 3. We parametrize the W-exchange and W-Annihilation contributions in the amplitudes by $\chi^{E(A)}$ and estimate them from phenomenological fits to data.

The exchange(annihilation) amplitudes are hence written as:

$$E_{q,s}(A_{q,s}) = \frac{G_F}{\sqrt{2}} V_{CKM} C_1(\mu) (C_2(\mu)) \chi_{q,s}^{E(A)} \frac{C_F}{N_c} f_D f_{P_1} f_{P_2} . \quad (2.5)$$

Since the initial charmed meson is annihilated and both the final mesons are produced from the weak vertex, after the production of a quark-antiquark pair from a gluon, these amplitudes are a product of the decay constants of the initial D meson (f_D) and that of $P_1(f_{P_1})$ and $P_2(f_{P_2})$. Apart from this, the strengths of the exchange(annihilation) amplitudes $\chi_{q,s}^{E(A)}$ are assumed to be the same for all modes and the subscripts distinguish the contributions of the pair production of the light quark-antiquark from that of the strange pair. Since the annihilation and exchange contributions are necessarily non-factorizable, they depend only on $C_{1,2}$ rather than the modified coefficients $a_{1,2}$.

We wish to emphasize that for the case of decays to two pseudoscalar mesons, it has been shown in Ref. [108] that in the annihilation contributions the quark-antiquark pair production happens with gluon emission from the initial state quark. Hence, this contribution is independent of the FSI effects that obviously involve the final state quarks and are discussed in Sec. 2.3. Hence inclusion of both weak annihilation/exchange contributions as well as FSI will not amount to double counting, as pointed out in Ref. [112].

The scale of the Wilson coefficients for the exchange and annihilation am-

plitudes must depend on both the mass ratios, $r_{1,2} = m_{P_{1,2}}/m_D$ and is taken to be, $\mu = \sqrt{\Lambda m_D(1 - r_1^2)(1 - r_2^2)}$.

2.2.3 Non-perturbative Inputs: Form Factors and Decay Constants

We start by specifying our convention for the different mesons involved in our analysis:

$$\begin{aligned}\pi^+ &= -u\bar{d}, & \pi^- &= d\bar{u}, & \pi^0 &= \frac{u\bar{u}-d\bar{d}}{\sqrt{2}}, \\ K^0 &= d\bar{s}, & \bar{K}^0 &= -s\bar{d}, & K^+ &= u\bar{s}, & K^- &= s\bar{u}, \\ D^0 &= c\bar{u}, & D^+ &= -c\bar{d}, & D_s^+ &= c\bar{s}.\end{aligned}$$

In the $D \rightarrow P_1$ transitions, the matrix element of the vector current is written in terms of the form factors F_+ and F_0 as,

$$\langle P_1(p') | \bar{q} \gamma^\mu c | D(p) \rangle \equiv F_+(q^2)(p^\mu + p'^\mu - \frac{m_D^2 - m_{P_1}^2}{q^2} q^\mu) + F_0(q^2) \frac{m_D^2 - m_{P_1}^2}{q^2} q^\mu, \quad (2.6)$$

where $q \equiv p - p'$. The matrix element for the production of the second meson P_2 , is given by,

$$\langle P_2(q) | \bar{q}_1 \gamma_\mu q_2 | 0 \rangle = i f_{P_2} q_\mu. \quad (2.7)$$

Hence, in the amplitude of the non-leptonic two pseudoscalar decay modes of charmed mesons involving the product of the two matrix elements specified in Eqs.(6) and (7), only the transition form factor F_0 appears.

Transition form factors can in principle be experimentally measured from the semi-leptonic decays, however, in the massless lepton limit, only the $F_+(q^2)$ contributes to the semi-leptonic amplitude distributions. However, the semi-leptonic information is still useful, since at zero momentum transfer the form factors obey the kinematic constraint $F_0(0) = F_+(0)$. The q^2 dependence of the F_0 on the other hand is accessible only with massive leptons in the semileptonic decays or in lattice simulations. Simple and modified pole models have been widely used to parametrize the q^2 dependence of the form factors, but these have poor convergence properties. Recently the z -expansion [113, 114] has been introduced as a model independent parametrization of the q^2 dependence of form factors over the entire kinematic range and has been shown to have improved convergence properties. In this approach, based on analyticity and unitarity, the form factors are expressed as a series expansion in powers of z^n , where z is a non-linear function of q^2 , with an overall multiplicative function accounting for the sub-threshold poles and branch cuts,

$$F(t) = \frac{1}{P(t)\phi(t, t_0)} \sum_{k=0}^{\text{inf}} a_k(t_0) z(t, t_0)^k . \quad (2.8)$$

The series coefficients and prefactors can only be determined from fits to lattice or experimental data. In fact, CLEO collaboration has determined these coefficients for the $D \rightarrow \pi, K, \eta$ form factors from the semileptonic decays but, in the massless lepton limit. Hence, for $F_0(q^2)$, we use lattice

results to determine the first two coefficients.

In the Becirevic and Kaidalov (BK) ansatz [115],

$$F_0(q^2) = \frac{F_0(0)}{1 - \frac{q^2}{\beta m_D^*}}, \quad (2.9)$$

where m_D^* is the mass of the vector meson with flavour $c\bar{d}$ or $c\bar{s}$, depending on the transition being $c \rightarrow d$ or $c \rightarrow s$ respectively. $F_0(0)$ and β are parameters to be fitted to experimental data and in fact, in Ref. [117], the Fermilab and Lattice MILC collaborations have fitted these parameters to CLEO-c data. The normalization $f(0)$ and shape parameter determine the physical observables describing the form factors at large recoil and are given by,

$$f(0) \equiv F_+(0) = F_0(0), \quad \frac{1}{\beta} \equiv \frac{(M_H^2 - M_L^2)}{F_+(0)} \frac{dF_0}{dq^2} \Big|_{q^2=0}. \quad (2.10)$$

Using these input parameters we can determine the first two coefficients of the series expansion in Eq. (2.8) for $F_0(q^2)$.

Few details regarding the z series form factor expansion can be found in Appendix B. If the series is rapidly converging, even two coefficients may be sufficient to determine the q^2 dependent form factor $F_0(q^2)$. Equating the normalization and slope obtained using Eq. (2.8) to that obtained from the lattice parameters $(f(0), \beta)$, which in turn had been obtained by fits to experimental data, we can obtain the z -expansion series (up to linear order)

¹It has been pointed out in Ref. [116] that F_0 , but not F_+ , can be modeled by a single pole.

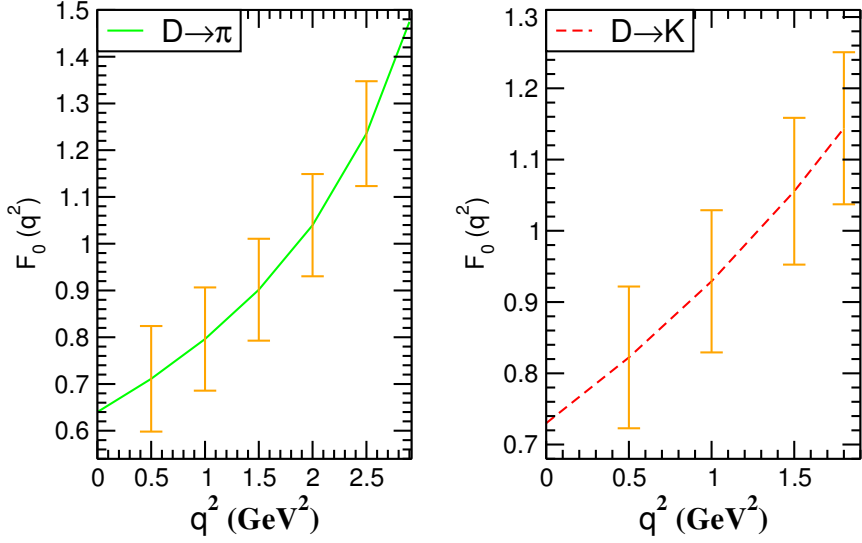


Figure 2.2: The q^2 dependence of the scalar form factors. The plot on the left displays $F_0(q^2)$ for $D \rightarrow \pi$ transition, while that on the right is for $D \rightarrow K$ transition.

for all the form factors.

In Fig. 2.2 we show the plots for our results for $D \rightarrow \pi$ and $D \rightarrow K$ where the lattice input parameters from Ref. [117] are used. We would like to point out that our $D \rightarrow \pi$ and $D \rightarrow K$ form factor values at $q^2 = 0$ are in very good agreement with that given in Refs. [118, 119] which are the most precise published calculations for $D \rightarrow \pi l \nu$ and $D \rightarrow K l \nu$ form factors, according to Lattice Review [120]. Further, the shape of $F_0(q^2)$ for $D \rightarrow \pi, K$ that we obtain after the z-series expansion are consistent with that of Ref. [119]. Moreover, the $f(0)$ values in Table 2.1 for $D \rightarrow \pi$ and $D \rightarrow K$ are also in agreement with CLEO results of Ref. [121].

Regarding $D \rightarrow \eta$ and $D \rightarrow \eta'$ form factors, since in these transitions, only the non-strange component η_q is involved, hence one expects, $F_0(q^2)$ for $D \rightarrow \eta_q, \eta'_q \sim D \rightarrow \pi$. For $D \rightarrow \eta$, CLEO has determined $F_+(0)V_{cd} =$

Table 2.1: Best fit values of BK parameters for the scalar form factors

| Decay | $f(0)$ | β |
|---------------------|--------------------------|--------------------------|
| $D \rightarrow \pi$ | $0.64 \pm 0.03 \pm 0.06$ | $1.41 \pm 0.06 \pm 0.07$ |
| $D \rightarrow K$ | $0.73 \pm 0.03 \pm 0.07$ | $1.31 \pm 0.07 \pm 0.13$ |

$0.086 \pm 0.006 \pm 0.001$ using the semileptonic decay mode $D^+ \rightarrow \eta e^+ \nu_e$ [122]. Hence we use this value to estimate $F_0(0)$. However, for η' , while the first observation of the decay mode $D^+ \rightarrow \eta' e^+ \nu_e$ has been reported by CLEO in the same paper, but the form factor was not determined in this case, and hence we approximate, the $F_0(0)$ for η' to be the same as that for η . Further, since it has been shown [123] that the form factors and particularly their shape is insensitive to the spectator quark, the shape for both η and η' , is assumed to be the same as that for the $D \rightarrow \pi$ case.

The $D_s \rightarrow \eta, \eta'$ have been estimated with some lattice studies using the $(f(0), \beta)$ values from a recent exploratory paper by Bali *et. al.* Ref. [124]. However, these have larger uncertainties, since even the lowest pion mass used is still far from the physical mass. Hence, for $D_s \rightarrow \eta, \eta'$ we take the form factors to be similar to that of $D \rightarrow K$ and for $D_s \rightarrow K$ we take them to be similar to $D \rightarrow \pi$. Note that in all these cases the masses of the final mesons for each of the respective decay process are used in obtaining their z-expansion coefficients, the approximations are used only for the input parameters, $f(0)$ and β . Due to this uncertainty, we have added an additional 3% theoretical error to these form factors.

Turning now to the decay constants, for π and K mesons, the $f_{\pi, K}$ are taken

Table 2.2: z-expansion coefficients obtained after using the BK parameters in Table 2.1

| Decay | a_0 | a_1 |
|----------------------|------------------|------------------|
| $D \rightarrow \pi$ | 0.19 ± 0.02 | -0.41 ± 0.05 |
| $D \rightarrow K$ | 0.08 ± 0.01 | -0.32 ± 0.03 |
| $D \rightarrow \eta$ | 0.06 ± 0.004 | -0.27 ± 0.02 |

from the Particle Data Group(PDG) [125]. For the η and η' , following the method described in [126], it is assumed that the decay constants in the quark flavour basis, follow the pattern of particle state mixing. The η and η' are expressed as linear combinations of the orthogonal flavour states,

$$\eta_q = \frac{1}{\sqrt{2}}(u\bar{u} + d\bar{d}), \quad \text{and} \quad \eta_s = s\bar{s}. \quad (2.11)$$

The physical states η and η' are related to these flavour states by,

$$\begin{pmatrix} \eta \\ \eta' \end{pmatrix} = \begin{pmatrix} \cos \phi & -\sin \phi \\ \sin \phi & \cos \phi \end{pmatrix} \begin{pmatrix} \eta_q \\ \eta_s \end{pmatrix},$$

where, the $\eta - \eta'$ mixing angle denoted by ϕ , represents the sum of the ideal mixing angle and the $\eta - \eta'$ mixing angle (θ) in the octet-singlet basis, $\phi = \theta + \tan^{-1} \sqrt{2}$. Hence the decay constants (form factors) f_q and f_s (F_{0_q} and F_{0_s}) corresponding to that for η_q and η_s ($D \rightarrow \eta_q$ and $D \rightarrow \eta_s$) respectively, are given by:

$$\begin{aligned} f_\eta^q &= f_q \cos \phi, & f_\eta^s &= -f_s \sin \phi, & F_{0_\eta}^q &= F_{0_q} \cos \phi, & F_{0_\eta}^s &= -F_{0_s} \sin \phi, \\ f_{\eta'}^q &= f_q \sin \phi, & f_{\eta'}^s &= f_s \cos \phi, & F_{0_{\eta'}}^q &= F_{0_q} \sin \phi, & F_{0_{\eta'}}^s &= F_{0_s} \cos \phi. \end{aligned}$$

Various ratios of decay rates having η' in the final state with respect to that with η , for example, $\Gamma(J/\psi \rightarrow \eta'\rho)/\Gamma(J/\psi \rightarrow \eta\rho)$, comparison of cross-sections of scattering processes for $\pi^- p \rightarrow \eta'n$ with that of $\pi^- p \rightarrow \eta n$ etc., had been used for a phenomenological fit for the decay constants as well as the angle ϕ in Ref. [126] and had been widely used. Recently, Babar with more accurate data on two photon widths of light pseudoscalar mesons, did a combined analysis [127] along with CLEO data to yield a mixing angle and decay constants with reduced uncertainties: $\phi = 37.66 \pm 0.70$, $\frac{f_q}{f_\pi} = 1.078 \pm 0.044$ and $\frac{f_s}{f_\pi} = 1.246 \pm 0.087$, which are used in this work.

With the above inputs, the un-unitarized amplitudes for all the two-body pseudoscalar-pseudoscalar (PP) modes: SCS, CF and DCS may be written and are listed as follows. For the decay modes involving η and η' , to distinguish the case in which η_q is the P_2 meson of eqn (4) from that where η_s is the one, the notation used is:

$$\begin{aligned}
C_{\eta_q}^f &= \frac{G_F}{\sqrt{2}} V_{CKM} a_2(\mu) f_q(m_D^2 - m_{P_1}^2) F_0^{DP_1}(m_{\eta'}^2), \\
C_{\eta_s}^f &= \frac{G_F}{\sqrt{2}} V_{CKM} a_2(\mu) f_s(m_D^2 - m_{P_1}^2) F_0^{DP_1}(m_{\eta'}^2), \\
C_{\eta'_q}^f &= \frac{G_F}{\sqrt{2}} V_{CKM} a_2(\mu) f_q(m_D^2 - m_{P_1}^2) F_0^{DP_1}(m_{\eta'}^2), \\
C_{\eta'_s}^f &= \frac{G_F}{\sqrt{2}} V_{CKM} a_2(\mu) f_s(m_D^2 - m_{P_1}^2) F_0^{DP_1}(m_{\eta'}^2).
\end{aligned}$$

SCS Decays

$$A(D^0 \rightarrow \pi^+ \pi^-) = -V_{cd}V_{ud}(T + E_q)$$

$$A(D^0 \rightarrow \pi^0 \pi^0) = \frac{V_{cd}V_{ud}}{\sqrt{2}}(-C + E_q)$$

$$A(D^0 \rightarrow \pi^0 \eta) = \frac{V_{cd}V_{ud}}{2}(-C_{\eta_q}^{F_0} + C_{\eta_q}^f) \cos \phi - V_{cs}V_{us}C_{\eta_s}^f \frac{\sin \phi}{\sqrt{2}} - V_{cd}V_{ud}E_q \cos \phi$$

$$A(D^0 \rightarrow \pi^0 \eta') = \frac{V_{cd}V_{ud}}{2}(-C_{\eta'_q}^{F_0} + C_{\eta'_q}^f) \sin \phi + V_{cs}V_{us}C_{\eta'_s}^f \frac{\cos \phi}{\sqrt{2}} - V_{cd}V_{ud}E_q \sin \phi$$

$$A(D^0 \rightarrow \eta \eta) = \frac{V_{cd}V_{ud}}{\sqrt{2}}(C_{\eta_q}^f + E_q) \cos^2 \phi + V_{cs}V_{us}(-C_{\eta_s}^f \frac{\sin 2\phi}{2\sqrt{2}} + \sqrt{2}E_s \sin^2 \phi)$$

$$A(D^0 \rightarrow \eta \eta') = V_{cd}V_{ud}(E_q \frac{\sin 2\phi}{2} + (C_{\eta_q}^f + C_{\eta'_q}^f) \frac{\sin 2\phi}{4}) + V_{cs}V_{us}(-C_{\eta_s}^f \frac{\sin^2 \phi}{\sqrt{2}} + C_{\eta'_s}^f \frac{\cos^2 \phi}{\sqrt{2}} - E_s \sin 2\phi)$$

$$A(D^0 \rightarrow K^+ K^-) = V_{cs}V_{us}(T + E_q)$$

$$A(D^0 \rightarrow K^0 \bar{K}^0) = -(V_{cs}V_{us}E_q + V_{cd}V_{ud}E_s)$$

$$A(D^+ \rightarrow \pi^+ \eta) = \frac{V_{cd}V_{ud}}{\sqrt{2}}(T_{\eta_q}^{F_0} + C_{\eta_q}^f + 2A_q) \cos \phi - V_{cs}V_{us}C_{\eta_s}^f \sin \phi$$

$$A(D^+ \rightarrow \pi^+ \eta') = \frac{V_{cd}V_{ud}}{\sqrt{2}}(T_{\eta'_q}^{F_0} + C_{\eta'_q}^f + 2A_q) \sin \phi + V_{cs}V_{us}C_{\eta'_s}^f \cos \phi$$

$$A(D^+ \rightarrow K^+ \bar{K}^0) = V_{cd}V_{ud}A_s + V_{cs}V_{us}T$$

$$A(D_s^+ \rightarrow \pi^+ K^0) = -(V_{cd}V_{ud}T + V_{cs}V_{us}A_q)$$

$$A(D_s^+ \rightarrow \pi^0 K^+) = -\frac{1}{\sqrt{2}}(V_{cd}V_{ud}C - V_{cs}V_{us}A_q)$$

$$A(D_s^+ \rightarrow K^+ \eta) = (V_{cd}V_{ud}C_{\eta_q}^f + V_{cs}V_{us}A_q) \frac{\cos \phi}{\sqrt{2}} - V_{cs}V_{us}(T_{\eta_s}^{F_0} + C_{\eta_s}^f + A_s) \sin \phi$$

$$A(D_s^+ \rightarrow K^+ \eta') = (V_{cd}V_{ud}C_{\eta'_q}^f + V_{cs}V_{us}A_q) \frac{\sin \phi}{\sqrt{2}} + V_{cs}V_{us}(T_{\eta'_s}^{F_0} + C_{\eta'_s}^f + A_s) \cos \phi$$

The $D^0 \rightarrow \pi\pi$ SCS decays obey the following triangular Isospin relation:

$$A(D^0 \rightarrow \pi^+\pi^-) + \sqrt{2}A(D^0 \rightarrow \pi^0\pi^0) = \sqrt{2}A(D^+ \rightarrow \pi^+\pi^0)$$

CF Decays

$$(D^0 \rightarrow K^-\pi^+) = -V_{cs}V_{ud}(T + E_q)$$

$$(D^0 \rightarrow \bar{K}^0\pi^0) = -V_{cs}V_{ud}\frac{(C - E_q)}{\sqrt{2}}$$

$$(D^0 \rightarrow \bar{K}^0\eta) = V_{cs}V_{ud}\left((-C_{\eta_q}^{F_0} - E_q)\frac{\cos\phi}{\sqrt{2}} + E_s \sin\phi\right)$$

$$(D^0 \rightarrow \bar{K}^0\eta') = V_{cs}V_{ud}\left((-C_{\eta'_q}^{F_0} - E_q)\frac{\sin\phi}{\sqrt{2}} - E_s \cos\phi\right)$$

$$(D^+ \rightarrow \bar{K}^0\pi^+) = -V_{cs}V_{ud}(T + C)$$

$$(D_s^+ \rightarrow \bar{K}^0K^+) = -V_{cs}V_{ud}(C + A_s)$$

$$(D_s^+ \rightarrow \pi^+\eta) = \frac{V_{cs}V_{ud}}{\sqrt{2}}(T_{\eta_s}^{F_0} \sin\phi - A_q \cos\phi)$$

$$(D_s^+ \rightarrow \pi^+\eta') = \frac{V_{cs}V_{ud}}{\sqrt{2}}(-T_{\eta'_s}^{F_0} \cos\phi - A_q \sin\phi)$$

The $D^0 \rightarrow K\pi$ CF decays obey the following triangular Isospin relation:

$$A(D^0 \rightarrow K^-\pi^+) + \sqrt{2}A(D^0 \rightarrow \bar{K}^0\pi^0) = A(D^+ \rightarrow \bar{K}^0\pi^+)$$

DCS Decays

$$(D^0 \rightarrow K^+\pi^-) = V_{cd}V_{us}(T + E_q)$$

$$(D^0 \rightarrow K^0\pi^0) = V_{cd}V_{us}\frac{(C - E_q)}{\sqrt{2}}$$

$$(D^0 \rightarrow K^0\eta) = V_{cd}V_{us}((C_{\eta_q}^{F_0} + E_q)\frac{\cos\phi}{\sqrt{2}} - E_s \sin\phi)$$

$$(D^0 \rightarrow K^0\eta') = V_{cd}V_{us}((C_{\eta'_q}^{F_0} + E_q)\frac{\sin\phi}{\sqrt{2}} + E_s \cos\phi)$$

$$(D^+ \rightarrow K^0\pi^+) = V_{cd}V_{us}(C + A_q)$$

$$(D^+ \rightarrow K^+\pi^0) = V_{cd}V_{us}\frac{T - A_q}{\sqrt{2}}$$

$$(D^+ \rightarrow K^+\eta) = -V_{cd}V_{us}((T_{\eta_q}^{F_0} + A_q)\frac{\cos\phi}{\sqrt{2}} - A_s \sin\phi)$$

$$(D^+ \rightarrow K^+\eta') = -V_{cd}V_{us}((T_{\eta'_q}^{F_0} + A_q)\frac{\sin\phi}{\sqrt{2}} + A_s \cos\phi)$$

$$(D_s^+ \rightarrow K^+K^0) = V_{cd}V_{us}(T + C)$$

The $D^0 \rightarrow K\pi$ DCS decays obey the following quadrilateral Isospin relation:

$$A(D^0 \rightarrow K^+\pi^-) + \sqrt{2}A(D^0 \rightarrow K^0\pi^0) = A(D^+ \rightarrow K^0\pi^+) + \sqrt{2}A(D^+ \rightarrow K^+\pi^0)$$

Similarly, to distinguish the cases where η_q or η_s is the P_1 meson, which incidentally appears in both Tree(T) and Colour Suppressed(C) amplitudes

(unlike for the case discussed above), we use the notation:

$$\begin{aligned}
C_{\eta_q}^{F_0}(T_{\eta_q}^{F_0}) &= \frac{G_F}{\sqrt{2}} V_{CKM} a_2(\mu) (a_1(\mu)) f_{P_2} (m_D^2 - m_{\eta}^2) F_0^{D\eta_q}(m_{P_2}^2), \\
C_{\eta_s}^{F_0}(T_{\eta_s}^{F_0}) &= \frac{G_F}{\sqrt{2}} V_{CKM} a_2(\mu) (a_1(\mu)) f_{P_2} (m_D^2 - m_{\eta}^2) F_0^{D\eta_s}(m_{P_2}^2), \\
C_{\eta'_q}^{F_0}(T_{\eta'_q}^{F_0}) &= \frac{G_F}{\sqrt{2}} V_{CKM} a_2(\mu) (a_1(\mu)) f_{P_2} (m_D^2 - m_{\eta'}^2) F_0^{D\eta'_q}(m_{P_2}^2), \\
C_{\eta'_s}^{F_0}(T_{\eta'_s}^{F_0}) &= \frac{G_F}{\sqrt{2}} V_{CKM} a_2(\mu) (a_1(\mu)) f_{P_2} (m_D^2 - m_{\eta'}^2) F_0^{D\eta'_s}(m_{P_2}^2).
\end{aligned}$$

2.3 Final State Interactions

Final state interaction effects are incorporated using unitarity relations, where the contribution to any channel is a result of sum over all possible hadronic intermediate states. Hence for all the $n D \rightarrow PP$ decays, the FSI corrected amplitudes or the 'unitarized' amplitudes, \mathcal{A}_i^U with $i = 1, \dots, n$ are given by ²

$$\mathcal{A}_i^U = \sum_{k=1}^N \mathcal{S}_{ik}^{1/2} \mathcal{A}_k, \quad (2.12)$$

where, \mathcal{S} is the strong interaction matrix and $k = 1, \dots, n, n + 1, \dots, N$, stands for all possible states that can rescatter into the PP states. In the heavy quark limit the hard rescattering dominates, in which case, the sum can be interpreted to be over all intermediate states of partons and the number of these states will hence be very large. Parton hadron duality will then permit this estimation. These corrections are incorporated into the hard scattering

²For part of the formalism used in this section, we closely follow Refs. [101, 128]

contributions in the QCD factorization approach of Ref. [108] for the case of B meson decays. For the case of charmed meson decays, since m_c is not large enough, we include these NF corrections in the modified Wilson coefficients, in terms of parameters χ_1 and χ_2 . However, some residual long distance FSI's may be left which are particularly important for charmed meson decays, due to the nearby resonances. This residual rescattering is considered in the limited set of $D \rightarrow PP$ decays, to which the duality cannot be applied and therefore these effects may not be incorporated in the NF corrections.

The \mathcal{S} matrix in Eq. (2.12) can be written in terms of a residual matrix (\mathcal{S}_{res}) for the rescattering among the $D \rightarrow PP$ states alone and the scattering matrix which accounts for the hard rescattering from all possible hadronic states into these channels, resulting in the factorization amplitudes as,

$$\begin{aligned}
\mathcal{S}_{ik} &= \sum_{j=1}^n (\mathcal{S}_1)_{ij} (\mathcal{S}_2)_{jk}, \text{ where, } \mathcal{S}_1 = \mathcal{S}_{\text{res}} \text{ and} \\
\mathcal{S}_2 &= \mathcal{S}_1^{-1} \mathcal{S}, \text{ with } \mathcal{A}_j^{\text{fac}} = \sum_{k=1}^N (\mathcal{S}_2^{1/2})_{jk} \mathcal{A}_k, \text{ resulting in} \\
\mathcal{A}_i^{\text{U}} &= \sum_{k=1}^n (\mathcal{S}_{\text{res}}^{1/2})_{ij} \mathcal{A}_j^{\text{fac}}. \tag{2.13}
\end{aligned}$$

Any \mathcal{S} matrix can be written in terms of a real, symmetric \mathbf{K} matrix as, $\mathcal{S} = (1 - i\mathbf{K})^{-1}(1 + i\mathbf{K})$. Hence, the unitarized amplitudes in Eq. (2.13),

may be written as,

$$\mathcal{A}_i^U = \sum_{k=1}^n ((1 - iK)^{-1})_{ij} \mathcal{A}_j^{\text{fac}}. \quad (2.14)$$

The K matrix parametrization has the advantage that the resonances coupling two body channels are represented by poles in the K matrix. The summation in Eq. (2.14), corresponds to summing the geometric series, where the final state hadrons are produced from scattering via resonance at different orders, starting from zero, i.e., directly from the decaying meson without the resonance contribution, resonant rescattering occurring once, twice and so on. While such coupled FSI's has been considered in the past in many papers [67, 99, 107, 111, 129] most of the papers on charm decays further assume $SU(3)$ to relate the parameters of the coupling matrix. Since $SU(3)$ is broken, we prefer to use the measured decay rates of the resonances to various channels to fix the K matrix parameters as far as possible and the ones not measured are left as parameters to be determined by fits of all the theoretical branching ratios to the observed values.

For each of the SCS, CF as well as DCS modes, states with the same isospin are coupled together. In general the K matrix coupling three channels will have the form:

$$K(s) = \frac{1}{(m_{Res}^2 - s)} \begin{bmatrix} k_1 \Gamma_{11} & \sqrt{k_1 k_2} \Gamma_{12} & \sqrt{k_1 k_3} \Gamma_{13} \\ \sqrt{k_2 k_1} \Gamma_{21} & k_2 \Gamma_{22} & \sqrt{k_2 k_3} \Gamma_{23} \\ \sqrt{k_3 k_1} \Gamma_{31} & \sqrt{k_3 k_2} \Gamma_{32} & k_3 \Gamma_{33}, \end{bmatrix}$$

where, m_{Res} denotes the mass of the resonance through which the different channels are coupled and k_1 , k_2 and k_3 are the cm momenta of the 3 decay modes. There are six independent parameters Γ_{ij} . To reduce the independent parameters to a manageable number, we impose the requirement that the diagonal cofactors of $K(s)$ vanish (or equivalently, $\det K(s) = 0$). This leads us to three conditions,

$$\Gamma_{12}^2 = \Gamma_{11}\Gamma_{22}, \quad \Gamma_{13}^2 = \Gamma_{11}\Gamma_{33} \quad \text{and} \quad \Gamma_{23}^2 = \Gamma_{22}\Gamma_{33}. \quad (2.15)$$

The Γ'_{ii} 's are related to the the partial decay width of the resonance to the i^{th} channel.

To illustrate this, we consider first the case of isospin zero states of SCS decay modes of D^0 meson. The isospin zero combination of the $\pi^+\pi^-$ and $\pi^0\pi^0$, K^+K^- and $K^0\bar{K}^0$, and the $\eta\eta$ modes, are coupled via Eq. (2.14) with the $f_0(1710)$ pole in the K matrix. Hence, for this specific case of coupling of the isospin zero states, in the K matrix, $m_{Res} = 1.720$ GeV, $k_1 = \frac{1}{2}(m_{D^0}^2 - 4m_{\pi^0}^2)$, $k_2 = \frac{1}{2}(m_{D^0}^2 - 4m_{K^0}^2)$, $k_3 = \frac{1}{2}(m_{D^0}^2 - 4m_{\eta}^2)$ and we have

$$\Gamma(f_0 \rightarrow \pi\pi) = \frac{\Gamma_{11}k_1}{m_{Res}}, \quad \Gamma(f_0 \rightarrow K\bar{K}) = \frac{\Gamma_{22}k_2}{m_{Res}}, \quad \text{and} \quad \Gamma(f_0 \rightarrow \eta\eta) = \frac{\Gamma_{33}k_3}{m_{Res}}.$$

Experimentally only the two ratios of the decay rates, $\Gamma(f_0 \rightarrow K\bar{K})/\Gamma(f_0 \rightarrow \pi\pi)$ and $\Gamma(f_0 \rightarrow K\bar{K})/\Gamma(f_0 \rightarrow \eta\eta)$ have been determined. Hence we keep $g_{pe} \equiv \Gamma(f_0 \rightarrow K\bar{K})$ as a parameter, to be determined from fits of our

theoretical estimates to the observed branching ratios.

Similarly, for the $I=1$ case, we take the $a_0(1450)$ resonance with $m_{Res} = 1.474$ GeV and $\Gamma_{Res} = 0.265$ GeV, to be responsible for the rescattering among the channels $K\bar{K}$, $\pi\eta$ and $\pi\eta'$, to which this resonance decays. Here again, the decay rate $\Gamma(a_0 \rightarrow \pi\eta)$ is not yet accurately measured and is treated as a parameter (h_{pe}) that may be predicted from the fits of all the branching ratios of the $D \rightarrow PP$ modes to experimental data. Note that the $K\bar{K}$, $\pi\eta$ and $\pi\eta'$ states appear as final states not only of SCS D^0 and D^+ decays, but also in the CF decays of the D_s^+ decays. For all these three sets of decays, the same K matrix (apart from tiny modifications in the cm momenta and the mass-squared of the decaying meson) will suffice, and more importantly with the same one unknown parameter, while many additional observables (all the branching ratios of these D^0 , D^+ and D_s^+) will get added to the χ^2 fit. If this one same parameter, along with the other unknowns in our analysis can simultaneously explain all the observed data, it would indicate that our naive technique of incorporating the FSI effects is satisfactory.

We also couple the isospin $1/2$ states of the $K\pi$, $K\eta$ and $K\eta'$ channels, that are the final states in the SCS decays of D_s^+ , CF decays of D^0 and DCS decays of D^0 and D^+ mesons. Here we use the $K_0^*(1950)$ resonance with $m_{Res} = 1.945$ GeV. Only the branching ratio, $\Gamma(K_0^* \rightarrow K\pi)/\Gamma_{total}$ has been measured. We take the other two decay rates, $\Gamma(K_0^* \rightarrow K\eta)$ and

$\Gamma(K_0^* \rightarrow K\eta')$ as parameters (j_{pe_1} and j_{pe_2}) that can be determined by the overall fits of all the branching ratios to data.

2.4 Numerical Analysis and Results

To estimate all the possible sets of coupled channels, the isospin decomposition of all the SCS, CF and DCS modes are listed on the next page. Here $A^{(U)}$ denote the bare or un-unitarized (unitarized or FSI corrected) amplitudes respectively, for each of the decay modes, while $A_i^{mode(U)}$ denotes the corresponding ununitarized (unitarized) isospin, $I = i$ amplitudes for those modes. With absence of resonances in particular isopin components with the right quantum numbers in the vicinity of the charmed meson masses, some of the isospin components of many modes remain un-unitarized.

SCS Decays

$$A^{(U)}(D^0 \rightarrow \pi^+\pi^-) \equiv \sqrt{2}\mathcal{A}_2^{\pi\pi} + \sqrt{2}\mathcal{A}_0^{\pi\pi(U)}$$

$$A^{(U)}(D^0 \rightarrow \pi^0\pi^0) \equiv 2\mathcal{A}_2^{\pi\pi} - \mathcal{A}_0^{\pi\pi(U)}$$

$$A^{(U)}(D^0 \rightarrow \pi^0\eta) \equiv \sqrt{3}\mathcal{A}_1^{\pi\eta(U)}$$

$$A^{(U)}(D^0 \rightarrow \pi^0\eta') \equiv \sqrt{3}\mathcal{A}_1^{\pi\eta'(U)}$$

$$A^{(U)}(D^0 \rightarrow \eta\eta) \equiv \sqrt{3}\mathcal{A}_0^{\eta\eta(U)}$$

$$A^{(U)}(D^0 \rightarrow K^+K^-) \equiv \sqrt{\frac{3}{2}}(\mathcal{A}_1^{KK(U)} + \mathcal{A}_0^{KK(U)})$$

$$A^{(U)}(D^0 \rightarrow K^0 \bar{K}^0) \equiv \sqrt{\frac{3}{2}} (\mathcal{A}_1^{KK(U)} - \mathcal{A}_0^{KK(U)})$$

$$A^{(U)}(D^+ \rightarrow \pi^+ \pi^0) \equiv 3\mathcal{A}_2^{\pi\pi}$$

$$A^{(U)}(D^+ \rightarrow K^+ \bar{K}^0) \equiv \mathcal{A}_1^{K^+K(U)}$$

$$A^{(U)}(D^+ \rightarrow \pi^+ \eta) \equiv \mathcal{A}_1^{\pi^+\eta(U)}$$

$$A^{(U)}(D^+ \rightarrow \pi^+ \eta') \equiv \mathcal{A}_1^{\pi^+\eta'(U)}$$

$$A^{(U)}(D_s^+ \rightarrow \pi^+ K^0) \equiv \frac{1}{\sqrt{3}} \mathcal{A}_{\frac{3}{2}}^{\pi K} + \sqrt{\frac{2}{3}} \mathcal{A}_{\frac{1}{2}}^{\pi K(U)}$$

$$A^{(U)}(D_s^+ \rightarrow \pi^0 K^+) \equiv \sqrt{\frac{2}{3}} \mathcal{A}_{\frac{3}{2}}^{\pi K} - \frac{1}{\sqrt{3}} \mathcal{A}_{\frac{1}{2}}^{\pi K(U)}$$

$$A^{(U)}(D_s^+ \rightarrow K^+ \eta) \equiv \mathcal{A}_{\frac{1}{2}}^{K^+\eta(U)}$$

$$A^{(U)}(D_s^+ \rightarrow K^+ \eta') \equiv \mathcal{A}_{\frac{1}{2}}^{K^+\eta'(U)}$$

CF Decays

$$A^{(U)}(D^0 \rightarrow K^- \pi^+) = \frac{1}{3} \mathcal{A}_{\frac{3}{2}}^{\bar{K}\pi} + \frac{2}{3} \mathcal{A}_{\frac{1}{2}}^{\bar{K}\pi(U)}$$

$$A^{(U)}(D^0 \rightarrow \bar{K}^0 \pi^0) = \frac{\sqrt{2}}{3} (\mathcal{A}_{\frac{3}{2}}^{\bar{K}\pi} - \mathcal{A}_{\frac{1}{2}}^{\bar{K}\pi(U)})$$

$$A^{(U)}(D^0 \rightarrow \bar{K}^0 \eta) = \sqrt{\frac{2}{3}} \mathcal{A}_{\frac{1}{2}}^{\bar{K}\eta(U)}$$

$$A^{(U)}(D^0 \rightarrow \bar{K}^0 \eta') = \sqrt{\frac{2}{3}} \mathcal{A}_{\frac{1}{2}}^{\bar{K}\eta'(U)}$$

$$A^{(U)}(D^+ \rightarrow \bar{K}^0 \pi^+) = \mathcal{A}_{\frac{3}{2}}^{\bar{K}\pi^+}$$

$$A^{(U)}(D_s^+ \rightarrow \bar{K}^0 K^+) = \mathcal{A}_1^{K\bar{K}(U)}$$

$$A^{(U)}(D_s^+ \rightarrow \pi^+ \eta) = \mathcal{A}_1^{\pi^+\eta(U)}$$

$$A^{(U)}(D_s^+ \rightarrow \pi^+ \eta') = \mathcal{A}_1^{\pi^+\eta'(U)}$$

DCS Decays

$$\begin{aligned}
A^{(U)}(D^0 \rightarrow K^+\pi^-) &= \frac{\sqrt{2}}{3}\mathcal{A}_{\frac{3}{2}}^{K\pi} - \frac{\sqrt{2}}{\sqrt{3}}\mathcal{A}_{\frac{1}{2}}^{K\pi(U)} \\
A^{(U)}(D^0 \rightarrow K^0\pi^0) &= \frac{2}{3}\mathcal{A}_{\frac{3}{2}}^{K\pi} + \frac{1}{\sqrt{3}}\mathcal{A}_{\frac{1}{2}}^{K\pi(U)} \\
A^{(U)}(D^0 \rightarrow K^0\eta) &= \mathcal{A}_{\frac{1}{2}}^{K\eta(U)} \\
A^{(U)}(D^0 \rightarrow K^0\eta') &= \mathcal{A}_{\frac{1}{2}}^{K\eta'(U)} \\
A^{(U)}(D^+ \rightarrow K^0\pi^+) &= \frac{\sqrt{2}}{3}\mathcal{A}_{\frac{3}{2}}^{K\pi^+} + \frac{\sqrt{2}}{\sqrt{3}}\mathcal{A}_{\frac{1}{2}}^{K\pi^+(U)} \\
A^{(U)}(D^+ \rightarrow K^+\pi^0) &= \frac{2}{3}\mathcal{A}_{\frac{3}{2}}^{K\pi^+} - \frac{1}{\sqrt{3}}\mathcal{A}_{\frac{1}{2}}^{K\pi^+(U)} \\
A^{(U)}(D^+ \rightarrow K^+\eta) &= \mathcal{A}_{\frac{1}{2}}^{K^+\eta(U)} \\
A^{(U)}(D^+ \rightarrow K^+\eta') &= \mathcal{A}_{\frac{1}{2}}^{K^+\eta'(U)} \\
A^{(U)}(D_s^+ \rightarrow K^+K^0) &= \frac{1}{\sqrt{2}}(\mathcal{A}_1^{KK} + \mathcal{A}_0^{KK})
\end{aligned}$$

With all the unitarized isospin amplitudes, we construct the corresponding unitarized decay amplitudes for all the decay modes. The decay rates for all the $D \rightarrow P_1P_2$ are then calculated as,

$$\Gamma(D \rightarrow P_1P_2) = \frac{p_c}{8\pi m_D^2} |A(D \rightarrow P_1P_2)|^2. \quad (2.16)$$

Here p_c is the centre of mass momentum of the mesons in the final state given by

$$p_c = \frac{\sqrt{(m_D^2 - (m_{P_1} + m_{P_2})^2)(m_D^2 - (m_{P_1} - m_{P_2})^2)}}{2m_D}.$$

The theoretical branching ratios for each of the decay modes of the D^0 , D^+ or the D_s^+ mesons are then obtained by dividing the corresponding decay rates by the total decay widths of these mesons. We then perform a χ^2 fit of these theoretical branching ratios with the experimentally measured branching fractions, estimating all the unknown parameters from the best fit to data.

The unknown parameters in our study are: the four parameters representing the NF corrections, χ_1 , χ_2 and their respective phases ϕ_1 , ϕ_2 , four parameters: $\chi_{q,s}^E$ and $\chi_{q,s}^A$ depicting the strength of the W-exchange and W-annihilation amplitudes with distinct strengths for $q\bar{q}$ and $s\bar{s}$ pair production, one unknown in each of the isospin zero and isospin one K matrices coupling modes from decays of D^0 and D^+ mesons, two parameters in the isospin half K matrix coupling various decay modes of D_s^+ , one parameter Λ , representing the momentum of the soft degrees of freedom in the charmed mesons, that is used to define the scale for each of the individual decay modes, making a total of 13 unknown parameters. On the other hand out of all the 33 decay modes considered, 28 have been measured, resulting in sufficient observables to determine all the unknown parameters and give predictions for five of the branching fractions of DCS modes that are not yet measured.

Apart from the experimental errors in the observed branching ratios, the calculated errors in our theoretical branching ratio estimates arise from the

errors in the form factors, the η and η' decay constants, the $\eta - \eta'$ mixing angle and the errors in the measured decay widths of the various resonances into the different channels that are included in our χ^2 fits. Errors due to the other theoretical inputs, like meson masses, decay constants of pion, Kaon, charmed mesons, CKM mixing elements (involving the first two generations) are negligibly small.

As discussed in Sec. 2.2.3, the z-series expansion has been obtained for the form factors, keeping the first two terms of this series. The coefficients a_0 and a_1 of these two terms are functions of normalization and shape parameters $f(0)$ and β , obtained from lattice results. The errors in these lattice parameters are used to obtain the errors in the expansion coefficient functions and then propagated to get the errors in the form factors. We find that the errors in the form factors vary from $\approx 5\%$ to $\approx 25\%$.

In the tables 2.4, 2.5 and 2.6, we list the values of the Branching Ratios of the all the SCS, CF and DCS $D \rightarrow PP$ modes obtained from our analysis, after incorporating the FSI effects (shown in the 2nd column), as well as in the absence of the FSI (column 3), absence of annihilation (column 4) along with the corresponding observed experimental branching ratios (column 5) given in PDG [125]. We also predict the B.R.'s for a few DCS modes that have not been experimentally measured yet and are given in the second column of Table 2.6

After incorporating all the errors, the χ^2 minimization results in the fol-

lowing best fit values of all the parameters:

Table 2.3: Parameter best fit values

| Name | Values | Name | Values | Name | Values |
|-----------|-----------|------------|--------------|------------|----------|
| Λ | 0.625645 | j_{pe_1} | 0.0000239368 | χ_q^A | 132.685 |
| χ_1 | -2.68215 | j_{pe_2} | 0.096456 | χ_s^A | 193.447 |
| χ_2 | 2.23605 | χ_q^E | -334.805 | ϕ_1 | 0.302258 |
| g_{pe} | 0.0471262 | χ_s^E | -81.3363 | ϕ_2 | 2.87681 |
| h_{pe} | 0.118834 | | | | |

Table 2.4: $D \rightarrow PP$ SCS B.R.'s, Columns 2 and 3 show our results with annihilation included, for the with and without FSI cases respectively, while column 4 which displays results without annihilation, includes FSI. All the numbers are in units of 10^{-3} .

| Modes | With FSI | Without FSI | Without Ann | Experimental Value |
|--------------------------------|-----------------|-----------------|-----------------|--------------------|
| $D^0 \rightarrow \pi^+\pi^-$ | (1.44 ± 0.027) | (4.35 ± 1.67) | (4.02 ± 1.75) | (1.402 ± 0.026) |
| $D^0 \rightarrow \pi^0\pi^0$ | (1.14 ± 0.56) | (3.66 ± 1.43) | (2.04 ± 0.79) | (0.8209 ± 0.035) |
| $D^0 \rightarrow K^+K^-$ | (4.06 ± 0.77) | (4.27 ± 2.34) | (6.78 ± 3.08) | (3.96 ± 0.08) |
| $D^0 \rightarrow K^0\bar{K}^0$ | (0.342 ± 0.052) | (0.561 ± 0.00) | (0.280 ± 0.084) | (0.34 ± 0.08) |
| $D^0 \rightarrow \pi^0\eta$ | (1.47 ± 0.90) | (6.47 ± 2.98) | (3.25 ± 1.51) | (0.68 ± 0.07) |
| $D^0 \rightarrow \pi^0\eta'$ | (2.17 ± 0.65) | (3.81 ± 1.43) | (1.85 ± 0.79) | (0.9 ± 0.14) |
| $D^0 \rightarrow \eta\eta$ | (1.27 ± 0.27) | (1.32 ± 0.41) | (1.34 ± 0.29) | (1.67 ± 0.20) |
| $D^0 \rightarrow \eta\eta'$ | (0.953 ± 0.183) | (1.04 ± 0.27) | (0.538 ± 0.163) | (1.05 ± 0.26) |
| $D^+ \rightarrow \pi^+\pi^0$ | (0.889 ± 0.451) | (0.870 ± 0.670) | (0.973 ± 0.394) | (1.19 ± 0.06) |
| $D^+ \rightarrow K^+K^0$ | (3.75 ± 0.63) | (10.2 ± 3.7) | (19.9 ± 5.6) | (5.66 ± 0.32) |
| $D^+ \rightarrow \pi^+\eta$ | (4.72 ± 0.21) | (23.4 ± 12.6) | (16.6 ± 7.7) | (3.53 ± 0.21) |
| $D^+ \rightarrow \pi^+\eta'$ | (6.76 ± 2.19) | (30.0 ± 7.6) | (9.78 ± 3.35) | (4.67 ± 0.29) |
| $D_s^+ \rightarrow \pi^+K^0$ | (1.96 ± 0.90) | (1.46 ± 1.10) | (1.32 ± 1.01) | (2.42 ± 0.12) |
| $D_s^+ \rightarrow \pi^0K^+$ | (0.817 ± 0.464) | (0.174 ± 0.100) | (1.01 ± 0.54) | (0.63 ± 0.21) |
| $D_s^+ \rightarrow K^+\eta$ | (1.50 ± 0.75) | (6.40 ± 4.52) | (2.23 ± 1.82) | (1.76 ± 0.35) |
| $D_s^+ \rightarrow K^+\eta'$ | (0.707 ± 0.049) | (2.09 ± 0.87) | (0.057 ± 0.047) | (1.8 ± 0.6) |

2.5 Conclusions

For several decades, various ratios of decay rates of many of the $D \rightarrow PP$ modes remained to be a puzzle as these were expected to be one in the $SU(3)$ limit, but the measured values exhibited large deviations from unity.

Table 2.5: $D \rightarrow PP$ CF B.R.'s, inclusion of Annihilation/FSI in our branching ratio estimates shown in various columns is the same as specified for Table 2.4. All the numbers are in units of 10^{-2} .

| Modes | With FSI | Without FSI | Without Ann | Experimental Value |
|-----------------------------------|-------------------|-------------------|-------------------|--------------------|
| $D^0 \rightarrow K^- \pi^+$ | (3.70 ± 1.33) | (8.83 ± 2.47) | (5.63 ± 1.81) | (3.88 ± 0.05) |
| $D^0 \rightarrow K^0 \pi^0$ | (1.88 ± 0.99) | (12.9 ± 4.4) | (3.30 ± 1.47) | (2.38 ± 0.08) |
| $D^0 \rightarrow K^0 \eta$ | (1.59 ± 0.48) | (0.97 ± 0.33) | (1.09 ± 0.34) | (0.958 ± 0.06) |
| $D^0 \rightarrow K^0 \eta'$ | (2.29 ± 0.43) | (2.06 ± 0.30) | (2.45 ± 0.47) | (1.88 ± 0.1) |
| $D^+ \rightarrow \bar{K}^0 \pi^+$ | (3.42 ± 1.78) | (13.5 ± 11.2) | (5.25 ± 3.34) | (2.94 ± 0.14) |
| $D_s^+ \rightarrow \bar{K}^0 K^+$ | (5.65 ± 1.29) | (17.0 ± 7.9) | (13.5 ± 5.3) | (2.95 ± 0.14) |
| $D_s^+ \rightarrow \pi^+ \eta$ | (2.26 ± 0.82) | (0.78 ± 0.56) | (2.14 ± 0.90) | (1.69 ± 0.10) |
| $D_s^+ \rightarrow \pi^+ \eta'$ | (2.64 ± 0.78) | (3.73 ± 1.52) | (2.52 ± 0.85) | (3.94 ± 0.25) |

Table 2.6: $D \rightarrow PP$ DCS B.R.'s, inclusion of Annihilation/FSI in our branching ratio estimates shown in various columns is the same as specified for Table 2.4. All the numbers are in units of 10^{-4} .

| Modes | With FSI | Without FSI | Without Ann | Experimental Value |
|-----------------------------|-------------------|-------------------|-------------------|--------------------|
| $D^0 \rightarrow K^+ \pi^-$ | (1.77 ± 0.88) | (3.71 ± 1.33) | (2.48 ± 1.07) | (1.38 ± 0.028) |
| $D^0 \rightarrow K^0 \pi^0$ | (2.11 ± 0.26) | (3.70 ± 1.35) | (0.68 ± 0.46) | – |
| $D^0 \rightarrow K^0 \eta$ | (0.94 ± 0.45) | (0.28 ± 0.10) | (0.96 ± 0.32) | – |
| $D^0 \rightarrow K^0 \eta'$ | (8.02 ± 3.32) | (0.59 ± 0.08) | (9.22 ± 1.61) | – |
| $D^+ \rightarrow K^0 \pi^+$ | (3.27 ± 1.86) | (11.9 ± 5.5) | (3.51 ± 2.11) | – |
| $D^+ \rightarrow K^+ \pi^0$ | (3.07 ± 1.02) | (2.15 ± 1.17) | (3.27 ± 1.39) | (1.83 ± 0.26) |
| $D^+ \rightarrow K^+ \eta$ | (0.98 ± 0.26) | (1.04 ± 0.23) | (0.89 ± 0.27) | (1.08 ± 0.17) |
| $D^+ \rightarrow K^+ \eta'$ | (1.40 ± 0.39) | (1.82 ± 0.18) | (1.35 ± 0.39) | (1.76 ± 0.22) |
| $D_s^+ \rightarrow K^+ K^0$ | (7.84 ± 2.31) | (0.68 ± 0.09) | (0.72 ± 0.44) | – |

We have evaluated the bare amplitudes of all the $D \rightarrow PP$ modes using factorization, however, we add non-factorizable corrections, weak annihilation and exchange contributions as parameters, and in the hadron matrix elements, the q^2 dependence of the form factors involved are evaluated using the z-expansion method and finally, resonant final state interaction effects are incorporated. The parameters of the K matrix coupling the various channels are defined using the measured decay widths of the resonances (where available) and those unobserved, are left as parameters to

be fitted from all the measured 28 $D \rightarrow PP$ branching ratios. Our best fit has a $\chi^2/\text{degree of freedom}$ of 2.25, which is an improvement over the previous results in Refs. [94, 110].

- We are able to get reasonable fits to almost all the observed branching ratios. In particular, our branching fractions for $D \rightarrow KK$, $D \rightarrow \pi\pi$ modes that have been a long standing puzzle are in agreement with the corresponding measured values.
- We have evaluated the cosine of the strong phase difference between the unitarized amplitudes for $D^0 \rightarrow K^-\pi^+$ and $D^0 \rightarrow K^+\pi^-$ and obtain, $\cos \delta_{K\pi} = 0.94 \pm 0.027$. This result is consistent with the recently measured BESIII result, $\cos \delta_{K\pi} = 1.02 \pm 0.11 \pm 0.06 \pm 0.01$ [130].
- The mode $D^0 \rightarrow K^0\bar{K}^0$ does not have any tree or colour suppressed contributions, but can come only from W-exchange. In fact, there are two exchange contributions, one appearing with a $d\bar{d}$ and the other with an $s\bar{s}$, which under exact $SU(3)$ symmetry would cancel each other, resulting in a null amplitude. However, since our parameters for these two contributions are distinct, our bare amplitude for this mode is small but non-vanishing. There have been speculations [107, 111] that this mode can arise just from final state interactions, even in the absence of a weak exchange contribution. However, from Table 2.4 it is clear that without the exchange contribution we are unable to generate a large enough rate: both final state interaction and the ex-

change contribution are necessary for consistency with the measured branching fraction.

- We have also evaluated the four ratios of amplitudes that had been specified in a recent paper [131]. In SU(3) limit these are all expected to be unity. Our theoretical estimates for these ratios are given below:

$$\begin{aligned}
R_1 &\equiv \frac{|A(D^0 \rightarrow K^+\pi^-)|}{|A(D^0 \rightarrow \pi^+K^-)| \tan^2 \theta_c} = 1.27 \pm 0.32, \\
R_2 &\equiv \frac{|A(D^0 \rightarrow K^+K^-)|}{|A(D^0 \rightarrow \pi^+\pi^-)|} = 1.27 \pm 0.42, \\
R_3 &\equiv \frac{|A(D^0 \rightarrow K^+K^-)| + |A(D^0 \rightarrow \pi^+\pi^-)|}{|A(D^0 \rightarrow \pi^+K^-)| \tan \theta_c + |A(D^0 \rightarrow K^+\pi^-)| \tan^{-1} \theta_c} = 1.19 \pm 0.28, \\
R_4 &\equiv \sqrt{\frac{|A(D^0 \rightarrow K^+K^-)||A(D^0 \rightarrow \pi^+\pi^-)|}{|A(D^0 \rightarrow \pi^+K^-)||A(D^0 \rightarrow K^+\pi^-)|}} = 1.19 \pm 0.26.
\end{aligned}$$

Furthermore, the following combination of these ratios is expected to be vanishing up to 4th order in U-spin breaking,

$$\Delta R \equiv R_3 - R_4 + \frac{1}{8} \left[\left(\sqrt{2R_1 - 1} - 1 \right)^2 - \left(\sqrt{2R_2 - 1} - 1 \right)^2 \right].$$

Using our unitarized amplitudes, we find the central value of ΔR to be indeed very tiny, however, with a large error.

$$\Delta R = -0.000013 \pm 0.006.$$

Our theoretical errors (in form factors, K-matrix parameters, etc.) are propagated to evaluate the errors in the ratios R_1, R_2, R_3, R_4 and finally

in ΔR .

- We would like to mention that in many modes involving η and η' , we have additional terms in our amplitude due to our distinction of the different form factors, compared to, for eg., those that appear in Ref. [94]. A naive look at the colour suppressed diagrams for $D \rightarrow \pi^0 \eta(\eta')$ will indicate that the contributions from the case where the spectator is part of the π^0 , and that, where it constitutes the $\eta(\eta')$ must cancel. However, in terms of the specific decay constants and form factors, one is proportional to $-f_\pi F_0^{D\eta_q}(m_\pi^2)$ while the other is proportional to $f_{\eta_q} F_0^{D\pi}(m_\eta^2)$, which are unequal and hence must survive.
- While the Particle Data Group [125] does not include a world average for $\Gamma(f_0(1710) \rightarrow K\bar{K})$ but it does list two values for the ratio $\frac{\Gamma(f_0(1710) \rightarrow K\bar{K})}{\Gamma_{total}}$: 0.36 ± 0.12 (Ref. [132]) and $0.38^{+0.09}_{-0.19}$ (Ref. [133]); our fit value of $g_{pe}(\equiv \Gamma(f_0(1710) \rightarrow K\bar{K}))$ corresponds to 0.35 for the branching ratio, which is consistent with these values.
- Our theoretical errors are rather large and could be reduced in future with more precise form factors available either from measurement of semileptonic D , D_s modes at BES III, where if even the lepton mass could be incorporated (eg. by looking at modes with muon in the final state), then the q^2 dependent F_0 could be known, or with improved lattice studies, specially for $D \rightarrow \eta'$, $D_s \rightarrow K$ and $D_s \rightarrow \eta, \eta'$.

- Accurate measurements of the decay widths of the resonances (used for the final state interactions) to many of the coupled channels can reduce the theoretical uncertainties and possibly allow for better fits to data. For example our fits seem to indicate a rather large value for h_{pe} or the width of $a_0(1450) \rightarrow \pi^0\eta$. This seems to result in larger branching fractions for many of the isospin one modes. Future measurement of this width can help reduce this uncertainty and perhaps result in better fits to data for these modes.
- Out of the 28 observed PP modes, we are unable to fit 7 of the modes well. Many of these modes involve η or η' in the final state. Including a gluonium component in the η , η' states may possibly be one way of improving these fits. This, along with improved form factor measurements, observation of decay rates of the resonances (playing a role in final state interactions) to these decay modes, as mentioned in the last two points above, could go a long way in improving our fits. One glaring misfit is the mode $D^+ \rightarrow K^+\bar{K}^0$. This mode does couple to $\pi^+\eta, \pi^+\eta'$ modes and hence, may possibly improve, along with the improvements in those modes. A fit excluding the modes which do not fit well (modes involving η or η' alongwith $K^+\bar{K}^0$) yields a still better $\chi^2/\text{d.o.f}$ of 1.44.
- The η and η' mesons have been subject to much theoretical discussion over the past number of years. Many authors have claimed that these

mesons might have a gluonium content and the QCD description for these mesons is still under a lot of research. Hence, it is not counter intuitive that the η and η' modes are do not fit well. The fits may become better in future with more accurate measurements for the $D \rightarrow \eta, \eta'$ form factors as well as a better understanding of the structure of these final state mesons.

- We emphasize that the Wilson coefficients which incorporate the NF pieces, are expected to be universal. On the other hand, the resonant final state interactions coupling different channels in various isospin states cannot be universal but have to be channel dependent. Hence, we have incorporated this separately. In Tables 2.4, 2.5 and 2.6, we have specifically added columns comparing the theoretical branching ratios for all the PP modes considered, for cases with and without the coupled channel FSI. It can be clearly seen that the fits to data are indeed much better with FSI.

2.A The Wilson Coefficients

The Wilson coefficients used in the evaluation of all the bare amplitudes have been calculated at the final state hadronic scale. This allows for an additional $SU(3)$ breaking effect and they have been incorporated using the procedure outlined in Ref. [110]. The Wilson coefficients at lower

scale are calculated in the Ref. [134]. The essential steps are following.

- In the first step, the Wilson coefficients $C_i(m_W)$ at weak scale are calculated by requiring the equality of the effective theory with five active flavors $q = u, d, s, c, b$ onto the full theory.
- Next, the coefficients undergo the evolution from the scale m_W to μ through the equation

$$C(\mu) = U_5(\mu, m_W)C(m_W). \quad (2.17)$$

- In the next step, coefficients are calculated at the scale of b quark

$$C(m_b) \rightarrow Z(m_b). \quad (2.18)$$

- Now, the Wilson coefficients can be evaluated at required scale (μ_c or μ_{hadron}) through the equation

$$C(\mu) = U_4(\mu, m_b)Z(m_b). \quad (2.19)$$

In the above steps, U_5 and U_4 are the 2×2 and 7×7 evolution matrices for five and four active flavors respectively. The $Z(m_b)$ is given in the Eqs.A.7 to A.10 of the Ref. [134].

The explicit expressions of the Wilson coefficients obtained after following the above steps are given in the Ref. [110]. They are:

$$C_1(\mu) = -0.2334\alpha^{1.444} + 0.0459\alpha^{0.7778} + 1.313\alpha^{0.4444} - 0.3041\alpha^{-0.2222}$$

$$C_2(\mu) = 0.2334\alpha^{1.444} + 0.0459\alpha^{0.7778} - 1.313\alpha^{0.4444} + 0.3041\alpha^{-0.2222}.$$

in terms of the running coupling constant α :

$$\alpha = \alpha_s(\mu) = \frac{4\pi}{\beta_0 \ln(\mu^2/\Lambda_{\overline{MS}}^2)} \left[1 - \frac{\beta_1 \ln \ln(\mu^2/\Lambda_{\overline{MS}}^2)}{\beta_0^2 \ln(\mu^2/\Lambda_{\overline{MS}}^2)} \right],$$

with the coefficients

$$\beta_0 = \frac{33 - 2f}{3} \quad , \quad \beta_1 = 102 - \frac{38}{3}N_f$$

We take active flavour number $N_f = 3$, and the QCD scale $\Lambda_{\overline{MS}} = \Lambda_{\overline{MS}} = 375$ MeV. Again, note that the scale dependent strong coupling constant $\alpha_s(\mu)$ is evaluated at the final state hadronic scales for each individual decay, to take care of the SU(3) breaking.

2.B Series Expansion Method for Form Factors

Using the analytic properties of $F(q^2)$, a transformation of variable is made which maps the cut on the q^2 plane onto a unit circle $|z| < 1$, where

$$z(t, t_0) = \frac{\sqrt{t_+ - t} - \sqrt{t_+ - t_0}}{\sqrt{t_+ - t} + \sqrt{t_+ - t_0}} \quad , \quad t = q^2,$$

where,

$$t_{\pm} = (m_D \pm m_{P_1})^2 \text{ and } t_0 = t_+ \left(1 - \left(1 - \frac{t_-}{t_+} \right)^{1/2} \right).$$

This transformation allows the form factors to be given by an expansion about $q^2 = t_0$, given as

$$F(t) = \frac{1}{P(t)\phi(t, t_0)} \sum_{k=0}^{\text{inf}} a_k(t_0) z(t, t_0)^k,$$

given also as Eq.(2.8) in the text. The function $P(t)$ in the above is 1 for $D \rightarrow \pi$ form factors. For $D_s \rightarrow \eta$ and $D \rightarrow K$ form factors, $P(t) = z(t, M_{D_{s0}^*}^2)$ (where $M_{D_{s0}^*}$) is the nearest 0^+ resonance mass). The outer function ϕ is given by [135]

$$\phi(t, t_0) = \sqrt{\frac{3t_+t_-}{32\pi\chi_0}} \left(\frac{z(q^2, 0)}{-q^2} \right)^2 \left(\frac{z(q^2, t_0)}{t_0 - q^2} \right)^{-1/2} \left(\frac{z(q^2, t_-)}{t_- - q^2} \right)^{-1/4} \frac{\sqrt{t_+ - q^2}}{(t_+ - t_0)^{1/4}},$$

where χ_0 has been calculated [135] using OPE and is given by:

$$\chi_0 = \frac{1 + 0.751\alpha_s(m_c)}{8\pi^2}.$$

For simplicity, we ignore condensate contribution which is of the order $O(m_c^{-3})$ and $O(m_c^{-4})$. The strong coupling at charm scale is computed with the package RunDec [136].

Chapter 3

Searching for New physics in Charm

Radiative decays

3.1 Introduction

The focus of this chapter will be the radiative decays of charmed mesons. While both the inclusive and exclusive radiative B meson decays have been extensively discussed in the literature, less attention has been paid to the D meson radiative decays as their branching ratios are expected to be much smaller due to the almost complete GIM suppression.

Moreover, charm radiative decays will be dominated by long distance contributions, which can hide the presence of new physics particles that may appear in the loop of the short distance penguin contributions. Nevertheless, in Ref. [137] it was pointed out that a measurement of the difference in the rates of the exclusive modes, $D^0 \rightarrow \rho\gamma$ and $D^0 \rightarrow \omega\gamma$ in which the

long distance effects are expected to cancel, would indicate short distance new physics if the data reveals a difference of rates which is more than 30%. But in general, due to the large uncertainties in the long distance contributions, any definite conclusion regarding NP will not be feasible from a measurement of the radiative decay rates for the inclusive $c \rightarrow u\gamma$ case nor for any individual exclusive channel, unless the NP short distance contribution is larger than that from the long distance effects. In fact, the possibility of enhancement above the otherwise dominant long distance effects, in presence of a fourth generation model with large mixing angles of the b' quark, $U_{ub'}U_{ub'}$ had been pointed out in Ref. [138]. Fourth generation models are now inconsistent with the LHC data, however, models with vector-like charge $-1/3$ quarks, for which the authors of Ref. [138] claimed that their results were also applicable, are still viable. In fact, in the last couple of years many detailed studies of the phenomenology of vector-like quarks and constraints from the flavour sector have been performed [139–143].

Apart from the enhancement in the decay rate, which will be subject to the relative size of the short distance and long distance effects, NP could also be searched through a measurement of the polarization of the photon produced in the decay. The SM has a robust prediction regarding the photon polarization in $c \rightarrow u\gamma$ decays and hence, a measurement of the photon polarization can pin down the presence of NP. This had been ear-

lier pointed out for the case of B radiative decays in Refs. [144, 145]. In the SM, the photons from the short distance (SD) penguin contribution in the $c \rightarrow u\gamma$ decays will be mostly left handed up to corrections of $O(m_u/m_c)$. This dominance of left handed polarization can get masked in the presence of long distance (LD) effects. However, the fraction of the right polarized photons will vary in different models and may possibly even allow one to distinguish between different models of NP. We explore the effects of the presence of a down-type isosinglet vector-like quark model on the $c \rightarrow u\gamma$ decay rate, as well as on the photon polarization for this model with an additional left-right symmetry. The decay rate evaluation requires an estimation of both the SD as well as LD components, which are described in the next section. In Sec. 3.3.1 some details of the down type isosinglet vector-like quark model are discussed, including the modifications to the Wilson coefficients in its presence. Sec. 3.3.2 contains a short discussion on LRSM and the results for the bare level SD contributions to the amplitudes for the emission of the left and right handed photons in this model. Sec. 3.4.1 gives our results for the branching ratios (BR's) in the SM and in the different NP models. In Sec. 3.4.2 we present our analysis of the polarization function in the LRSM and the LRSM with vector-like quark.



Figure 3.1: The two types of pole contribution effects. Type-I (left) and type II (right).

3.2 Amplitudes within the Standard Model

3.2.1 Long distance contributions

The long distance contributions being non-perturbative in nature are hard to estimate. They can be separated into two classes. At the quark level, the first corresponds to the annihilation (or exchange) diagrams $c\bar{q}_1 \rightarrow q_2\bar{q}_3$ with a photon attached to any of the four quark lines. At the hadronic level these diagrams manifest as long distance pole diagrams. The second, corresponds to the underlying quark process $c \rightarrow q_1\bar{q}_2q$, followed by $\bar{q}_2q \rightarrow \gamma$. At the hadronic level this is the vector meson dominance mechanism (VMD).

Pole Contributions

The pole amplitudes are a subset of a more general class of long distance contributions, which include two-particle intermediate states and extend up to all higher n-particle intermediate states. Phenomenologically however, the single-particle or pole terms are the most accessible. The pole contributions to charm meson radiative weak decays are shown in Fig. 3.1.

If the incoming meson undergoes a weak transition before the photon emission, it is referred to as a Type I transition, while the transition is of Type II, if the final state meson is created from the weak transition of the intermediate virtual states, after the photon emission. In both cases, all possible spin-zero and spin-one virtual particles can contribute respectively, however, only the lightest of the virtual particles are included in practice.

The transition amplitude for the processes $D(p) \rightarrow V(k_1, \lambda_1) + \gamma(k_2, \lambda_2)$ can be written in gauge invariant form as

$$\begin{aligned} & \mathcal{M}(D \rightarrow V\gamma) \\ &= \epsilon_\mu^\dagger(k_1, \lambda_1) \epsilon_\nu^\dagger(k_2, \lambda_2) \left(\mathcal{A}^{PV} (p^\mu p^\nu - g^{\mu\nu} k_2 \cdot p) + i \mathcal{A}^{PC} \epsilon^{\mu\nu\alpha\beta} k_{1\alpha} p_\beta \right). \end{aligned} \quad (3.1)$$

In general both \mathcal{A}^{PV} (the parity-violating amplitude) and \mathcal{A}^{PC} (the parity-conserving amplitude) will be present. The decay rate is given by

$$\Gamma(D \rightarrow V\gamma) = \frac{|\mathbf{k}_2|^3}{4\pi} \left(|\mathcal{A}^{PV}|^2 + |\mathcal{A}^{PC}|^2 \right), \quad (3.2)$$

where \mathbf{k}_2 is the decay momentum in the rest frame of D meson.

Pole amplitude of type I

If the initial particle is a pseudoscalar meson, the intermediate meson has to be a scalar (parity-violating case) or a pseudoscalar meson (parity-conserving). However since our detailed theoretical and experimental un-

derstanding about scalar states is lacking, we consider mixing with pseudoscalar mesons only and therefore will only get parity conserving contributions from the type-I amplitudes¹. The pseudoscalar meson will propagate virtually until it decays to a vector meson V via electromagnetic transition which is parity conserving. The amplitude is then given by

$$\mathcal{M}_{V\gamma P} = h_{V\gamma P} \epsilon_\mu^\dagger(k_1, \lambda_1) \epsilon_\nu^\dagger(k_2, \lambda_2) \epsilon^{\mu\nu\alpha\beta} k_{1\alpha} p_\beta, \quad (3.3)$$

where $h_{V\gamma P}$ is the electromagnetic coupling of the photon with the mesons V, P and is determined phenomenologically by

$$|h_{V\gamma P}|^2 = \begin{cases} \frac{12\pi\Gamma_{V\rightarrow P\gamma}}{|\mathbf{k}_2|^3}, & (M_V > M_P) \\ \frac{4\pi\Gamma_{P\rightarrow V\gamma}}{|\mathbf{k}_2|^3}, & (M_P > M_V). \end{cases} \quad (3.4)$$

The type-I decay amplitude is then given by

$$\mathcal{A}_I^{PC}(D \rightarrow V\gamma) = \sum_n h_{V\gamma P_n} \frac{1}{m_D^2 - m_{P_n}^2} \langle P_n | \mathcal{H}_W^{(\text{eff})} | D \rangle, \quad (3.5)$$

where $\mathcal{H}_W^{(\text{eff})}$ is the effective weak Hamiltonian of Bauer, Stech and Wirbel [146](BSW), which is given for the Cabibbo-favoured (CF) and

¹However, the current data on scalar states does allow us to estimate the parity violating LD contributions to $D^0 \rightarrow \phi\gamma$, numbers for which has been displayed in Table 3.8.

Cabibbo-suppressed (CS) modes as,

$$\begin{aligned}
\mathcal{H}_\omega^{CF} &= -V_{ud}V_{cs}^* \frac{G_F}{\sqrt{2}} [a_1(\bar{u}d)(\bar{s}c) + a_2(\bar{s}d)(\bar{u}c)], \\
\mathcal{H}_\omega^{CS} &= -\frac{G_F}{\sqrt{2}} [a_1 (V_{ud}V_{cd}^*(\bar{u}d)(\bar{d}c) + V_{us}V_{cs}^*(\bar{u}s)(\bar{s}c)) \\
&\quad + a_2 (V_{us}V_{cs}^*(\bar{s}s)(\bar{u}c) + V_{ud}V_{cd}^*(\bar{d}d)(\bar{u}c))], \tag{3.6}
\end{aligned}$$

where V 's are the CKM matrix elements, a_1 and a_2 are free parameters and will depend on the mass scale being probed. For our case we use the value of a_1 and a_2 from the $D \rightarrow \bar{K}\pi$ data [147].

$$a_1(m_c^2) = 1.2 \pm 0.1, \quad a_2(m_c^2) = -0.5 \pm 0.1. \tag{3.7}$$

It is possible in principle to extend the discussion of the $V\gamma$ final states to a larger set of meson-photon final states $M\gamma$, where the spin of the meson M should be greater than zero. We can write the gauge invariant amplitude and the interaction vertex in the same way as Eq. 3.1 and Eq. 3.4 respectively. The interaction vertex will then be denoted by $h_{M\gamma P_n}$ instead of $h_{V\gamma P_n}$. We consider here final states of the type $A\gamma$, $T\gamma$ where A and T are axial vector and tensor mesons. The formalism for $D \rightarrow A\gamma$ decays is exactly the same as $D \rightarrow V\gamma$ decays. The coupling and the total decay rate are found via Eq. (3.4) and Eq. (3.2) respectively. For the $T\gamma$ final states,

the coupling and the decay rate are given by

$$|h_{T\gamma P}|^2 = \frac{40\pi\Gamma_{T\rightarrow P\gamma}}{|\mathbf{k}_2|^5} \quad (3.8)$$

and

$$\Gamma_{D\rightarrow T\gamma} = \frac{|\mathbf{k}_2|^5}{4\pi} |\mathcal{A}_I^{PC}|^2 \quad (3.9)$$

respectively.

Pole amplitude of type II

Since for the amplitude of type II, the photon emission occurs before the weak transition, hence, the intermediate meson will be vector in nature. The type II pole amplitude can be written in a similar way to the type I amplitude:

$$\mathcal{A}_{II}^{PC}(D \rightarrow V\gamma) = \sum_n \langle V|\mathcal{H}_w|D_n^* \rangle \frac{1}{m_D^2 - m_{D_n^*}^2} h_{D_n^*\gamma D}. \quad (3.10)$$

Vector Meson Dominance (VMD) contributions

Fig 3.2 shows the VMD contribution for radiative charm meson decays. We describe briefly the formalism for obtaining the $D \rightarrow V_1\gamma$ amplitude from $D \rightarrow V_1 V_2$ amplitude in the following. For a more detailed description we refer to [148].

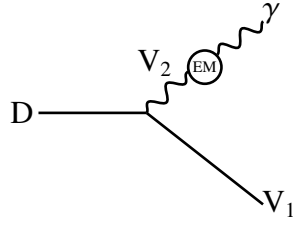


Figure 3.2: The vector meson dominance (VMD) contribution

- First, the amplitude for the processes $D \rightarrow V_1 V_2$ is constructed. This is then multiplied by the factor $\frac{e}{f_{V_2}}$, where e is the electric charge and f_{V_2} is defined as,

$$\langle 0 | e J_{em}^\mu(0) | V(k, \lambda) \rangle = e \frac{m_V^2}{f_V} \epsilon^\mu(k, \lambda). \quad (3.11)$$

Here f_V is determined in terms of $V \rightarrow e^+ e^-$ data,

$$\Gamma_{V \rightarrow e^+ e^-} = \frac{4\pi\alpha^2 m_V}{3 f_V^2} \left[1 - \frac{4m_e^2}{m_V^2} \right]^{\frac{1}{2}} \left[1 + \frac{2m_e^2}{m_V^2} \right]. \quad (3.12)$$

- Since V_2 propagates as a massless virtual particle and is converted to a photon, one needs to extrapolate the $D \rightarrow V_1 V_2$ amplitude and $V_2 \rightarrow \gamma$ vertex from $k_2^2 = m_2^2$ to $k_2^2 = 0$. As a result of this extrapolation f_{V_2} in general will not be the same as determined from Eq. 3.12.

We use the factorization assumption [148, 149] and the BSW Hamiltonian [146] to obtain a theoretical description of $D \rightarrow V_1 V_2$ amplitude. The

squared VMD amplitude is given by

$$\begin{aligned}
|\mathcal{A}_{VMD}|^2 &= \frac{G_F^2 |V_{cq}^* V_{uq'}|^2}{2m_D^2 \mathbf{k}^2} a_i^2(m_c^2) f_X^2 I \times \left[(m_D + m_Y)^2 A_1^2(q_0^2) + \frac{4\mathbf{k}^2 m_D^2 V^2(q_0^2)}{(m_D + m_Y)^2} \right] \times \frac{4\pi\alpha}{\bar{f}_{V_2}^2} \\
&= |\mathcal{A}_{VMD}^{PV}|^2 + |\mathcal{A}_{VMD}^{PC}|^2, \tag{3.13}
\end{aligned}$$

where \bar{f}_{V_2} is the off-shell extension of f_{V_2} ; $q, q' = d, s$; $a_1(m_c^2), a_2(m_c^2)$ are the color favored and color suppressed BSW operators, \mathbf{k} is the photon spatial momentum, X is the final meson which couples to vacuum and the other meson, Y comes in the matrix element $\langle Y(p_Y) | J^\mu | D(P) \rangle$, which is given by

$$\begin{aligned}
\langle Y(p_Y) | J^\mu | D(P) \rangle &= \frac{2V(q^2)}{m_D + m_Y} \epsilon^{\mu\nu\rho\sigma} \epsilon_\nu^* P_\rho p_{Y\sigma} + 2m_Y i A_0(q^2) \frac{(\epsilon^* \cdot q)}{q^2} q^\mu + i \\
&\left[(m_D + m_Y) A_1(q^2) \epsilon^{*\mu} - \frac{(\epsilon^* \cdot q) A_2(q^2)}{m_D + m_Y} (P + p_Y)^\mu - 2m_Y A_3(q^2) \frac{(\epsilon^* \cdot q)}{q^2} q^\mu \right] \tag{3.14}
\end{aligned}$$

X can be V_1 or V_2 ; for $X = V_1, q_0^2 = m_1^2$, where m_1 is the mass of vector meson V_1 ; for $X = V_2, q_0^2 = 0$. To calculate the form factors at $q_0^2 \neq 0$, we use the form

$$A_1(q_0^2) = \frac{A_1(0)}{1 - b'x}, \quad V(q_0^2) = \frac{V(0)}{(1 - x)(1 - ax)},$$

where $x = \frac{q_0^2}{m_{H^*}^2}$. The quantities m_{H^*}, b', a can be found in ref [150]. All these long distance effects are rather hard to calculate from first principles but can be estimated in models. Hence, it is important that the observables chosen for uncovering short distance NP, have different values

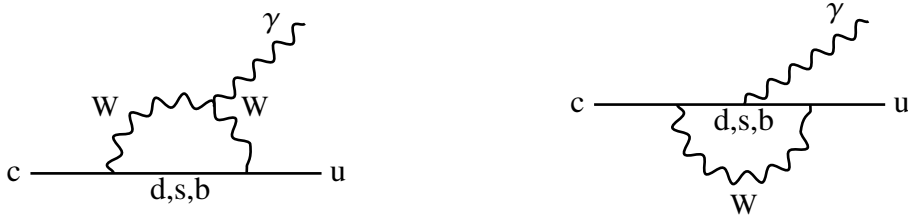


Figure 3.3: The Feynman diagrams for the process $c \rightarrow u\gamma$.

from the SM case, even in the presence of the large long distance contributions. We provide an updated estimate for the long distance amplitudes and branching ratios for charm decays following the methods of Ref. [148] in appendix 3.A.

3.2.2 Short distance contribution

The amplitude for the flavour changing radiative transitions were first evaluated by Inami and Lim [151]. As pointed out in Ref. [152], those formulae need to be appropriately modified for the case of $c \rightarrow u\gamma$ decay. The SM Lagrangian for the processes $c \rightarrow u\gamma$, which arises at the loop level as shown in Fig.3.3 is given by,

$$\mathcal{L}_{\text{int}} = -\frac{4G_F}{\sqrt{2}}A^{SM} \frac{e}{16\pi^2} m_c (\bar{u}\sigma_{\mu\nu}P_R c) F^{\mu\nu}, \quad (3.15)$$

where the mass of the final quark u has been neglected and $P_R = \frac{1+\gamma_5}{2}$. The coefficient A^{SM} is a function of the internal quark masses and the (QCD

uncorrected) contribution to the amplitude A^{SM} is given by,

$$\begin{aligned}
A^{SM} &= \sum_{p=1,2} Q_p \left[V_{cb}^* V_{ub} G_p^{LL}(r_b) + V_{cs}^* V_{us} G_p^{LL}(r_s) + V_{cd}^* V_{ud} G_p^{LL}(r_d) \right] \\
&= \sum_{p=1,2} Q_p \sum_{q=d,s,b} V_{ci}^* V_{ui} G_p^{LL}(r_q),
\end{aligned} \tag{3.16}$$

where $r_q = \frac{m_q^2}{M_W^2}$ with m_q ($q = d, s, b$) being the masses of the down-type quarks running in the fermion loop in the penguin diagrams. The functions G_p^{LL} , $p = 1, 2$ defined in [152] are given in appendix 3.C. Q_1 and Q_2 are the charges of the W boson emitted from the initial quark in the loop diagram, and that of the internal quark running in the loop, respectively. The inclusive decay rate for a $c \rightarrow u\gamma$ process within the SM is given by,

$$\Gamma_{c \rightarrow u\gamma}^0 = \frac{\alpha G_F^2}{128\pi^4} m_c^5 |A^{SM}|^2. \tag{3.17}$$

This results in the following inclusive BR for the $c \rightarrow u\gamma$ process,

$$BR(c \rightarrow u\gamma) = \frac{3\alpha}{4\pi} \frac{|A^{SM}|^2}{|V_{cs}|^2 I(\frac{m_s^2}{m_c^2}) + |V_{cd}|^2 I(\frac{m_d^2}{m_c^2})} BR(D^+ \rightarrow X e^+ \nu_e), \tag{3.18}$$

which is normalized with respect to the inclusive semi-leptonic BR for D^+ decays, to get rid of the uncertainty in the charm quark mass. The function I is the phase space suppression factor and is given by,

$$I(x) = 1 - 8x + 8x^3 - x^4 + 12x^2 \ln\left(\frac{1}{x}\right). \tag{3.19}$$

In the case of $b \rightarrow s\gamma$ decay, up-type quarks flow in the loop and the heavy top quark contribution dominates and induces penguin operators already at the electroweak scale. In contrast, all the down type quarks are massless compared to the electroweak scale, resulting in no penguin contribution at this scale within the SM for the case of $c \rightarrow u\gamma$. However, the presence of a heavy down type vector-like quark, will result in a non-vanishing penguin contribution at the electroweak scale. Within the SM, the enhancement of the radiative decay rates in presence of QCD corrections was pointed out in Ref. [148]. While the enhancement was by a factor of two in the case of $b \rightarrow s\gamma$, it was expected to be more dramatic in the case of charm radiative decays [148, 153]. It is hence important to write down the weak effective Hamiltonian with all the dimension-6 operators and calculate the corresponding Wilson coefficients within the renormalization-group improved perturbation theory which are discussed below.

The RG evolution and the coefficient $C_{7\text{eff}}$

The RG evolution of the Wilson coefficients for charm decays in context of the SM to the next-to-leading order (NLO) in QCD corrections is performed. The calculation for the complete set of operators relevant for charm decays had previously been done up to NLO in the NDR scheme [154] and to the next-to-next-to-leading order (NNLO) in the $\overline{\text{MS}}$ scheme [155]. In this article, we work in the $\overline{\text{MS}}$ scheme since the anoma-

lous dimension matrices at the leading order (LO) ($\hat{\gamma}_{eff}^0$) and at NLO ($\hat{\gamma}_{eff}^1$) are readily available in Ref. [155]. The short distance evolution of the Wilson coefficients has to be divided into two steps. The first task is to integrate out the weak gauge bosons at a scale $\mu \sim M_W$. This is done by calculating the C_i 's at the scale $\mu \sim M_W$ by matching the effective theory with five active flavors $q = u, d, s, c, b$ onto the full theory. As mentioned earlier, no penguin operators are generated at this point, since all the down-type quarks (d, s and b) are to be treated as massless [153] and the GIM mechanism is in full effect. The effective hamiltonian for the scale $m_b < \mu < M_W$ is then given by,

$$\mathcal{H}_{eff}(m_b < \mu < M_W) = \frac{4G_F}{\sqrt{2}} \sum_{q=d,s,b} V_{cq}^* V_{uq} [C_1(\mu) Q_1^q + C_2(\mu) Q_2^q]. \quad (3.20)$$

Here,

$$Q_1^q = (\bar{u}_L \gamma_\mu T^a q_L) (\bar{q}_L \gamma^\mu T^a c_L), \quad Q_2^q = (\bar{u}_L \gamma_\mu q_L) (\bar{q}_L \gamma^\mu c_L). \quad (3.21)$$

The effective anomalous dimension matrix $\hat{\gamma}_{eff}$ is calculated in the effective theory with five flavours. Using this matrix, the $C_i(M_W)$'s are evolved down to the scale $\mu \sim m_b$, and the $C_i(m_b)$'s are obtained.

The next step is to integrate out the b quark as an effective degree of freedom at the scale $\mu \sim m_b$. This is accomplished by matching the effective five flavour theory onto the effective theory for four flavours. This generates the penguin operators with the Wilson coefficients depending upon

M_W solely through the coefficients $C_{1,2}(m_b)$. The effective hamiltonian at the scale $m_c < \mu < m_b$ is then given by

$$\mathcal{H}_{eff}(m_c < \mu < m_b) = \frac{4G_F}{\sqrt{2}} \sum_{q=d,s} V_{cq}^* V_{uq} [C_1(\mu) Q_1^q + C_2(\mu) Q_2^q + \sum_{i=3}^{10} C_i(\mu) Q_i] \quad (3.22)$$

where

$$Q_3 = \bar{u}_L \gamma_\mu c_L \sum_{q=u,d,s,c} \bar{q} \gamma^\mu q, \quad Q_4 = \bar{u}_L \gamma_\mu T^a c_L \sum_{q=u,d,s,c} \bar{q} \gamma^\mu T^a q, \quad (3.23)$$

$$Q_5 = \bar{u}_L \gamma_\mu \gamma_\nu \gamma_\rho c_L \sum_{q=u,d,s,c} \bar{q} \gamma^\mu \gamma^\nu \gamma^\rho q, \quad (3.24)$$

$$Q_6 = \bar{u}_L \gamma_\mu \gamma_\nu \gamma_\rho T^a c_L \sum_{q=u,d,s,c} \bar{q} \gamma^\mu \gamma^\nu \gamma^\rho T^a q, \quad (3.25)$$

$$Q_7 = -\frac{g_{em}}{16\pi^2} m_c \bar{u}_L \sigma^{\mu\nu} c_R F_{\mu\nu}, \quad Q_8 = -\frac{g_s}{16\pi^2} m_c \bar{u}_L \sigma^{\mu\nu} T^a c_R G_{\mu\nu}^a. \quad (3.26)$$

In all of the above, $q_L = P_L q$ and $P_{R,L} = (1 \pm \gamma_5)/2$ are the chirality projection operators. The T^a are the generators of $SU(3)$. The C_i 's are the Wilson coefficients which contain the complete short distance (perturbative QCD) corrections. For the case of radiative charm decays under consideration here, the operators Q_9 and Q_{10} are not relevant and therefore not shown in the above list. We will hence consider only the set of Wilson coefficients $C_{1,\dots,8}$ which are evolved down from the m_b scale to the m_c scale using the $\hat{\gamma}_{eff}$ matrix now evaluated in the effective theory with four flavours to obtain the $C_i(m_c)$'s.

Hence, at each order (O), the vector of the Wilson coefficients C_i at the

scale $\mu = m_c$ may be schematically written as

$$C_i^{(O)}(m_c) = U_{(f=4)}^{(O)}(m_c, m_b) R_{match}^{(O)} U_{(f=5)}^{(O)}(m_b, M_W) C_i^{(O)}(M_W) \quad (3.27)$$

where f is the number of active flavours at the corresponding scale, $R_{match}^{(O)}$ is the matching matrix between the effective five flavour theory above the scale $\mu = m_b$ to the effective four flavour theory below the scale $\mu = m_b$, the index $O = \{\text{LO}, \text{NLO}\}$ specifies the order in QCD corrections at which the corresponding quantities are being calculated and the U 's are the evolution matrices related to the effective anomalous dimension matrix $\hat{\gamma}_{eff}$ and are discussed in detail below. We use the formalism given in Ref. [156, 157] to obtain the evolution matrices for LO and NLO. We also closely follow Ref. [155] in the following discussion.

The leading order(LO) evolution

Let us start with the full 8×8 effective anomalous dimension matrix at the leading order ($\hat{\gamma}_{eff}^0$) which can be assimilated in parts from [155, 158–160]. It is given in eqn. (3.52) in appendix 3.B with the full dependence on the number of active flavours(f) and charges(q_1, q_2) of the internal quark and the decaying quark.

Now, let V be the matrix that diagonalizes $\hat{\gamma}_{eff}^{0T}$, so that

$$V^{-1} \hat{\gamma}_{eff}^{0T} V = [\hat{\gamma}_{eff_i}^{(0)T}]_{diag}. \quad (3.28)$$

The LO evolution matrix $U^{(0)}$ for evolving the C_i 's down from the scale μ_2 to μ_1 is then given by

$$U^{(0)}(\mu_1, \mu_2) = V \left[\begin{array}{c} \left(\frac{\alpha_s(\mu_1)}{\alpha_s(\mu_2)} \right)^{-\hat{\gamma}_{eff_i}^{(0)}/2\beta_0} \\ \vdots \\ \left(\frac{\alpha_s(\mu_1)}{\alpha_s(\mu_2)} \right)^{-\hat{\gamma}_{eff_i}^{(0)}/2\beta_0} \end{array} \right]_{diag} V^{-1} \quad (3.29)$$

where α_s is the strong coupling constant.

A few comments are in order at this point. It was specified previously that the only operators relevant for the case of charm decays within the SM, above the scale $\mu = m_b$ are Q_1^q and Q_2^q . Hence, the matrix $U^{(0)}(m_b, M_W)$ is essentially a 2×2 matrix. The LO values of $C_{1,2}(M_W)$, which are basically the initial conditions are well known and are given by:

$$C_1(M_W) = 0, \quad C_2(M_W) = 1. \quad (3.30)$$

Hence we have, for the scale $m_b < \mu < M_W$

$$\begin{pmatrix} C_1(m_b) \\ C_2(m_b) \end{pmatrix} = U^{(0)}(m_b, M_W) \begin{pmatrix} C_1(M_W) \\ C_2(M_W) \end{pmatrix}. \quad (3.31)$$

At this point, all the other Wilson coefficients (C_3 to C_8) are zero. They get their values from the matching at the scale m_b . However, the matching matrix $R_{match} = \delta_{ij}$ to LO and hence, for the LO evolution, the coefficients C_3 to C_8 remain vanishing even after the matching procedure. The resulting 8×1 column vector $(C_1(m_b), C_2(m_b), 0, 0, 0, 0, 0, 0)$ is then multiplied with the 8×8 evolution matrix $U^{(0)}(m_c, m_b)$ to obtain the values of the C_i 's at the

charm scale. The renormalization scheme independent Wilson coefficient $C_{7_{eff}}$ relevant for radiative charm decays is then obtained at LO using the relation

$$C_{7_{eff}} = C_7 + \sum_{i=1}^6 y_i C_i \quad (3.32)$$

where $y_i = \frac{2}{3}\{0, 0, 1, \frac{4}{3}, 20, \frac{80}{3}\}$ [155].

The next-to-leading order(NLO) evolution

The NLO expression for the evolution matrix is given by

$$U^{(1)}(\mu_1, \mu_2) = (1 + \alpha_s(\mu_1)J^{(1)})U^{(0)}(\mu_1, \mu_2)(1 - \alpha_s(\mu_2)J^{(1)}) \quad (3.33)$$

where

$$J^{(1)} = VH^{(1)}V^{-1}. \quad (3.34)$$

V was defined previously in eqn. (3.28) and the matrix H is defined by

$$H_{ij}^{(1)} = \delta_{ij}\hat{\gamma}_{eff_i}^{(0)}\frac{\beta_1}{2\beta_0^2} - \frac{G_{ij}^{(1)}}{2\beta_0 + \hat{\gamma}_{eff_i}^{(0)} - \hat{\gamma}_{eff_j}^{(0)}}. \quad (3.35)$$

with

$$G^{(1)} = V^{-1}\hat{\gamma}_{eff}^{(1)T}V. \quad (3.36)$$

The expression for the 8×8 $\hat{\gamma}_1$ matrix with the complete effective flavour and charge dependence can again be collected in parts from [155, 158–160]. Due to its large size, we provide the matrix in two separate 8×6 and

8×2 blocks in appendix 3.B (see eqns. 3.54 and 3.53).

It is easy to see that one encounters a term of the order of α_s^2 on expanding the expression for $U^{(1)}(\mu_1, \mu_2)$ (eqn. (3.33)). However, a calculation of the NLO contribution necessarily requires that all terms higher than the first order in α_s be discarded and hence, special care should be taken in using eqn.(3.33) for the NLO evolution.

Similar to the case of the LO evolution, the only relevant coefficients above the m_b scale are $C_1(M_W)$ and $C_2(M_W)$, calculated up to the NLO order this time. The expressions can be found in [161] and in the $\overline{\text{MS}}$ scheme are given by

$$C_1(M_W) = \frac{15\alpha_s(M_W)}{4\pi}, \quad C_2(M_W) = 1. \quad (3.37)$$

The coefficients $C_i(i = 3, \dots, 8)$ however are non-vanishing after the matching procedure at NLO, since the matching matrix R_{match} is now defined by

$$R_{match_{ij}} = \delta_{ij} + \frac{\alpha_s(m_b)}{4\pi} R_{ij}^{(1)}. \quad (3.38)$$

The non-zero elements of the matrix $R^{(1)}$ for charm decays being [155]

$$\begin{aligned} R_{41}^{(1)} &= -R_{42}^{(1)}/6 = 1/9, \\ R_{71}^{(1)} &= -R_{72}^{(1)}/6 = 8/81, \\ R_{81}^{(1)} &= -R_{82}^{(1)}/6 = -1/54. \end{aligned} \quad (3.39)$$

The full set of NLO coefficients (C_1, \dots, C_8) for the case of charm decays in the SM is then given by

$$C(m_c) = U^{(1)}(m_c, m_b)R_{match}C(m_b). \quad (3.40)$$

where $C(m_b)$ is an 8×1 column vector whose first two elements are $C_1(m_b)$ and $C_2(m_b)$ and the rest are zero. Once the values at the charm scale are obtained, the corresponding value for $C_{7_{eff}}$ can be obtained from eqn. (3.32).

3.3 New Physics models

3.3.1 Down type isosinglet vector-like quark

The SM contains three generation of quarks, however, the number of generations is not predicted by the theory. A simple extension of the SM would be to have a chiral fourth generation of quarks and leptons. Presence of a fourth generation would have a significant effect on the Higgs sector of the SM and is now ruled out by the Higgs production and decay processes data at the LHC. However, the so called vector-like quarks, which do not receive their masses from Yukawa couplings to a Higgs doublet, are consistent with the present Higgs data. They are distinguished from the SM quarks by their vector coupling to gauge bosons, i.e., both the left handed, Ψ_L and right handed, Ψ_R chiralities of these fermions transform the same way under the SM gauge groups $SU(3)_c \times SU(2)_L \times U(1)_Y$. These exotic

fermions occur for example in the grand unified theory based on E_6 [162]. In general these fermions could either be singlets or doublets or triplets under $SU(2)_L$. Here we consider the case of a down type isosinglet quark. In the SM, the quark mixing matrix is a 3×3 unitary matrix which is specified in terms of three angles $(\theta_{12}, \theta_{13}, \theta_{23})$ and a CP -violating phase, δ_{13} . A 4×4 unitary quark mixing matrix (A) is parametrized in terms of 3 additional angles $(\theta_{14}, \theta_{24}, \theta_{34})$ and two more CP violating phases, δ_{14}, δ_{24} . In Ref. [143], a chi-squared fit to many flavour observables was performed to obtain the preferred central values, along with the errors of all the elements of the measurable 3×4 quark mixing matrix (V). To evaluate the SD contribution of the radiative decay rate in the presence of the vector-like isosinglet quark, the central values of the mass and mixing angles are obtained from the results of the fit in Ref. [143] are used. The relevant charged current Lagrangian is given by,

$$\mathcal{L}_W = \frac{g}{\sqrt{2}} \bar{u}_{iL} V_{i\alpha} \gamma^\mu d_\alpha W_\mu,$$

where V is a 3×4 CKM matrix mentioned above.

Modified Wilson coefficients in presence of a vector-like quark

Having discussed the evolution of the Wilson coefficients for the SM in full detail we will now simply specify how the contribution of the vector-like quark model modifies the SM coefficients.

Table 3.1: Central values of CKM matrix elements in SM and in SM+VLQ.

| Parameter | SM | $m_{b'} = 800 \text{ GeV}$ | $m_{b'} = 1200 \text{ GeV}$ |
|---------------|--------|----------------------------|-----------------------------|
| θ_{12} | 0.2273 | 0.2271 | 0.2270 |
| θ_{13} | 0.0035 | 0.0038 | 0.0038 |
| θ_{23} | 0.0397 | 0.0391 | 0.0391 |
| δ_{13} | 1.10 | 1.04 | 1.04 |
| θ_{14} | – | 0.0151 | 0.0147 |
| θ_{24} | – | 0.0031 | 0.0029 |
| θ_{34} | – | 0.0133 | 0.0123 |
| δ_{14} | – | 0.11 | 0.11 |
| δ_{24} | – | 3.23 | 3.23 |

The down-type vector-like quark induces a Z-mediated FCNC in the down-type quark sector. In Ref. [163] it was pointed out for the case of singlet up type vector like quark, that only the Wilson coefficients are modified. Similarly for the $c \rightarrow u$ transitions that are of interest to us, no new set of operators are introduced and hence the anomalous dimension matrices along with the coefficients $C_1(M_W)$ and $C_2(M_W)$, remain exactly the same as that in the SM, up to NLO.²

The fundamental difference in this model is that at the electroweak scale, the coefficients $C_{7,8}$ will not be zero. While the down-type quarks running in the penguin loop in the SM³ can be treated as massless and hence do not contribute, the vector-like b' quark, which couples with all the up-type SM quarks being heavier than M_W will generate a value for the coefficients C_7

²However, at the NNLO order, one encounters terms dependent on $\frac{m_t^2}{M_W^2}$ which arise as a result of integrating out the top quark as a heavier degree of freedom at the electroweak scale. Since the b' is also heavier than the W boson, one needs to integrate it out too at this scale. Hence, at the NNLO level, the expressions for $C_1(M_W)$ and $C_2(M_W)$ change for this model as compared to SM.

³The relevant diagrams in the Feynman gauge can be found in [152].

and C_8 at the electroweak scale itself. The values are

$$C_7 = \frac{1}{2} \left(G_1^{LL} \left(\frac{m_{b'}^2}{M_W^2} \right) - \frac{1}{3} G_2^{LL} \left(\frac{m_{b'}^2}{M_W^2} \right) \right) \quad (3.41)$$

$$C_8 = \frac{1}{2} G_2^{LL} \left(\frac{m_{b'}^2}{M_W^2} \right) \quad (3.42)$$

where the functions $G_p^{LL}(r)$ defined in [152] are given in appendix 3.C.

We have calculated these coefficients in this model for two benchmark values for the mass of the b' quark in accordance with [143]. Our results are displayed in Table 3.2. Our values for the coefficients in the SM match exactly with Ref. [155] if we use their values for the parameters m_t , m_b , M_W and μ . We find there is more than an order enhancement in the values of the coefficients $C_{7_{eff}}$ and $C_{8_{eff}}$ at the NLO level in the case of this vector-like quark model compared to the SM. However, we should mention here that our NLO results for the NP model are not exact in the sense that we have not calculated the expressions for these coefficients at the NLO level at the W scale. The LO results are exact. From the values in Table 3.2 it is evident that the dimension six operators $O_{1,\dots,6}$ do not mix with the dimension five operators $O_{7,8}$ (a fact that is well known and clear from the form of the anomalous dimension matrices).

Table 3.2: The values of the Wilson coefficients at the charm scale in SM and a heavy vector-like quark(VLQ) model with the benchmark values of 800 GeV and 1200 GeV for the heavy-quark mass. We take the mass of the charm quark $m_c = 1.275$ GeV, the \overline{MS} mass of the bottom quark $m_b = 4.18$ and the mass of the W boson $M_W = 80.385$. The four-loop expression for the strong constant α_s has been used.

| Coefficients | LO | | | NLO | | |
|-----------------|---------|--------------------|---------------------|---------|--------------------|---------------------|
| | SM | VLQ | VLQ | SM | VLQ | VLQ |
| | | $m_{b'} = 800$ GeV | $m_{b'} = 1200$ GeV | | $m_{b'} = 800$ GeV | $m_{b'} = 1200$ GeV |
| C_1 | -1.0769 | -1.0769 | -1.0769 | -0.7434 | -0.7434 | -0.7434 |
| C_2 | 1.1005 | 1.1005 | 1.1005 | 1.0503 | 1.0503 | 1.0503 |
| C_3 | -0.0043 | -0.0043 | -0.0043 | -0.0060 | -0.0060 | -0.0060 |
| C_4 | -0.0665 | -0.0665 | -0.0665 | -0.1015 | -0.1015 | -0.1015 |
| C_5 | 0.0004 | 0.0004 | 0.0004 | 0.0003 | 0.0003 | 0.0003 |
| C_6 | 0.0008 | 0.0008 | 0.0008 | 0.0009 | 0.0009 | 0.0009 |
| C_7 | 0.0837 | 0.3324 | 0.3276 | 0.6095 | 0.2820 | 0.2778 |
| C_8 | -0.0582 | -0.2259 | -0.2253 | -0.0690 | -0.2197 | -0.2192 |
| $ C_{7_{eff}} $ | 0.0424 | 0.2911 | 0.2863 | 0.0119 | 0.2159 | 0.2117 |

3.3.2 Left-right symmetric model

The minimal Left Right symmetric model is based on the gauge group $SU(3)_c \times SU(2)_L \times SU(2)_R \times U(1)_{B-L}$ [164–166] with the fermions represented as doublet representations of $SU(2)_L$ and $SU(2)_R$. The electric charge Q and the third components of the weak isospin I_{3L} and I_{3R} are related as $Q = I_{3L} + I_{3R} + \frac{B-L}{2}$. To ensure perturbative interactions between right-handed gauge boson and fermions, $\zeta_g = \frac{g_R}{g_L}$ (where the g_R and g_L are the right and left handed couplings respectively) should not be large. As in the low energy weak interaction L-R symmetry is broken, in general $g_L \neq g_R$. Direct search results impose the the bound $\zeta_g M_{W_2} > 2.5$ TeV [167, 168]. In order to generate active neutrino mass through see-saw mechanism, ν_R should be in the TeV range. All these constraints result in the range for ζ_g being $[0, 2]$. The charged gauge boson W_L and W_R are mix-

ture of the mass eigenstates W_1 and W_2 , with a mixing angle ζ restricted to lie in the range $[0, 10^{-3}]$ [169, 170]. Since the minimal LRSM models with an exact symmetry between the left and right handed sectors are becoming harder to realize, we use a right handed mixing matrix which is distinct from the left handed CKM matrix. To decrease the number of parameters, we take the right-handed CKM matrix to be,

$$\begin{pmatrix} c_{12} & s_{12} & 0 \\ -s_{12} & c_{12} & 0 \\ 0 & 0 & 1 \end{pmatrix}, \quad (3.43)$$

where $c_{12} = \cos \phi_{12}$ and $s_{12} = \sin \phi_{12}$. This parametrization of the right handed CKM matrix is inspired by Ref. [170, 171]. The CP violating phases have been taken to be zero and $\phi_{13} = \phi_{23} = 0$, where ϕ_{ij} is the mixing angle between the i^{th} and j^{th} generations. For the case of the LRSM with a heavy vector-like quark b' , there are three additional parameters ($\phi_{14}, \phi_{24}, \phi_{34}$). The explicit form of the right-handed CKM matrix in this case is given by,

$$\begin{pmatrix} c_{12}c_{13}c_{14} & c_{13}c_{14}s_{12} & 0 & s_{14} \\ -c_{24}s_{12} - c_{12}s_{14}s_{24} & c_{12}c_{24} - s_{12}s_{14}s_{24} & 0 & c_{14}s_{24} \\ -c_{12}c_{24}s_{14}s_{34} + s_{12}s_{24}s_{34} & -c_{12}s_{24}s_{34} - c_{24}s_{12}s_{14}s_{34} & c_{34} & c_{14}c_{24}s_{34} \end{pmatrix}, \quad (3.44)$$

where $c_{ij} = \cos \phi_{ij}$, and $s_{ij} = \sin \phi_{ij}$.

The effective lagrangian given in eqn. (3.15) (for SM) may now be written for the case of LRSM as,

$$\mathcal{L}_{eff} = -\frac{eG_F}{4\sqrt{2}\pi^2}[\mathcal{A}\bar{u}\sigma^{\mu\nu}RcF_{\mu\nu} + \mathcal{B}\bar{u}\sigma^{\mu\nu}LcF_{\mu\nu}] \quad (3.45)$$

where \mathcal{A} and \mathcal{B} are the bare SD contributions to c_L and c_R respectively.

$$\begin{aligned} \mathcal{A} = \sum_{\ell} \left\{ Q_1(M\cos^2\zeta\lambda_{\ell}^{LL}G_1^{LL} + m\zeta_g^2\sin^2\zeta\lambda_{\ell}^{RR}G_1^{RR} + m_{\ell}\zeta_g\sin\zeta\cos\zeta e^{i\phi}\lambda_{\ell}^{LR}G_1^{LR} \right. \\ \left. + m_{\ell}\zeta_g\sin\zeta\cos\zeta e^{-i\phi}\lambda_{\ell}^{RL}G_1^{RL}) + Q_2(M\cos^2\zeta\lambda_{\ell}^{LL}G_2^{LL} + m\zeta_g^2\sin^2\zeta\lambda_{\ell}^{RR}G_2^{RR} \right. \\ \left. + m_{\ell}\zeta_g\sin\zeta\cos\zeta e^{i\phi}\lambda_{\ell}^{LR}G_2^{LR} + m_{\ell}\zeta_g\sin\zeta\cos\zeta e^{-i\phi}\lambda_{\ell}^{RL}G_2^{RL}) \right\} \quad (3.46) \end{aligned}$$

$$\begin{aligned} \mathcal{B} = \sum_{\ell} \left\{ Q_1(m\cos^2\zeta\lambda_{\ell}^{LL}H_1^{LL} + M\zeta_g^2\sin^2\zeta\lambda_{\ell}^{RR}H_1^{RR} + m_{\ell}\zeta_g\sin\zeta\cos\zeta e^{i\phi}\lambda_{\ell}^{LR}H_1^{LR} \right. \\ \left. + m_{\ell}\zeta_g\sin\zeta\cos\zeta e^{-i\phi}\lambda_{\ell}^{RL}H_1^{RL}) + Q_2(m\cos^2\zeta\lambda_{\ell}^{LL}H_2^{LL} + M\zeta_g^2\sin^2\zeta\lambda_{\ell}^{RR}H_2^{RR} \right. \\ \left. + m_{\ell}\zeta_g\sin\zeta\cos\zeta e^{i\phi}\lambda_{\ell}^{LR}H_2^{LR} + m_{\ell}\zeta_g\sin\zeta\cos\zeta e^{-i\phi}\lambda_{\ell}^{RL}H_2^{RL}) \right\}. \quad (3.47) \end{aligned}$$

For the case of $c \rightarrow u\gamma$ decays, $Q_1 = 1$, $Q_2 = -1/3$, $M = m_c$ and $m = m_u$. l is the down type quark running in the penguin loop with mass m_l . For the case of LRSM with a vector like quark this will include $m_{b'}$ also. λ_i 's are the CKM factors, $\lambda_{\ell}^{LL} = V_{c\ell}^{*L}V_{\ell u}^L$, $\lambda_{\ell}^{RR} = V_{c\ell}^{*R}V_{\ell u}^R$, $\lambda_{\ell}^{LR} = V_{c\ell}^{*L}V_{\ell u}^R$, $\lambda_{\ell}^{RL} = V_{c\ell}^{*R}V_{\ell u}^L$. The functions G_p^{ij} and H_p^{ij} for $p = 1, 2$ and $i = j = L$ are given in Ref. [152]. G_p and H_p are also included in appendix 3.C. We calculate the SD contributions \mathcal{A} and \mathcal{B} only at the bare level. For the $c \rightarrow u\gamma$ decays in the LRSM model, the operator basis with and without the heavy vector-like quark now consists of 20 operators. They are the 8 operators described in

Table 3.3: LRSM, LRSM+VLQ parameter and their allowed range

| Parameters | Ranges | |
|---|---------------------|---------------|
| | LRSM | LRSM+VLQ |
| ζ | $0 - 10^{-3}$ | $0 - 10^{-3}$ |
| ζ_g | $0 - 2$ | $0 - 2$ |
| ϕ_{12} | $0 - 2\pi$ | $0 - 2\pi$ |
| LRSM+VLQ | | |
| Parameter | Range | |
| $m_{b'}$ | 800, 1200GeV | |
| $\phi_{i4}(i = 1, 2, 3)$ | $0 - 2\pi$ | |
| $\theta_{ij}(i = 1, 2, 3; j = 2, 3, 4)$ | listed in Table 3.1 | |

sec. 3.2.2 which contribute to \mathcal{A} along with the following two operators,

$$Q_9^q = (\bar{u}_L \gamma_\mu T^a q_L) (\bar{q}_R \gamma^\mu T^a c_R), \quad Q_{10}^q = (\bar{u}_L \gamma_\mu q_L) (\bar{q}_R \gamma^\mu c_R), \quad (3.48)$$

which are the left-right analogues of Q_1^q and Q_2^q . 10 more operators with the chiralities of these operators flipped, contribute to \mathcal{B} . Since the strong interactions preserve chirality, these two sets of operators with different chiralities do not mix with each other and the RG group mixing of the two sets are the same. However, the additional operators require an additional $\gamma_{4 \times 4}$ which although present in the literature for radiative b decays [169], is not available for the case of the radiative charm decays. Hence incorporating the QCD corrections for the LRSM case, is beyond the scope of this work.

3.4 Results and discussions

3.4.1 Branching ratios in the SM and for the NP models

The inclusion of QCD corrections result in an enhancement of the coefficient A^{SM} (defined in eqn. 3.16) from $\mathcal{O}(10^{-7})$ at the bare (QCD uncorrected) level to $\mathcal{O}(10^{-6})$ at the LO and $\mathcal{O}(10^{-3})$ at the NLO level. At the LO, the contributions from the intermediate d and s quarks differ only in the CKM factors $V_{cd}^* V_{ud}$ and $V_{cs}^* V_{us}$. Their sum, using unitarity is $-V_{cb}^* V_{ub}$, leading to a large suppression in the amplitude. At the NLO, the functional dependence of the amplitudes on the s and d quark masses becomes substantial and hence the net amplitude is no longer just the sum of the CKM factors. In fact, since $V_{cs}^* V_{us} = -V_{cd}^* V_{ud}$, this results in $A^{SM} \propto V_{cs}^* V_{us} [f(\frac{m_s}{mc})^2 - f(\frac{m_d}{mc})^2]$, where the function f [153] is given by:

$$\begin{aligned}
 f(x) = & -\frac{1}{243}((3672 - 288\pi^2 - 1296\zeta_3 + (1944 - 324\pi^2)\ln x + 108\ln^2 x \\
 & + 36\ln^3 x)x + 576\pi^2 x^{\frac{3}{2}} + (324 - 576\pi^2 + (1728 - 216\pi^2)\ln x \\
 & + 324\ln^2 x + 36\ln^3 x)x^2 + (1296 - 12\pi^2 + 1776\ln x - 2052\ln^2 x)x^3) \\
 & - \frac{4\pi i}{81}((144 - 6\pi^2 + 18\ln x + 18\ln^2 x)x + (-54 - 6\pi^2 + 108\ln x \\
 & + 18\ln^2 x)x^2 + (116 - 96\ln x)x^3). \tag{3.49}
 \end{aligned}$$

Table 3.4: The values for $|A|$ and the inclusive $c \rightarrow u\gamma$ BR in the SM and vector-like quark(VLQ) model. For the vector-like quark model, the values have been calculated for the benchmark values $m'_b = 800$ GeV and 1200 GeV.

| QCD | $ A $ | | | BR($c \rightarrow u\gamma$) | | |
|------|-----------------------|---------------------------|----------------------------|-------------------------------|---------------------------|----------------------------|
| | SM | VLQ $m_{b'} = 800$ GeV | VLQ $m_{b'} = 1200$ GeV | SM | VLQ $m_{b'} = 800$ GeV | VLQ $m_{b'} = 1200$ GeV |
| Bare | 2.73×10^{-7} | 2.49×10^{-5} | 2.35×10^{-5} | 2.04×10^{-17} | 1.70×10^{-13} | 1.51×10^{-13} |
| LO | 5.89×10^{-6} | 4.32×10^{-5} | 4.25×10^{-5} | 9.48×10^{-15} | 5.11×10^{-13} | 4.94×10^{-13} |
| NLO | 2.61×10^{-3} | 4.46×10^{-2} | 4.37×10^{-2} | 1.86×10^{-9} | 5.46×10^{-7} | 5.23×10^{-7} |

Hence, the coefficient A^{SM} at LO and NLO is given by,

$$A_{LO}^{SM} = -V_{cb}^* V_{ub} C_{7eff}^{LO} \quad A_{NLO}^{SM} = V_{cs}^* V_{us} C_{7eff}^{NLO}. \quad (3.50)$$

Note that $|C_{7eff}|$ itself is not enhanced at NLO compared to LO within the SM as is evident from the values in Table 3.2, rather the different CKM coefficients appearing in A_{LO}^{SM} and A_{NLO}^{SM} result in the enhancement of the coefficient A^{SM} at the NLO level.

Since the vector-like quark b' generates a non-vanishing value for the coefficients C_7 and C_8 at the electroweak scale itself, its presence results in an increased magnitude of C_{7eff} as can be seen in Table 3.2. This results in the BR enhancement by 2 orders of magnitude in the vector-like quark model at NLO compared to that in the SM. The values for $|A|$ and the corresponding BR's for the QCD uncorrected, LO and NLO corrected contributions for SM and the vector-like quark model (with $m'_b = 800, 1200$ GeV) are given in table 3.4.

Table 3.5 shows the bare level BR's for the LRSM as well as LRSM with a heavy vector-like quark model. Comparing with the bare level BR's from

Table 3.5: Branching ratios for the LRSM model without and with contribution from heavy vector-like quark(VLQ). The Branching ratio is expressed as a function of ζ , ζ_g and θ_{12} (for LRSM) and of ζ , ζ_g , θ_{12} , θ_{14} , θ_{24} and θ_{34} (for LRSM+VLQ). The corresponding parameters are varied to determine the maximum and minimum values.

| Model | | BR |
|---------------------|-----|------------------------|
| LRSM | Max | 1.96×10^{-11} |
| | Min | 0.67×10^{-15} |
| LRSM+VLQ (800 GeV) | Max | 4.65×10^{-8} |
| | Min | 1.69×10^{-13} |
| LRSM+VLQ (1200 GeV) | Max | 0.96×10^{-7} |
| | Min | 1.42×10^{-13} |

Table 3.4, it is evident that for LRSM alone an enhancement of $\mathcal{O}(10^2)$ to $\mathcal{O}(10^6)$ is feasible, depending on the values of the parameters of LRSM, compared to the SM. LRSM along with vector-like quark can enhance the BR by even upto $\mathcal{O}(10^{10})$.

For the SM (vector-like quark model), the enhancement of the BR from the bare level to that with QCD corrections at NLO level is $\mathcal{O}(10^8)$ ($\mathcal{O}(10^6)$). For the case of LRSM with vector-like quark, QCD corrections are expected to lead to similar large enhancement. Even if the enhancement from these corrections is considerably less ($\sim \mathcal{O}(10^4)$), the QCD corrected SD contribution from the LRSM with vector-like quark could result in BR's much larger than that from the LD effects. This enhancement could possibly point towards the presence of such a NP.

3.4.2 Photon polarization as a probe for new physics

Within the SM, in the penguin diagram responsible for the $c \rightarrow u\gamma$ process only left-handed components of the external fermions couple to the W boson. A helicity flip on the c quark leg, proportional to m_c , contributes to the amplitude for the emission of left polarized photons, while, that on the u quark leg, proportional to m_u , results in right polarized photons.

In the LRSM since the physical W_1 boson couples to both left and right handed quarks, a helicity flip is also possible on the internal (d, s, b) quark lines and will result in additional left handed photons with an amplitude involving a new coefficient function and proportional to $m_b\zeta$ and similarly there will be additional right-handed photons proportional to $m_b\zeta$. In the presence of a vector-like quark, each of these contributions will be proportional to $m_{b'}\zeta$.

In analogy to Ref. [145], we define the photon polarization for the inclusive process $c \rightarrow u\gamma$ as

$$\lambda_\gamma = \frac{|c_R|^2 - |c_L|^2}{|c_R|^2 + |c_L|^2}, \quad (3.51)$$

where c_R, c_L denote the amplitudes for the right and left polarized photons in the process.

For the SM, since the SD contributions to c_R are negligible ($\mathcal{O}(m_u)$ suppressed), if one only includes the SD contributions to estimate λ_γ , its value would be -1 . However, the exclusive decay modes corresponding to the

$c \rightarrow u\gamma$ process are dominated by LD contributions. To account for these we add the values of the pole type and VMD amplitudes of all the exclusive processes (given in appendix 3.A). Due to uncertainty in the sign of the VMD contributions, the long distance amplitudes can lie in the range $(2.08 \times 10^{-9} - 8.78 \times 10^{-7}) \text{ GeV}^{-1}$. Since the LD amplitude does not have any preferred polarization, it contributes equally to both c_R and c_L . This results in an almost vanishing value of $\lambda_\gamma \sim (\mathcal{O}(10^{-8} - 10^{-5}))$ within the SM. This is in contrast to the $b \rightarrow s\gamma$ case [145], where the LD contributions are less significant, and hence the λ_γ value is -1 in SM. Without LR symmetry, an isosinglet vector-like quark can only couple to W_L and hence its addition will only enhance the left handed polarized amplitude. For this case we find that in presence of LD contribution, λ_γ lies in the range -6.1×10^{-6} to -2.6×10^{-3} . The bare SD contributions to the $|c_R|$ and $|c_L|$ amplitudes within the LRSM are given by eqns. (3.46) and (3.47). Here again the LD contribution is appropriately added to $|c_R|$ and $|c_L|$.

The photon polarization can be expressed as a function of ζ , ζ_g and ϕ_{12} (LRSM) and of ζ , ζ_g , ϕ_{12} , ϕ_{14} , ϕ_{24} and ϕ_{34} (for LRSM+VLQ). We vary the parameters ζ_g and ζ within their allowed ranges ($0 \leq \zeta_g \leq 2$ and $0 \leq \zeta \leq 10^{-3}$) and look for the ϕ_{12} (LRSM) and of ϕ_{12} , ϕ_{14} , ϕ_{24} and ϕ_{34} (for LRSM+VLQ) values for the maximum deviation of the polarization from its SM value of ≈ 0 .

The contour plots for the variation of λ_γ for LRSM with no LD contribution

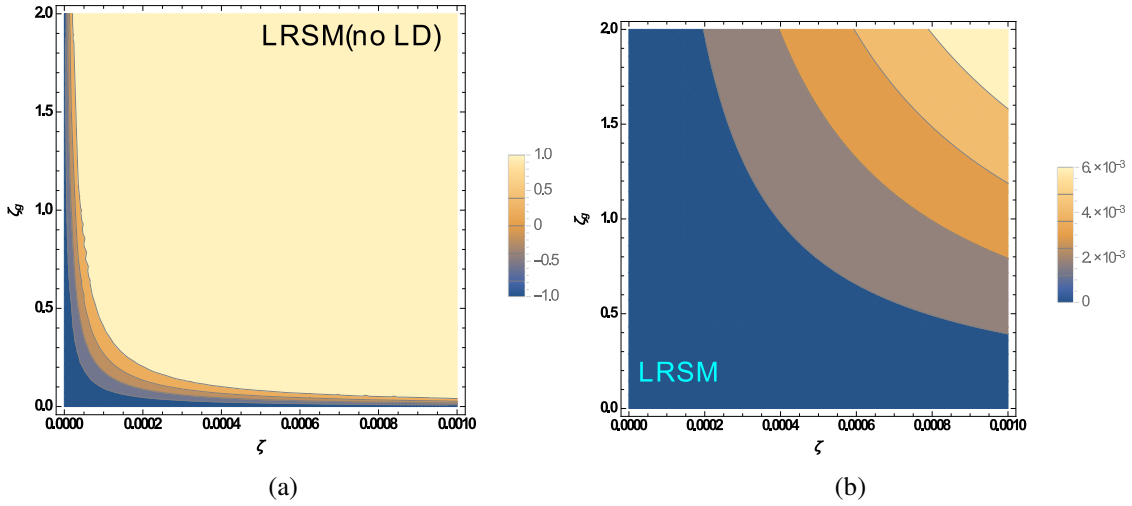


Figure 3.4: Contour plots showing the variation of the polarization λ_γ as a function of ζ and ζ_g for LRSM with no LD contribution on left and LRSM with LD amplitude of $2 \times 10^{-9} \text{ GeV}^{-1}$ on right. For both the cases, the right-handed CKM elements are set for maximum deviation of the polarization function from its SM value. The bar-legends for the different contours of λ_γ are displayed along with the respective figures. Here $0 < \zeta < 10^{-3}$ and $0 < \zeta_g < 2$.

and LRSM with LD amplitude of $2 \times 10^{-9} \text{ GeV}^{-1}$ are shown in Fig. 3.4.

As seen in Fig. 3.4(a), for very small values of ζ and ζ_g , LRSM approaches the SM and hence in absence of long distance contribution, the polarization is left handed ($\lambda_\gamma = -1$), however as the parameters ζ and ζ_g increase, the polarization value changes from -1 to +1. This picture completely changes in the presence of the long distance effects, shown in Fig. 3.4(b). Left and right pannels of Fig. 3.5 show the λ_γ contours for LRSM with an isosinglet down type vector-like quark of mass 800 GeV and 1200 GeV respectively, with LD amplitudes (in units of GeV^{-1}) of 2×10^{-9} , 1×10^{-8} and 8×10^{-8} , corresponding to the top, middle and bottom rows. At the lower end of the range estimated for the LD amplitude, in a model with a vector like quark along with LRSM, polarization can be large, even +1 as both ζ and ζ_g approach their maximum values. If the LD contributions are larger \sim

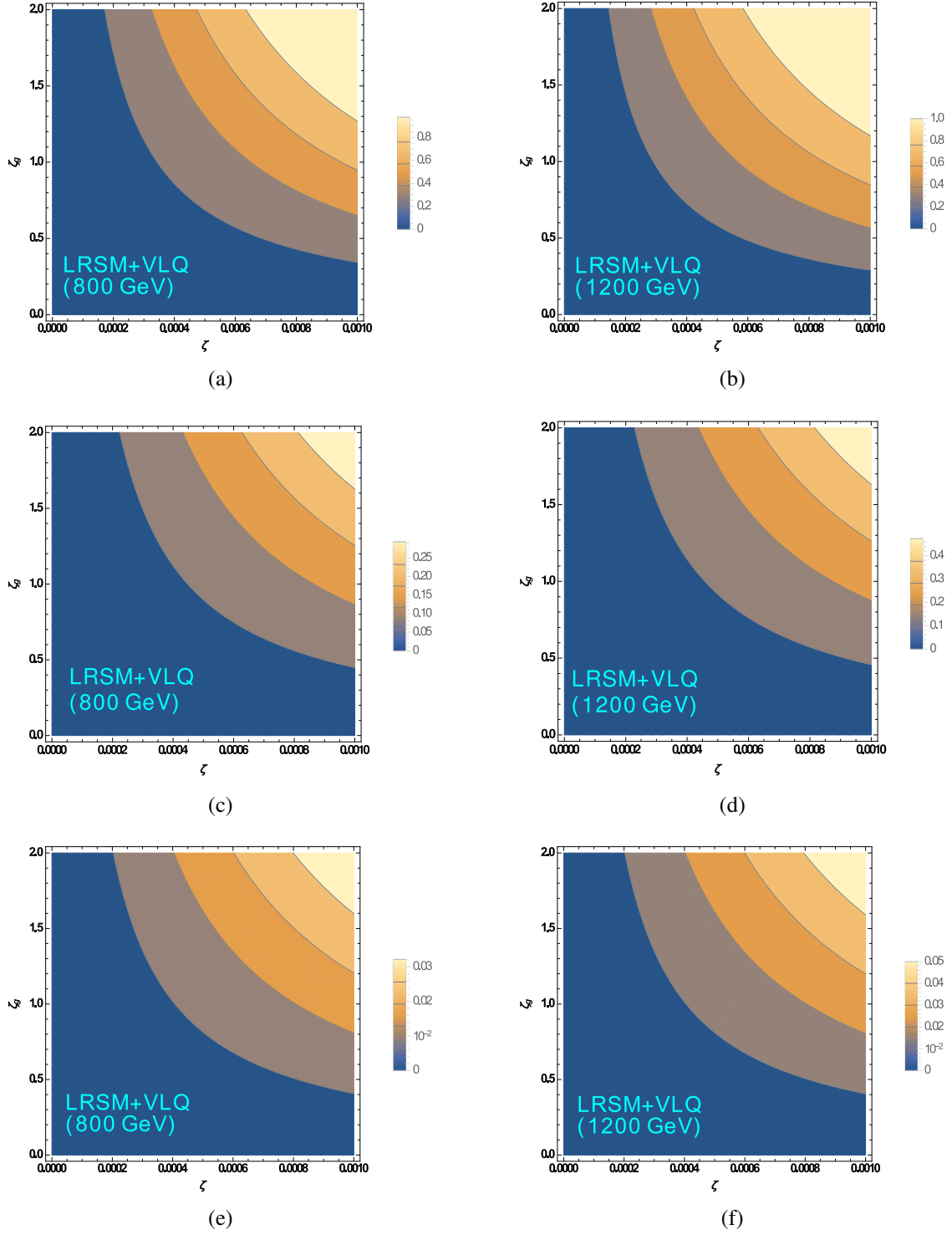


Figure 3.5: Contour plots showing the variation of the polarization λ_γ as a function of ζ and ζ_g . The left panels show the plots for LRSM with a VLQ of mass 800 GeV, while the right panels display the plots for LRSM with a VLQ of mass 1200 GeV. The LD amplitudes (in units of GeV^{-1}) are 2×10^{-9} , 1×10^{-8} , and 8×10^{-8} , for the top, middle and bottom rows respectively. For all the cases, the right-handed CKM elements are set for maximum deviation of the polarization function from its SM value. The bar-legends for the different contours of λ_γ are displayed along with the respective figures. Here $0 < \zeta < 10^{-3}$ and $0 < \zeta_g < 2$.

$1 \times 10^{-8} \text{ GeV}^{-1}$, the maximum polarization value is ~ 0.5 , which further reduces to 0.05 for LD amplitude of $8 \times 10^{-8} \text{ GeV}^{-1}$.

On the experimental side, branching ratios of some of the radiative decays of the D^0 meson have been measured by the Belle collaboration [172],

$$\text{BR}(D^0 \rightarrow \rho^0 \gamma) = (1.77 \pm 0.3 \pm 0.07) \times 10^{-5},$$

$$\text{BR}(D^0 \rightarrow \phi \gamma) = (2.76 \pm 0.19 \pm 0.10) \times 10^{-5},$$

$$\text{BR}(D^0 \rightarrow \bar{K}^{*0} \gamma) = (4.66 \pm 0.21 \pm 0.21) \times 10^{-4}.$$

If the LD contribution is at its lower limit, then the measured $\text{BR}(D^0 \rightarrow \rho^0 \gamma)$ can allow some enhancement from the NP SD contribution, on the other hand, the upper limit of LD saturates the observe BR. The measured $\text{BR}(D^0 \rightarrow \phi \gamma)$ also allows some NP SD contribution. The upper limit for $\text{BR}(D^0 \rightarrow \omega \gamma)$ is 2.4×10^{-4} [35] and cannot be saturated by the SM contribution. Also, recently an observation of the photon polarization in the $b \rightarrow s \gamma$ transition was reported by LHCb [173]. Photon polarization is obtained by the angular distribution of the photon direction with respect to the plane defined by the momenta of the three final-state hadrons in their centre of mass frame. A similar technique could be used to measure the photon polarization for the case of $D \rightarrow \omega \gamma$, since the decay of ω into three pions will permit the measurement of an up-down asymmetry between the number of events with photons on either side of the plane. For the model with left-right symmetry and a vector-like quark, the enhancement in the

$\text{BR}(c \rightarrow u\gamma)$, as well as the photon polarization value being different from that of the SM, should be reflected in the exclusive modes as well, although the results may be weaker. All the form factors required to estimate the exclusive BR's are neither available from experimental data nor yet extracted from lattice calculations. Hence, we do not attempt to calculate the exact BR's for specific exclusive modes. Very recently exclusive radiative charm decays have been studied [174] in heavy quark and hybrid formalism.

3.5 Conclusions

Charmed decay modes including radiative ones are expected to be plagued by long distance contributions. For the SM, NLO QCD corrections enhance the short distance $c \rightarrow u\gamma$ branching ratio by about $\mathcal{O}(10^8)$. Further enhancement of the branching ratio is possible in various new physics models. We show that for certain values of the parameter space, an enhancement by even up to $\mathcal{O}(10^{10})$ is possible in a left-right symmetric model with a down type vector-like singlet quark at the bare level. This could be enhanced further by many orders of magnitude after incorporating QCD corrections, enabling the short distance branching fraction to be possibly even larger than the long distance contribution. Such an enhancement could signal the presence of physics beyond the SM. However, the uncertainty in the size of the long distance contributions, may not allow this to be easily feasible. Nevertheless measurements of branching ratios

of all possible charm radiative modes should be made. A clearer signature of new physics could be obtained by measurement of the photon polarization, for eg. for the radiative $D \rightarrow \omega\gamma$ mode via a technique similar to that used recently by LHCb [173] for the $b \rightarrow s\gamma$ case. We find that for a large region of the parameter space for the vector-like quark model with left-right symmetry, the photon polarization can be right handed. For the modes $D \rightarrow K^*\gamma, \rho\gamma$ the photon polarization could possibly be determined by looking at the photon conversion to e^+e^- [175].

3.A Additional Information regarding the long distance contributions

To calculate the long distance contributions, we have closely followed Ref. [148]. Here, we give the numerical values of various parameters used for our estimates, as well as update the previous results in [148] using the latest values of the input parameters.

In table 3.8 we display the results for the calculation of the long-distance $D \rightarrow V\gamma$ amplitudes. The individual numbers for type-I pole and VMD contributions are shown separately along with the branching ratios. These results are essentially an update of the results in Ref. [148] using the same techniques. The major updates are:

- Inclusion of new modes like $D_s^+ \rightarrow \pi_2^+(1670)\gamma$, $D^+ \rightarrow \pi_2^+(1670)\gamma$,

Table 3.6: Decay width and poles masses used in Type I and Type II pole amplitude analysis.

| Decay width used to calculate $h_{V\gamma P_n}$ (GeV) | Type I pole, P_n (GeV) | Type II pole, D_n^* (GeV) |
|---|-----------------------------|--------------------------------|
| $\Gamma_{\rho^+ \rightarrow \pi^+ \gamma} = 6.734 \times 10^{-5}$ | $M_{\pi^+} = 0.140$ | $M_{D^{*+}(2010)} = 2.011$ |
| $\Gamma_{\rho^0 \rightarrow \pi^0 \gamma} = 9.008 \times 10^{-5}$ | $M_{\pi^0} = 0.135$ | |
| $\Gamma_{\rho^0 \rightarrow \eta \gamma} = 4.504 \times 10^{-5}$ | $M_{K^+} = 0.494$ | |
| $\Gamma_{\omega \rightarrow \pi^0 \gamma} = 7.029 \times 10^{-4}$ | $M_{K^0} = 0.498$ | |
| $\Gamma_{\omega \rightarrow \eta \gamma} = 3.905 \times 10^{-6}$ | $M_{\eta} = 0.548$ | |
| $\Gamma_{\phi \rightarrow \pi^0 \gamma} = 5.418 \times 10^{-6}$ | $M_{\eta'} = 0.958$ | |
| $\Gamma_{\phi \rightarrow \eta \gamma} = 5.584 \times 10^{-5}$ | $M_{D^+} = 1.869$ | |
| $\Gamma_{\phi \rightarrow \eta' \gamma} = 2.666 \times 10^{-7}$ | $M_{f_0(980)} = 0.990$ | |
| $\Gamma_{\phi \rightarrow f^0 \gamma} = 1.374 \times 10^{-6}$ | $M_{a_0(980)} = 0.980$ | |
| $\Gamma_{\phi \rightarrow a^0 \gamma} = 3.242 \times 10^{-7}$ | | |
| $\Gamma_{b_1^+ \rightarrow \pi^+ \gamma} = 2.272 \times 10^{-4}$ | | |
| $\Gamma_{a_1^+ \rightarrow \pi^+ \gamma} = 6.4 \times 10^{-4}$ | | |
| $\Gamma_{a_2 \rightarrow \pi^+ \gamma} = 3.114 \times 10^{-4}$ | | |
| $\Gamma_{\omega(1420) \rightarrow \pi^0 \gamma} = 2.03 \times 10^{-8}$ | | |
| $\Gamma_{\rho(1450) \rightarrow \eta \gamma} = 2.2 \times 10^{-9}$ | | |
| $\Gamma_{\pi_2^+(1670) \rightarrow \pi^+ \gamma} = 1.82 \times 10^{-4}$ | | |
| $\Gamma_{K^{*+}(898) \rightarrow K^+ \gamma} = 4.801 \times 10^{-5}$ | | |
| $\Gamma_{K^*(892) \rightarrow K^0 \gamma} = 1.166 \times 10^{-4}$ | | |
| $\Gamma_{K_1(1270) \rightarrow K^0 \gamma} = 6.588 \times 10^{-9}$ | | |
| $\Gamma_{K_1(1400) \rightarrow K^0 \gamma} = 4.886 \times 10^{-8}$ | | |
| $\Gamma_{K_2^{*+}(1430) \rightarrow K^+ \gamma} = 2.364 \times 10^{-4}$ | | |

Table 3.7: Pole masses, electromagnetic coupling and form factors used in VMD amplitude analysis.

| VMD Poles and Coupling | | Form Factors | | | | |
|------------------------------|-----------------|--------------------------|--------|----------|------|------|
| $H^*(\text{GeV})$ | $\frac{e}{f_V}$ | Decays | $V(0)$ | $A_1(0)$ | a | b' |
| $M_{D^{*+}(2010)} = 2.01027$ | $0.06(\rho^0)$ | $D^0 \rightarrow K^{*-}$ | 0.99 | 0.62 | 0.57 | 0.74 |
| $M_{D^{*+}} = 2.7$ | $0.018(\omega)$ | $D^0 \rightarrow \rho^-$ | 1.05 | 0.61 | 0.55 | 0.69 |
| | $0.024(\phi)$ | $D^+ \rightarrow K^{0*}$ | 0.99 | 0.62 | 0.57 | 0.74 |
| | | $D^+ \rightarrow \rho^0$ | 1.05 | 0.61 | 0.55 | 0.69 |
| | | $D^+ \rightarrow \omega$ | 1.05 | 0.61 | 0.55 | 0.69 |
| | | $D_s \rightarrow \phi$ | 1.10 | 0.61 | 0.57 | 0.74 |
| | | $D_s \rightarrow K^{0*}$ | 1.16 | 0.60 | 0.55 | 0.69 |

Table 3.8: The pole-I, pole-II and VMD amplitudes and the exclusive radiative branching ratios.

| Mode | $A^{PC}(10^{-8})$ | | | $A^{PV}(10^{-8})$ | | B.R. |
|--|-------------------|------|-------------|-------------------|------------|------------------------------|
| | P-I | P-II | VMD | P-I | VMD | |
| $D_s^+ \rightarrow \rho^+ \gamma$ | 7.07 | | ± 8.36 | | ± 11.5 | $(4.7-13) \times 10^{-4}$ |
| $D_s^+ \rightarrow b_1^+(1235) \gamma$ | 6.19 | | | | | 4.9×10^{-5} |
| $D_s^+ \rightarrow a_1^+(1260) \gamma$ | 10.4 | | | | | 1.4×10^{-4} |
| $D_s^+ \rightarrow a_2^+(1320) \gamma$ | 18.2 | | | | | 9.4×10^{-5} |
| $D_s^+ \rightarrow K^{*+} \gamma$ | 2.30 | | ± 1.44 | | ± 2.22 | $(1.6-5.4) \times 10^{-5}$ |
| $D_s^+ \rightarrow K^{**}(1430) \gamma$ | 5.15 | | | | | 3.6×10^{-6} |
| $D_s^+ \rightarrow \pi_2^+(1670) \gamma$ | 7.62 | | | | | 5.4×10^{-7} |
| $D^+ \rightarrow \rho^+ \gamma$ | -1.30 | 0.74 | ± 1.85 | | ± 2.34 | $(4.2 - 6.7) \times 10^{-5}$ |
| $D^+ \rightarrow K^{*+} \gamma$ | | | ± 0.46 | | ± 0.6 | 2.7×10^{-6} |
| $D^+ \rightarrow b_1^+(1235) \gamma$ | -1.13 | | | | | 2.4×10^{-6} |
| $D^+ \rightarrow a_1^+(1260) \gamma$ | -1.91 | | | | | 6.8×10^{-6} |
| $D^+ \rightarrow a_2^+(1320) \gamma$ | -3.36 | | | | | 3.2×10^{-6} |
| $D^+ \rightarrow \pi_2^+(1670) \gamma$ | -1.40 | | | | | 5.6×10^{-9} |
| $D^0 \rightarrow \bar{K}^{*0} \gamma$ | -5.21 | | ± 3.62 | | ± 4.77 | $(4.6-18) \times 10^{-5}$ |
| $D^0 \rightarrow K_1(1270) \gamma$ | -0.016 | | | | | 1.6×10^{-10} |
| $D^0 \rightarrow K_1(1400) \gamma$ | -0.038 | | | | | 4.7×10^{-10} |
| $D^0 \rightarrow K^*(1410) \gamma$ | -0.018 | | | | | 1×10^{-10} |
| $D^0 \rightarrow \rho^0 \gamma$ | 1.36 | | ± 1.05 | | ± 1.46 | $(5.12-18) \times 10^{-6}$ |
| $D^0 \rightarrow \omega \gamma$ | -0.703 | | ± 0.897 | | ± 1.20 | $(3.2-9) \times 10^{-6}$ |
| $D^0 \rightarrow \phi \gamma$ | 0.318 | | ± 0.956 | -0.428 | ± 1.32 | $(4.8-6.4) \times 10^{-6}$ |

$D^0 \rightarrow K_1(1270) \gamma$, $D^0 \rightarrow K_1(1400) \gamma$, $D^0 \rightarrow K_1(1410) \gamma$ in the type-I pole amplitudes.

- Updated form factors taken from Ref. [150] used in calculating the VMD amplitudes.
- Updated $V \rightarrow P$ (vector-pseudoscalar) and $T \rightarrow P$ (tensor-pseudoscalar) decay widths from Ref. [35] used for the evaluation of the couplings $h_{V\gamma P}$ and $h_{T\gamma P}$ respectively for the type-I pole amplitudes.
- Inclusion of $\eta - \eta'$ mixing in calculating the type-I $D^0 \rightarrow \rho^0 \gamma$, $D^0 \rightarrow$

$\omega\gamma$ and $D^0 \rightarrow \phi\gamma$ amplitudes. The corresponding mixing angles and decay constants have been obtained from Ref. [176].

- Inclusion of the parity-violating (PV) part for the $D^0 \rightarrow \phi\gamma$ type-I pole amplitude. The decay constants for the corresponding scalars involved have been taken from Ref. [177] for $f_0(980)$ and [178] for $a_0(980)$ respectively.
- The decay constants are taken from Ref. [179] for the light vector mesons and from Ref. [35] for the light pseudoscalar mesons. For the decay constants of the D^* and D_s^* mesons, we use Ref. [180].

We have only calculated the type-II pole contribution to the mode $D^+ \rightarrow \rho^+\gamma$. This is because:

- The corresponding decay widths for $D_s^* \rightarrow D_s$ and $D^{0*} \rightarrow D^0$ essential for calculating the type-II pole contributions to the D_s and D^0 decay modes respectively are only given as limits in Ref. [35].
- For decay modes of D^+ other than $\rho^+\gamma$ (for eg. $b_1^+(1235)\gamma$, $a_1^+(1260)\gamma$ etc.), the corresponding decay constants for the final state particles are not available.

3.B The LO and NLO anomalous dimension matrices

We provide the effective anomalous dimension matrix in the $\overline{\text{MS}}$ scheme in this appendix. For the case of charm decays we have $q_1 = -1/3$, $q_2 = 2/3$ and $\bar{q} = q_1 - q_2$. While evolving the C_i 's down from the M_W to the m_b scale, one has to make the assignments $n = 3$ and $f = 5$. For the corresponding evolution from the m_b to the m_c scale, the values are $n = 2$ and $f = 4$.

At the LO level, it is given by

$$\hat{\gamma}_{eff}^0 = \begin{pmatrix} -4\frac{8}{3} & 0 & -\frac{2}{9} & 0 & 0 & -\frac{4q_1}{3} - \frac{8q_2}{81} & \frac{173}{162} \\ 12 & 0 & 0 & \frac{4}{3} & 0 & 0 & 8q_1 + \frac{16q_2}{27} & \frac{70}{27} \\ 0 & 0 & 0 & -\frac{52}{3} & 0 & 2 & \frac{176q_2}{27} & \frac{14}{27} \\ 0 & 0 & -\frac{40}{9} & \frac{4f}{3} - \frac{160}{9} & \frac{4}{9} & \frac{5}{6} & \left(\frac{16f}{27} - \frac{88}{81}\right)q_2 & \frac{74}{81} - \frac{49f}{54} \\ 0 & 0 & 0 & -\frac{256}{3} & 0 & 20 & \frac{6272q_2}{27} & 36f + \frac{1736}{27} \\ 0 & 0 & -\frac{256}{9} & \frac{40f}{3} - \frac{544}{9} & \frac{40}{9} & -\frac{2}{3} & 48n\bar{q} + \left(\frac{1456f}{27} - \frac{3136}{81}\right)q_2 & \frac{160f}{27} + \frac{2372}{81} \\ 0 & 0 & 0 & 0 & 0 & 0 & \frac{32}{3} & 0 \\ 0 & 0 & 0 & 0 & 0 & 0 & \frac{32q_2}{3} & \frac{28}{3} \end{pmatrix}. \quad (3.52)$$

At the NLO level, due to its large size, we present the matrix in 8×6 and 8×2 blocks. It reads

$$\hat{\gamma}_{eff}^{1^{8 \times 2}} = \begin{pmatrix} \left(\frac{2f}{27} - \frac{374}{27}\right)q_1 + \left(\frac{64f}{729} - \frac{12614}{729}\right)q_2 & \frac{431f}{5832} + \frac{65867}{5832} \\ \left(\frac{136}{9} - \frac{4f}{9}\right)q_1 + \left(\frac{2332}{243} - \frac{128f}{243}\right)q_2 & \frac{10577}{486} - \frac{917f}{972} \\ -\frac{112n\bar{q}}{3} - \left(\frac{4720f}{243} + \frac{97876}{243}\right)q_2 & \frac{42524}{243} - \frac{2398f}{243} \\ \left(-\frac{32f^2}{243} + \frac{4448f}{729} + \frac{70376}{729}\right)q_2 - \frac{140n\bar{q}}{9} & -\frac{253f^2}{486} - \frac{39719f}{5832} - \frac{159718}{729} \\ -\frac{3136n\bar{q}}{3} - \left(\frac{188608f}{243} + \frac{1764752}{243}\right)q_2 & -14f^2 + \frac{140954f}{243} + \frac{2281576}{243} \\ \left(-\frac{56f}{3} - \frac{1136}{9}\right)n\bar{q} - \left(\frac{5432f^2}{243} - \frac{232112f}{729} + \frac{4193840}{729}\right)q_2 & -\frac{6031f^2}{486} - \frac{15431f}{1458} - \frac{3031517}{729} \\ \frac{1936}{9} - \frac{224f}{27} & 0 \\ \left(\frac{368}{3} - \frac{224f}{27}\right)q_2 & \frac{1456}{9} - \frac{61f}{27} \end{pmatrix}. \quad (3.53)$$

$$\hat{\gamma}_{eff}^{1^{8 \times 6}} = \begin{pmatrix} \frac{16f}{9} - \frac{145}{3} & \frac{40f}{27} - 26 & -\frac{1412}{243} & -\frac{1369}{243} & \frac{134}{243} & -\frac{35}{162} \\ \frac{20f}{3} - 45 & -\frac{28}{3} & -\frac{416}{81} & \frac{1280}{81} & \frac{56}{81} & \frac{35}{27} \\ 0 & 0 & -\frac{4468}{81} & -\frac{52f}{9} - \frac{29129}{81} & \frac{400}{81} & \frac{3493}{108} - \frac{2f}{9} \\ 0 & 0 & \frac{368f}{81} - \frac{13678}{243} & \frac{1334f}{81} - \frac{79409}{243} & \frac{509}{486} - \frac{8f}{81} & \frac{13499}{648} - \frac{5f}{27} \\ 0 & 0 & -\frac{160f}{9} - \frac{244480}{81} & -\frac{2200f}{9} - \frac{29648}{81} & \frac{16f}{9} + \frac{23116}{81} & \frac{148f}{9} + \frac{3886}{27} \\ 0 & 0 & \frac{77600}{243} - \frac{1264f}{81} & \frac{164f}{81} - \frac{28808}{243} & \frac{400f}{81} - \frac{20324}{243} & \frac{622f}{27} - \frac{21211}{162} \\ 0 & 0 & 0 & 0 & 0 & 0 \\ 0 & 0 & 0 & 0 & 0 & 0 \end{pmatrix}, \quad (3.54)$$

3.C The functions G_p

In this appendix, we provide the form of the G_p and H_p functions.

$$G_p^{ij}(r_\ell) = \int_0^1 dx \int_0^{1-x} dy \frac{1}{\Lambda_p} g_p^{ij}(r_\ell, x, y)$$

$$H_p^{ij}(r_\ell) = \int_0^1 dx \int_0^{1-x} dy \frac{1}{\Lambda_p} h_p^{ij}(r_\ell, x, y)$$

$$\Lambda_1(r_\ell, x, y) = 1 - x + r_\ell x - r_i xy - r_f xz$$

$$\Lambda_2(r_\ell, x, y) = x + r_\ell(1 - x) - r_i xy - r_f xz$$

$$z = 1 - x - y$$

$$g_1^{LL}(r_\ell, x, y) = 1 - x + z + y(1 - 2x) + r_\ell x(1 - y) - r_f xz$$

$$h_1^{LL}(r_\ell, x, y) = 1 - x + y + z(1 - 2x) + r_\ell x(1 - z) - r_i xy$$

$$g_1^{LR}(x) = 3(x - 1) - x^2 \sqrt{r_i r_f}$$

$$h_1^{LR}(r_\ell, x, y) = xy r_i + xz r_f - xr_\ell + (x - 1)$$

$$g_2^{LL}(r_\ell, x, y) = -2x(1 - y) + r_\ell(-1 + x + xy) + r_f xz$$

$$h_2^{LL}(r_\ell, x, y) = -2x(1 - z) + r_\ell(-1 + x + xz) + r_i xy$$

$$g_2^{LR}(x) = (1 - x)^2 \sqrt{r_i r_f}$$

$$g_1^{LR} = h_1^{RL} \quad h_1^{LR} = g_1^{RL}$$

$$\begin{aligned}
g_2^{LL} &= h_2^{RR} & h_2^{LL} &= g_2^{RR} \\
g_2^{LR} &= h_2^{RL} & h_2^{LR} &= g_2^{RL}
\end{aligned}
\tag{3.55}$$

In the above, $r_i = m_c^2/M_W^2$, $r_f = m_u^2/M_W^2$ and $r_\ell = m_\ell^2/M_W^2$ with m_c , m_u and M_W denoting the masses of the charm quark, up quark and the W-boson respectively. The m stands for the masses of the down-type quarks running in the fermionic penguin loop for a $c \rightarrow u\gamma$ transition. Hence, for the SM $m = (m_d, m_s, m_b)$ and for the vector-like quark model $m = (m_d, m_s, m_b, m_{b'})$ with m_d , m_s , m_b and $m_{b'}$ standing for the masses of the d , s , b and b' quarks respectively.

Chapter 4

Conclusion and future directions

This chapter highlights the main conclusions of the works described in chapters 2 and 3. I also briefly discuss the probable future directions of my research career.

Chapter 2 is about the $D \rightarrow PP$ decays. The theoretical challenges in dealing with hadronic charm decays posed due to the mass of the charm quark have been discussed in detail. The importance of the annihilation and exchange diagrams for such decays is thoroughly discussed and are accounted for as free parameters. We also highlight the justifications towards the need for adding non-factorizable corrections as free parameters in case of using the factorization approximation for estimating the charm decays. A detailed description of the form factors used in our analysis is provided. In addition to these, resonant final state interactions are expected to play a dominant role in $D \rightarrow PP$ decays due to the proximity of the charm meson mass to that of some short lived hadronic resonances. We account for these

types of effects via a K-matrix formalism, relying as much as possible on data whereas treating the unknown elements in the K matrix as free parameters. We fit our 13 parameters to the 28 $D \rightarrow PP$ branching ratios that are experimentally available and find a $\chi^2/\text{d.o.f}$ of 2.25, which, though not a good fit, is a substantial improvement over previous works of this kind. Most the $D \rightarrow PP$ modes fit well and we are able to satisfactorily explain important ratios and phase differences that have been discussed in detail in section 2.5. The modes which do not fit well are mostly those involving η and/or η' and $D^+ \rightarrow K^+ \bar{K}^0$. A fit carried out without these yields a better $\chi^2/\text{d.o.f}$ of 1.44.

In Chapter 3, we explore the effect of the presence of a down type isosinglet vector like quark in the presence of a left-right symmetry on the inclusive $c \rightarrow u\gamma$ BR. Although the uncorrected inclusive radiative charm branching ratio is quite small, QCD corrections enhance it substantially within the SM. However, even with such a large enhancement, the SM short distance contribution is still overshadowed by dominant long distance effects. A detailed discussion regarding the long distance estimation is provided. We also discuss the RG evolution for the short distance Wilson coefficients within the SM in a thorough manner. This is followed by a discussion of the new physics models that we use and the corresponding effect that the RG evolution will have on the coefficients of such new physics. The incorporation of these models results in a further enhancement of the short

distance coefficients. We also propose an observable termed the "photon polarization" which may be instrumental in identifying such new physics.

The direct search for physics beyond the SM has so far been unsuccessful. There have been anomalies in some of the observables in the flavour sector, with deviations from the SM predictions at the level of few sigma [181]. Tensions between SM expectations and experimental results have been found in B physics for observables such as the $R_{D^*}^{\tau,l} = \frac{\text{BR}(B \rightarrow D^* \tau \nu_\tau)}{\text{BR}(B \rightarrow D^* l \nu_l)}$, $R_D^{\tau,l} = \frac{\text{BR}(B \rightarrow D \tau \nu_\tau)}{\text{BR}(B \rightarrow D l \nu_l)}$ [182–188] and $R_K = \frac{\text{BR}(B \rightarrow K \mu^+ \mu^-)}{\text{BR}(B \rightarrow K e^+ e^-)}$ [189, 190]. The disagreement of these observables with their SM predictions hints towards the violation of lepton flavour universality. Attention has also been drawn towards the P'_5 anomaly in the angular distribution for the $B \rightarrow K^* \mu^+ \mu^-$ decays [191, 192], reported by LHCb [193]. The $B_s \rightarrow \phi \mu^+ \mu^-$ rate in the $1 < q^2 < 6 \text{GeV}^2$ region has been reported to be about 3σ below theoretical calculations [194]. After the completion of my PhD, I want to explore some of these tensions. I would also like to look at the rare charm decays other than the radiative decays, and explore the possibility of using them as a probe for the identification of New Physics.

Bibliography

- [1] C.-N. Yang and R. L. Mills, “Conservation of Isotopic Spin and Isotopic Gauge Invariance,” *Phys. Rev.*, vol. 96, pp. 191–195, 1954.
- [2] C.-N. Yang and R. L. Mills, “Isotopic spin conservation and a generalized gauge invariance,” 1954.
- [3] J. S. Schwinger, “A Theory of the Fundamental Interactions,” *Annals Phys.*, vol. 2, pp. 407–434, 1957.
- [4] M. Gell-Mann, “A Schematic Model of Baryons and Mesons,” *Phys. Lett.*, vol. 8, pp. 214–215, 1964.
- [5] J. D. Bjorken and S. L. Glashow, “Elementary Particles and SU(4),” *Phys. Lett.*, vol. 11, pp. 255–257, 1964.
- [6] J. H. Christenson, J. W. Cronin, V. L. Fitch, and R. Turlay, “Evidence for the 2π Decay of the K^0 Meson,” *Phys. Rev. Lett.*, vol. 13, pp. 138–140, 1964.
- [7] M. Y. Han and Y. Nambu, “Three Triplet Model with Double SU(3) Symmetry,” *Phys. Rev.*, vol. 139, pp. B1006–B1010, 1965.

- [8] O. W. Greenberg, “Spin and Unitary Spin Independence in a Paraquark Model of Baryons and Mesons,” *Phys. Rev. Lett.*, vol. 13, pp. 598–602, 1964.
- [9] S. Weinberg, “A Model of Leptons,” *Phys. Rev. Lett.*, vol. 19, pp. 1264–1266, 1967.
- [10] A. Salam, “Weak and Electromagnetic Interactions,” *Conf. Proc.*, vol. C680519, pp. 367–377, 1968.
- [11] S. L. Glashow, J. Iliopoulos, and L. Maiani, “Weak Interactions with Lepton-Hadron Symmetry,” *Phys. Rev.*, vol. D2, pp. 1285–1292, 1970.
- [12] H. Fritzsch, M. Gell-Mann, and H. Leutwyler, “Advantages of the Color Octet Gluon Picture,” *Phys. Lett.*, vol. B47, pp. 365–368, 1973.
- [13] D. J. Gross and F. Wilczek, “ASYMPTOTICALLY FREE GAUGE THEORIES. 2.,” *Phys. Rev.*, vol. D9, pp. 980–993, 1974.
- [14] H. D. Politzer, “Reliable Perturbative Results for Strong Interactions?,” *Phys. Rev. Lett.*, vol. 30, pp. 1346–1349, 1973.
- [15] J. J. Aubert *et al.*, “Experimental Observation of a Heavy Particle J,” *Phys. Rev. Lett.*, vol. 33, pp. 1404–1406, 1974.

- [16] J. E. Augustin *et al.*, “Discovery of a Narrow Resonance in $e^+ e^-$ Annihilation,” *Phys. Rev. Lett.*, vol. 33, pp. 1406–1408, 1974. [Adv. Exp. Phys.5,141(1976)].
- [17] G. Goldhaber *et al.*, “Observation in $e^+ e^-$ Annihilation of a Narrow State at $1865\text{-MeV}/c^2$ Decaying to $K \pi$ and $K \pi \pi \pi$,” *Phys. Rev. Lett.*, vol. 37, pp. 255–259, 1976.
- [18] M. L. Perl *et al.*, “Evidence for Anomalous Lepton Production in $e^+ e^-$ Annihilation,” *Phys. Rev. Lett.*, vol. 35, pp. 1489–1492, 1975.
- [19] S. W. Herb *et al.*, “Observation of a Dimuon Resonance at 9.5-GeV in 400-GeV Proton-Nucleus Collisions,” *Phys. Rev. Lett.*, vol. 39, pp. 252–255, 1977.
- [20] C. Y. Prescott *et al.*, “Parity Nonconservation in Inelastic Electron Scattering,” *Phys. Lett.*, vol. B77, pp. 347–352, 1978.
- [21] C. S. Wu, E. Ambler, R. W. Hayward, D. D. Hoppes, and R. P. Hudson, “Experimental test of parity conservation in beta decay,” *Phys. Rev.*, vol. 105, pp. 1413–1415, Feb 1957.
- [22] D. P. Barber *et al.*, “Discovery of Three Jet Events and a Test of Quantum Chromodynamics at PETRA Energies,” *Phys. Rev. Lett.*, vol. 43, p. 830, 1979.
- [23] G. Arnison *et al.*, “Experimental Observation of Isolated Large Transverse Energy Electrons with Associated Missing Energy at

- $s^{*(1/2)} = 540\text{-GeV}$,” *Phys. Lett.*, vol. B122, pp. 103–116, 1983.
[611(1983)].
- [24] G. Arnison *et al.*, “Experimental Observation of Lepton Pairs of Invariant Mass Around $95\text{-GeV}/c^{*2}$ at the CERN SPS Collider,” *Phys. Lett.*, vol. B126, pp. 398–410, 1983.
- [25] F. Abe *et al.*, “Observation of top quark production in $\bar{p}p$ collisions,” *Phys. Rev. Lett.*, vol. 74, pp. 2626–2631, 1995.
- [26] S. Abachi *et al.*, “Observation of the top quark,” *Phys. Rev. Lett.*, vol. 74, pp. 2632–2637, 1995.
- [27] G. Aad *et al.*, “Observation of a new particle in the search for the Standard Model Higgs boson with the ATLAS detector at the LHC,” *Phys. Lett.*, vol. B716, pp. 1–29, 2012.
- [28] S. Chatrchyan *et al.*, “Observation of a new boson at a mass of 125 GeV with the CMS experiment at the LHC,” *Phys. Lett.*, vol. B716, pp. 30–61, 2012.
- [29] [https://en.wikipedia.org/wiki/Standard_Model_\(mathematical_formulation\)](https://en.wikipedia.org/wiki/Standard_Model_(mathematical_formulation)).
- [30] <http://hyperphysics.phy-astr.gsu.edu/hbase/forces/couple.html>.
- [31] http://www.physnet.org/modules/pdf_modules/m281.pdf.
- [32] <http://www.particleadventure.org/electroweak.html>.
- [33] <http://www.people.fas.harvard.edu/~hgeorgi/weak.pdf>.

- [34] M. Kobayashi and T. Maskawa, “CP Violation in the Renormalizable Theory of Weak Interaction,” *Prog. Theor. Phys.*, vol. 49, pp. 652–657, 1973.
- [35] C. Patrignani, “Review of Particle Physics,” *Chin. Phys.*, vol. C40, no. 10, p. 100001, 2016.
- [36] N. Cabibbo, “Unitary Symmetry and Leptonic Decays,” *Phys. Rev. Lett.*, vol. 10, pp. 531–533, 1963. [,648(1963)].
- [37] M. Artuso, B. Meadows, and A. A. Petrov, “Charm Meson Decays,” *Ann. Rev. Nucl. Part. Sci.*, vol. 58, pp. 249–291, 2008.
- [38] A. Ryd and A. A. Petrov, “Hadronic D and D(s) Meson Decays,” *Rev. Mod. Phys.*, vol. 84, pp. 65–117, 2012.
- [39] G. Burdman and I. Shipsey, “ $D^0 - \bar{D}^0$ mixing and rare charm decays,” *Ann. Rev. Nucl. Part. Sci.*, vol. 53, pp. 431–499, 2003.
- [40] G. Burdman, E. Golowich, J. L. Hewett, and S. Pakvasa, “Rare charm decays in the standard model and beyond,” *Phys. Rev.*, vol. D66, p. 014009, 2002.
- [41] A. A. Petrov, “Searching for New Physics with Charm,” *PoS*, vol. BEAUTY2009, p. 024, 2009.
- [42] G. D’Ambrosio and D.-N. Gao, “The Diquark model: New physics effects for charm and kaon decays,” *Phys. Lett.*, vol. B513, pp. 123–129, 2001.

- [43] B. D. Yabsley, “Experimental limits on new physics from charm decay,” *Int. J. Mod. Phys.*, vol. A19, p. 949, 2004.
- [44] F. E. Close and H. J. Lipkin, “Puzzles in Cabibbo suppressed charm decays,” *Phys. Lett.*, vol. B551, pp. 337–342, 2003.
- [45] S. Fajfer, S. Prelovsek, and P. Singer, “Rare charm meson decays $D \rightarrow P \text{ lepton}^+ \text{ lepton}^-$ and $c \rightarrow u \text{ lepton}^+ \text{ lepton}^-$ in SM and MSSM,” *Phys. Rev.*, vol. D64, p. 114009, 2001.
- [46] Y. Grossman, A. L. Kagan, and Y. Nir, “New physics and CP violation in singly Cabibbo suppressed D decays,” *Phys. Rev.*, vol. D75, p. 036008, 2007.
- [47] N. Sinha, R. Sinha, T. E. Browder, S. Pakvasa, and N. G. Deshpande, “Method for determining the D^0 - anti- D^0 mixing parameters,” *Phys. Rev. Lett.*, vol. 99, p. 262002, 2007.
- [48] J. M. Link *et al.*, “A Measurement of lifetime differences in the neutral D meson system,” *Phys. Lett.*, vol. B485, pp. 62–70, 2000.
- [49] G. Brandenburg *et al.*, “Rate measurement of $D^0 \rightarrow K^+ \pi^- \pi^0$ and constraints on D^0 - anti- D^0 mixing,” *Phys. Rev. Lett.*, vol. 87, p. 071802, 2001.
- [50] R. Aaij *et al.*, “Evidence for CP violation in time-integrated $D^0 \rightarrow h^- h^+$ decay rates,” *Phys. Rev. Lett.*, vol. 108, p. 111602, 2012.

- [51] T. Aaltonen *et al.*, “Measurement of the difference of CP-violating asymmetries in $D^0 \rightarrow K^+K^-$ and $D^0 \rightarrow \pi^+\pi^-$ decays at CDF,” *Phys. Rev. Lett.*, vol. 109, p. 111801, 2012.
- [52] T. Feldmann, S. Nandi, and A. Soni, “Repercussions of Flavour Symmetry Breaking on CP Violation in D-Meson Decays,” *JHEP*, vol. 06, p. 007, 2012.
- [53] J. Brod, Y. Grossman, A. L. Kagan, and J. Zupan, “A Consistent Picture for Large Penguins in $D \rightarrow \pi^+ \pi^-, K^+ K^-$,” *JHEP*, vol. 10, p. 161, 2012.
- [54] J. Brod, A. L. Kagan, and J. Zupan, “Size of direct CP violation in singly Cabibbo-suppressed D decays,” *Phys. Rev.*, vol. D86, p. 014023, 2012.
- [55] H.-Y. Cheng and C.-W. Chiang, “Direct CP violation in two-body hadronic charmed meson decays,” *Phys. Rev.*, vol. D85, p. 034036, 2012. [Erratum: *Phys. Rev.*D85,079903(2012)].
- [56] B. Bhattacharya, M. Gronau, and J. L. Rosner, “CP asymmetries in singly-Cabibbo-suppressed D decays to two pseudoscalar mesons,” *Phys. Rev.*, vol. D85, p. 054014, 2012. [*Phys. Rev.*D85,no.7,079901(2012)].

- [57] E. Franco, S. Mishima, and L. Silvestrini, “The Standard Model confronts CP violation in $D^0 \rightarrow \pi^+\pi^-$ and $D^0 \rightarrow K^+K^-$,” *JHEP*, vol. 05, p. 140, 2012.
- [58] G. Isidori, J. F. Kamenik, Z. Ligeti, and G. Perez, “Implications of the LHCb Evidence for Charm CP Violation,” *Phys. Lett.*, vol. B711, pp. 46–51, 2012.
- [59] Y. Grossman and D. J. Robinson, “SU(3) Sum Rules for Charm Decay,” *JHEP*, vol. 04, p. 067, 2013.
- [60] D. Atwood and A. Soni, “Searching for the Origin of CP violation in Cabibbo Suppressed D-meson Decays,” *PTEP*, vol. 2013, no. 9, p. 093B05, 2013.
- [61] G. F. Giudice, G. Isidori, and P. Paradisi, “Direct CP violation in charm and flavor mixing beyond the SM,” *JHEP*, vol. 04, p. 060, 2012.
- [62] G. Hiller, Y. Hochberg, and Y. Nir, “Supersymmetric ΔA_{CP} ,” *Phys. Rev.*, vol. D85, p. 116008, 2012.
- [63] Y. Hochberg and Y. Nir, “Relating direct CP violation in D decays and the forward-backward asymmetry in $t\bar{t}$ production,” *Phys. Rev. Lett.*, vol. 108, p. 261601, 2012.

- [64] W. Altmannshofer, R. Primulando, C.-T. Yu, and F. Yu, “New Physics Models of Direct CP Violation in Charm Decays,” *JHEP*, vol. 04, p. 049, 2012.
- [65] G. Isidori and J. F. Kamenik, “Shedding light on CP violation in the charm system via D to V gamma decays,” *Phys. Rev. Lett.*, vol. 109, p. 171801, 2012.
- [66] G. Hiller, M. Jung, and S. Schacht, “SU(3)-flavor anatomy of non-leptonic charm decays,” *Phys. Rev.*, vol. D87, no. 1, p. 014024, 2013.
- [67] F. Buccella, M. Lusignoli, A. Pugliese, and P. Santorelli, “CP violation in D meson decays: Would it be a sign of new physics?,” *Phys. Rev.*, vol. D88, no. 7, p. 074011, 2013.
- [68] S. MAijller, U. Nierste, and S. Schacht, “Topological amplitudes in D decays to two pseudoscalars: A global analysis with linear $SU(3)_F$ breaking,” *Phys. Rev.*, vol. D92, no. 1, p. 014004, 2015.
- [69] M. J. Charles, “CKM studies in the charm sector,” in *8th International Workshop on the CKM Unitarity Triangle (CKM 2014) Vienna, Austria, September 8-12, 2014*, 2014.
- [70] H. D. Politzer and M. B. Wise, “Effective Field Theory Approach to Processes Involving Both Light and Heavy Fields,” *Phys. Lett.*, vol. B208, pp. 504–507, 1988.

- [71] M. Beneke, G. Buchalla, M. Neubert, and C. T. Sachrajda, “QCD factorization for exclusive, nonleptonic B meson decays: General arguments and the case of heavy light final states,” *Nucl. Phys.*, vol. B591, pp. 313–418, 2000.
- [72] M. Beneke, G. Buchalla, M. Neubert, and C. T. Sachrajda, “QCD factorization for $B \rightarrow \pi\pi$ decays: Strong phases and CP violation in the heavy quark limit,” *Phys. Rev. Lett.*, vol. 83, pp. 1914–1917, 1999.
- [73] Y.-Y. Keum, H.-n. Li, and A. I. Sanda, “Fat penguins and imaginary penguins in perturbative QCD,” *Phys. Lett.*, vol. B504, pp. 6–14, 2001.
- [74] Y. Y. Keum, H.-N. Li, and A. I. Sanda, “Penguin enhancement and $B \rightarrow K\pi$ decays in perturbative QCD,” *Phys. Rev.*, vol. D63, p. 054008, 2001.
- [75] C.-D. Lu, K. Ukai, and M.-Z. Yang, “Branching ratio and CP violation of $B \rightarrow \pi\pi$ decays in perturbative QCD approach,” *Phys. Rev.*, vol. D63, p. 074009, 2001.
- [76] C.-D. Lu and M.-Z. Yang, “ $B \rightarrow \pi\rho, \pi\omega$ decays in perturbative QCD approach,” *Eur. Phys. J.*, vol. C23, pp. 275–287, 2002.
- [77] C. W. Bauer, D. Pirjol, and I. W. Stewart, “Soft collinear factorization in effective field theory,” *Phys. Rev.*, vol. D65, p. 054022, 2002.

- [78] M. Bauer, B. Stech, and M. Wirbel, “Exclusive Nonleptonic Decays of D, D(s), and B Mesons,” *Z. Phys.*, vol. C34, p. 103, 1987.
- [79] M. Wirbel, B. Stech, and M. Bauer, “Exclusive Semileptonic Decays of Heavy Mesons,” *Z. Phys.*, vol. C29, p. 637, 1985.
- [80] A. Ali, G. Kramer, and C.-D. Lu, “CP violating asymmetries in charmless nonleptonic decays $B \rightarrow P P, P V, V V$ in the factorization approach,” *Phys. Rev.*, vol. D59, p. 014005, 1999.
- [81] A. Ali, G. Kramer, and C.-D. Lu, “Experimental tests of factorization in charmless nonleptonic two-body B decays,” *Phys. Rev.*, vol. D58, p. 094009, 1998.
- [82] A. J. Buras, J. M. Gerard, and R. Ruckl, “ $1/n$ Expansion for Exclusive and Inclusive Charm Decays,” *Nucl. Phys.*, vol. B268, pp. 16–48, 1986.
- [83] B. Yu. Blok and M. A. Shifman, “Towards a Theory of Weak Hadronic Decays of Charmed Particles,” *Sov. J. Nucl. Phys.*, vol. 45, p. 135, 1987. [*Yad. Fiz.*45,211(1987)].
- [84] B. Yu. Blok and M. A. Shifman, “Weak Nonleptonic Decays of Charmed Mesons in QCD Sum Rules,” *Sov. J. Nucl. Phys.*, vol. 45, p. 301, 1987. [*Yad. Fiz.*45,478(1987)].

- [85] B. Yu. Blok and M. A. Shifman, “Weak Nonleptonic Decays of Charmed Mesons: Theory Versus Experiment,” *Sov. J. Nucl. Phys.*, vol. 45, p. 522, 1987. [*Yad. Fiz.*45,841(1987)].
- [86] L.-L. Chau and H.-Y. Cheng, “Analysis of Exclusive Two-Body Decays of Charm Mesons Using the Quark Diagram Scheme,” *Phys. Rev.*, vol. D36, p. 137, 1987.
- [87] L.-L. Chau and H.-Y. Cheng, “Analysis of the Recent Data of Exclusive Two-body Charm Decays,” *Phys. Lett.*, vol. B222, pp. 285–292, 1989.
- [88] J. L. Rosner, “Final state phases in charmed meson two-body nonleptonic decays,” *Phys. Rev.*, vol. D60, p. 114026, 1999.
- [89] C.-W. Chiang and J. L. Rosner, “Final state phases in doubly-Cabibbo suppressed charmed meson nonleptonic decays,” *Phys. Rev.*, vol. D65, p. 054007, 2002.
- [90] C.-W. Chiang, Z. Luo, and J. L. Rosner, “Two-body Cabibbo suppressed charmed meson decays,” *Phys. Rev.*, vol. D67, p. 014001, 2003.
- [91] B. Bhattacharya and J. L. Rosner, “Flavor symmetry and decays of charmed mesons to pairs of light pseudoscalars,” *Phys. Rev.*, vol. D77, p. 114020, 2008.

- [92] B. Bhattacharya and J. L. Rosner, “Charmed meson decays to two pseudoscalars,” *Phys. Rev.*, vol. D81, p. 014026, 2010.
- [93] B. Bhattacharya and J. L. Rosner, “Effect of η - η' mixing on $D \rightarrow PV$ decays,” *Phys. Rev.*, vol. D82, p. 037502, 2010.
- [94] H.-Y. Cheng and C.-W. Chiang, “Two-body hadronic charmed meson decays,” *Phys. Rev.*, vol. D81, p. 074021, 2010.
- [95] L.-L. Chau and H.-Y. Cheng, “SU(3) breaking effects in charmed meson decays,” *Phys. Lett.*, vol. B333, pp. 514–518, 1994.
- [96] Y.-L. Wu, M. Zhong, and Y.-F. Zhou, “Exploring final state hadron structure and SU(3) flavor symmetry breaking effects in $D \rightarrow PP$ and $D \rightarrow PV$ decays,” *Eur. Phys. J.*, vol. C42, p. 391, 2005.
- [97] H. J. Lipkin, “Troubles with Nonleptonic Charm Decays,” *Phys. Rev. Lett.*, vol. 44, pp. 710–712, 1980.
- [98] J. F. Donoghue and B. R. Holstein, “Dynamical Effects in Two-body Charm Decay,” *Phys. Rev.*, vol. D21, p. 1334, 1980.
- [99] C. Sorensen, “Final State Interactions in the Decays of Charmed Mesons,” *Phys. Rev.*, vol. D23, p. 2618, 1981.
- [100] A. N. Kamal and E. D. Cooper, “HADRONIC INTERACTION CORRECTIONS TO TWO-BODY D_0 DECAYS,” *Z. Phys.*, vol. C8, p. 67, 1981.

- [101] C.-K. Chua and W.-S. Hou, “Implications of anti-B \rightarrow D0 h0 decays on anti-B \rightarrow D anti-K, anti-D anti-K decays,” *Phys. Rev.*, vol. D72, p. 036002, 2005.
- [102] M. Gronau, D. London, and J. L. Rosner, “Rescattering Contributions to rare B-Meson Decays,” *Phys. Rev.*, vol. D87, no. 3, p. 036008, 2013.
- [103] S. P. Rosen, “Remarks on the Differing Lifetimes of Charmed Mesons,” *Phys. Rev. Lett.*, vol. 44, p. 4, 1980.
- [104] I. I. Y. Bigi and M. Fukugita, “A Clean Test of the W Boson Exchange Model for the Decays of Charm and Bottom Mesons,” *Phys. Lett.*, vol. B91, pp. 121–123, 1980.
- [105] J. F. Donoghue, “Is D0 \rightarrow phi anti-K0 Really a Clear Signal for the Annihilation Diagram?,” *Phys. Rev.*, vol. D33, pp. 1516–1518, 1986.
- [106] A. N. Kamal, N. Sinha, and R. Sinha, “A Coupled Channel Treatment of Cabibbo Angle Favored ($D, D(s) \rightarrow VP$) Decays,” *Z. Phys.*, vol. C41, p. 207, 1988.
- [107] H.-Y. Cheng, “Weak annihilation and the effective parameters $a(1)$ and $a(2)$ in nonleptonic D decays,” *Eur. Phys. J.*, vol. C26, pp. 551–565, 2003.

- [108] M. Beneke and M. Neubert, “QCD factorization for $B \rightarrow PP$ and $B \rightarrow PV$ decays,” *Nucl. Phys.*, vol. B675, pp. 333–415, 2003.
- [109] M. Beneke, G. Buchalla, M. Neubert, and C. T. Sachrajda, “QCD factorization for $B \rightarrow \pi K$ decays,” in *High energy physics. Proceedings, 30th International Conference, ICHEP 2000, Osaka, Japan, July 27-August 2, 2000. Vol. 1, 2*, pp. 882–885, 2000.
- [110] H.-n. Li, C.-D. Lu, and F.-S. Yu, “Branching ratios and direct CP asymmetries in $D \rightarrow PP$ decays,” *Phys. Rev.*, vol. D86, p. 036012, 2012.
- [111] P. Zenczykowski, “Dispersive contribution to CP violation in hyperon decays,” *Phys. Rev.*, vol. D55, pp. 1688–1690, 1997.
- [112] J.-H. Lai and K.-C. Yang, “Weak annihilation topologies and final state interactions in $D \rightarrow PP$ decays,” *Phys. Rev.*, vol. D72, p. 096001, 2005.
- [113] T. Becher and R. J. Hill, “Comment on form-factor shape and extraction of $|V(ub)|$ from $B \rightarrow \pi l \nu$,” *Phys. Lett.*, vol. B633, pp. 61–69, 2006.
- [114] R. J. Hill, “The Modern description of semileptonic meson form factors,” *eConf*, vol. C060409, p. 027, 2006.
- [115] D. Becirevic and A. B. Kaidalov, “Comment on the heavy \rightarrow light form-factors,” *Phys. Lett.*, vol. B478, pp. 417–423, 2000.

- [116] R. J. Hill, “Heavy-to-light meson form-factors at large recoil,” *Phys. Rev.*, vol. D73, p. 014012, 2006.
- [117] C. Bernard *et al.*, “Visualization of semileptonic form factors from lattice QCD,” *Phys. Rev.*, vol. D80, p. 034026, 2009.
- [118] H. Na, C. T. H. Davies, E. Follana, G. P. Lepage, and J. Shigemitsu, “The $D \rightarrow K, l\nu$ Semileptonic Decay Scalar Form Factor and $|V_{cs}|$ from Lattice QCD,” *Phys. Rev.*, vol. D82, p. 114506, 2010.
- [119] H. Na, C. T. H. Davies, E. Follana, J. Koponen, G. P. Lepage, and J. Shigemitsu, “ $D \rightarrow \pi, l\nu$ Semileptonic Decays, $|V_{cd}|$ and 2^{nd} Row Unitarity from Lattice QCD,” *Phys. Rev.*, vol. D84, p. 114505, 2011.
- [120] S. Aoki *et al.*, “Review of lattice results concerning low-energy particle physics,” *Eur. Phys. J.*, vol. C74, p. 2890, 2014.
- [121] D. Besson *et al.*, “Improved measurements of D meson semileptonic decays to pi and K mesons,” *Phys. Rev.*, vol. D80, p. 032005, 2009.
- [122] J. Yelton *et al.*, “Studies of $D^+ \rightarrow \{\eta', \eta, \phi\}e^+\nu_e$,” *Phys. Rev.*, vol. D84, p. 032001, 2011.
- [123] J. Koponen, C. T. H. Davies, and G. Donald, “D to K and D to pi semileptonic form factors from Lattice QCD,” in *Proceedings, 5th International Workshop on Charm Physics (Charm 2012): Honolulu, Hawaii, USA, May 14-17, 2012*, 2012.

- [124] G. S. Bali, S. Collins, S. D'Almeida, and I. Kanamori, “ $D_s \rightarrow \eta, \eta'$ semileptonic decay form factors with disconnected quark loop contributions,” *Phys. Rev.*, vol. D91, no. 1, p. 014503, 2015.
- [125] K. A. Olive *et al.*, “Review of Particle Physics,” *Chin. Phys.*, vol. C38, p. 090001, 2014.
- [126] T. Feldmann, P. Kroll, and B. Stech, “Mixing and decay constants of pseudoscalar mesons,” *Phys. Rev.*, vol. D58, p. 114006, 1998.
- [127] F.-G. Cao, “Determination of the η - η' mixing angle,” *Phys. Rev.*, vol. D85, p. 057501, 2012.
- [128] C.-K. Chua, “Rescattering effects in charmless anti-B(u,d,s) \rightarrow PP decays,” *Nucl. Phys.*, vol. A844, pp. 260C–265C, 2010.
- [129] A. N. Kamal and R. Sinha, “A Coupled Channel Treatment of Cabibbo Angle Suppressed ($D, D(s)^+$) \rightarrow pp Decays,” *Phys. Rev.*, vol. D36, p. 3510, 1987.
- [130] M. Ablikim *et al.*, “Measurement of the $D \rightarrow K^- \pi^+$ strong phase difference in $\psi(3770) \rightarrow D^0 \bar{D}^0$,” *Phys. Lett.*, vol. B734, pp. 227–233, 2014.
- [131] M. Gronau, “SU(3) in D decays: From 30% symmetry breaking to 10^{-4} precision,” *Phys. Rev.*, vol. D91, no. 7, p. 076007, 2015.
- [132] M. Albaladejo and J. A. Oller, “Identification of a Scalar Glueball,” *Phys. Rev. Lett.*, vol. 101, p. 252002, 2008.

- [133] R. S. Longacre *et al.*, “A Measurement of $\pi^- p \rightarrow K^0(s) K^0(s) n$ at 22-GeV/ c and a Systematic Study of the 2^{++} Meson Spectrum,” *Phys. Lett.*, vol. B177, pp. 223–227, 1986.
- [134] S. Fajfer, P. Singer, and J. Zupan, “The Radiative leptonic decays $D^0 \rightarrow e^+ e^- \gamma$, $\mu^+ \mu^- \gamma$ in the standard model and beyond,” *Eur. Phys. J.*, vol. C27, pp. 201–218, 2003.
- [135] M. C. Arnesen, B. Grinstein, I. Z. Rothstein, and I. W. Stewart, “A Precision model independent determination of $|V(ub)|$ from $B \rightarrow \pi e \nu$,” *Phys. Rev. Lett.*, vol. 95, p. 071802, 2005.
- [136] K. G. Chetyrkin, J. H. Kuhn, and M. Steinhauser, “RunDec: A Mathematica package for running and decoupling of the strong coupling and quark masses,” *Comput. Phys. Commun.*, vol. 133, pp. 43–65, 2000.
- [137] S. Fajfer, S. Prelovsek, P. Singer, and D. Wyler, “A Possible arena for searching new physics: The Gamma ($D^0 \rightarrow \rho^0 \gamma$) / Gamma ($D^0 \rightarrow \omega \gamma$) ratio,” *Phys. Lett.*, vol. B487, pp. 81–86, 2000.
- [138] K. S. Babu, X. G. He, X. Li, and S. Pakvasa, “Fourth Generation Signatures in D^0 - Anti- d^0 Mixing and Rare D Decays,” *Phys. Lett.*, vol. B205, pp. 540–544, 1988.

- [139] G. Cacciapaglia, A. Deandrea, L. Panizzi, N. Gaur, D. Harada, and Y. Okada, “Heavy Vector-like Top Partners at the LHC and flavour constraints,” *JHEP*, vol. 03, p. 070, 2012.
- [140] F. J. Botella, M. Nebot, and G. C. Branco, “Vector-like quarks and New Physics in the flavour sector,” *J. Phys. Conf. Ser.*, vol. 447, p. 012061, 2013.
- [141] K. Ishiwata, Z. Ligeti, and M. B. Wise, “New Vector-Like Fermions and Flavor Physics,” *JHEP*, vol. 10, p. 027, 2015.
- [142] C. Bobeth, A. J. Buras, A. Celis, and M. Jung, “Patterns of Flavour Violation in Models with Vector-Like Quarks,” 2016.
- [143] A. K. Alok, S. Banerjee, D. Kumar, and S. U. Sankar, “Flavor signatures of isosinglet vector-like down quark model,” *Nuclear Physics B*, vol. 906, pp. 321 – 341, 2016.
- [144] D. Atwood, T. Gershon, M. Hazumi, and A. Soni, “Clean Signals of CP-violating and CP-conserving New Physics in $B \rightarrow P V \gamma$ Decays at B Factories and Hadron Colliders,” 2007.
- [145] M. Gronau and D. Pirjol, “Photon polarization in radiative B decays,” *Phys. Rev.*, vol. D66, p. 054008, 2002.
- [146] M. Wirbel, B. Stech, and M. Bauer, “Exclusive Semileptonic Decays of Heavy Mesons,” *Z. Phys.*, vol. C29, p. 637, 1985.

- [147] M. Wirbel, “Description of Weak Decays of D and B Mesons,” *Prog. Part. Nucl. Phys.*, vol. 21, pp. 33–98, 1988.
- [148] G. Burdman, E. Golowich, J. L. Hewett, and S. Pakvasa, “Radiative weak decays of charm mesons,” *Phys. Rev.*, vol. D52, pp. 6383–6399, 1995.
- [149] R. Aleksan, F. Buccella, A. Le Yaouanc, L. Oliver, O. Pene, and J. C. Raynal, “Uncertainties on the cp phase α due to penguin diagrams,” *Phys. Lett.*, vol. B356, pp. 95–106, 1995.
- [150] S. Fajfer and J. Kamenik, “Charm meson resonances and $d \rightarrow \nu$ semileptonic form factors,” *Phys. Rev. D*, vol. 72, p. 034029, Aug 2005.
- [151] T. Inami and C. S. Lim, “Effects of Superheavy Quarks and Leptons in Low-Energy Weak Processes $k(L) \rightarrow \mu \text{ anti-}\mu$, $K^+ \rightarrow \pi^+ \text{ Neutrino anti-neutrino}$ and $K^0 \leftrightarrow \text{ anti-}K^0$,” *Prog. Theor. Phys.*, vol. 65, p. 297, 1981. [Erratum: *Prog. Theor. Phys.*65,1772(1981)].
- [152] Q. Ho-Kim and X.-Y. Pham, “One loop flavor changing electromagnetic transitions,” *Phys. Rev.*, vol. D61, p. 013008, 2000.
- [153] C. Greub, T. Hurth, M. Misiak, and D. Wyler, “The $c \rightarrow u$ gamma contribution to weak radiative charm decay,” *Phys. Lett.*, vol. B382, pp. 415–420, 1996.

- [154] S. Fajfer, P. Singer, and J. Zupan, “The Radiative leptonic decays $D_0 \rightarrow e^+ e^- \gamma$, $\mu^+ \mu^- \gamma$ in the standard model and beyond,” *Eur. Phys. J.*, vol. C27, pp. 201–218, 2003.
- [155] S. de Boer, B. MÅijller, and D. Seidel, “Higher-order Wilson coefficients for $c \rightarrow u$ transitions in the standard model,” *JHEP*, vol. 08, p. 091, 2016.
- [156] G. Buchalla, A. J. Buras, and M. E. Lautenbacher, “Weak decays beyond leading logarithms,” *Rev. Mod. Phys.*, vol. 68, pp. 1125–1144, 1996.
- [157] M. Beneke, T. Feldmann, and D. Seidel, “Systematic approach to exclusive $B \rightarrow V l^+ l^-$, $V \gamma$ decays,” *Nucl. Phys.*, vol. B612, pp. 25–58, 2001.
- [158] K. G. Chetyrkin, M. Misiak, and M. Munz, “ $|\Delta F| = 1$ nonleptonic effective Hamiltonian in a simpler scheme,” *Nucl. Phys.*, vol. B520, pp. 279–297, 1998.
- [159] M. Gorbahn and U. Haisch, “Effective Hamiltonian for non-leptonic $|\Delta F| = 1$ decays at NNLO in QCD,” *Nucl. Phys.*, vol. B713, pp. 291–332, 2005.
- [160] M. Gorbahn, U. Haisch, and M. Misiak, “Three-loop mixing of dipole operators,” *Phys. Rev. Lett.*, vol. 95, p. 102004, 2005.

- [161] K. G. Chetyrkin, M. Misiak, and M. Munz, “Weak radiative B meson decay beyond leading logarithms,” *Phys. Lett.*, vol. B400, pp. 206–219, 1997. [Erratum: *Phys. Lett.*B425,414(1998)].
- [162] J. L. Hewett and T. G. Rizzo, “Fourth Generation and Exotic Quarkonium in $E(6)$ Theories,” *Phys. Rev.*, vol. D35, p. 2194, 1987.
- [163] A. K. Alok, S. Banerjee, D. Kumar, S. U. Sankar, and D. London, “New-physics signals of a model with a vector-singlet up-type quark,” *Phys. Rev.*, vol. D92, p. 013002, 2015.
- [164] J. C. Pati and A. Salam, “Lepton Number as the Fourth Color,” *Phys. Rev.*, vol. D10, pp. 275–289, 1974. [Erratum: *Phys. Rev.*D11,703(1975)].
- [165] R. N. Mohapatra and J. C. Pati, “A Natural Left-Right Symmetry,” *Phys. Rev.*, vol. D11, p. 2558, 1975.
- [166] G. Senjanovic and R. N. Mohapatra, “Exact Left-Right Symmetry and Spontaneous Violation of Parity,” *Phys. Rev.*, vol. D12, p. 1502, 1975.
- [167] G. Aad *et al.*, “ATLAS search for a heavy gauge boson decaying to a charged lepton and a neutrino in pp collisions at $\sqrt{s} = 7$ TeV,” *Eur. Phys. J.*, vol. C72, p. 2241, 2012.
- [168] S. Chatrchyan *et al.*, “Search for leptonic decays of W ’ bosons in pp collisions at $\sqrt{s} = 7$ TeV,” *JHEP*, vol. 08, p. 023, 2012.

- [169] P. L. Cho and M. Misiak, “ $b \rightarrow s \gamma$ decay in $SU(2)_L \times SU(2)_R \times U(1)$ extensions of the Standard Model,” *Phys. Rev.*, vol. D49, pp. 5894–5903, 1994.
- [170] E. Kou, C.-D. Lü, and F.-S. Yu, “Photon Polarization in the $b \rightarrow s \gamma$ processes in the Left-Right Symmetric Model,” *JHEP*, vol. 12, p. 102, 2013.
- [171] P. Langacker and S. U. Sankar, “Bounds on the Mass of $W(R)$ and the $W(L)$ - $W(R)$ Mixing Angle ξ in General $SU(2)_L \times SU(2)_R \times U(1)$ Models,” *Phys. Rev.*, vol. D40, pp. 1569–1585, 1989.
- [172] A. Abdesselam *et al.*, “Observation of $D^0 \rightarrow \rho^0 \gamma$ and search for CP violation in radiative charm decays,” 2016. [*Phys. Rev. Lett.*118,051801(2017)].
- [173] R. Aaij *et al.*, “Observation of Photon Polarization in the $b \rightarrow s \gamma$ Transition,” *Phys. Rev. Lett.*, vol. 112, no. 16, p. 161801, 2014.
- [174] S. de Boer and G. Hiller, “Rare radiative charm decays within the standard model and beyond,” 2017.
- [175] Y. Grossman and D. Pirjol, “Extracting and using photon polarization information in radiative B decays,” *JHEP*, vol. 06, p. 029, 2000.
- [176] F.-G. Cao, “Determination of the η - η' mixing angle,” *Phys. Rev.*, vol. D85, p. 057501, 2012.

- [177] I. Bediaga, F. S. Navarra, and M. Nielsen, “The structure of $f_0(980)$ from charmed mesons decays,” *Physics Letters B*, vol. 579, no. 1–2, pp. 59 – 66, 2004.
- [178] C. Aydin and A. H. Yilmaz, “Coupling constants $g(a(0) \omega \gamma)$ as derived from light cone QCD sum rules,” *Mod. Phys. Lett.*, vol. A21, pp. 1297–1304, 2006.
- [179] D. Ebert, R. N. Faustov, and V. O. Galkin, “Relativistic treatment of the decay constants of light and heavy mesons,” *Phys. Lett.*, vol. B635, pp. 93–99, 2006.
- [180] S. Narison, “Decay Constants of Heavy-Light Mesons from QCD,” *Nucl. Part. Phys. Proc.*, vol. 270-272, pp. 143–153, 2016.
- [181] Z. Ligeti, “Flavor Constraints on New Physics,” *PoS*, vol. Lepton-Photon2015, p. 031, 2016.
- [182] R. Aaij *et al.*, “Measurement of the ratio of branching fractions $\mathcal{B}(\bar{B}^0 \rightarrow D^{*+}\tau^-\bar{\nu}_\tau)/\mathcal{B}(\bar{B}^0 \rightarrow D^{*+}\mu^-\bar{\nu}_\mu)$,” *Phys. Rev. Lett.*, vol. 115, no. 11, p. 111803, 2015. [Addendum: *Phys. Rev. Lett.*115,no.15,159901(2015)].
- [183] J. P. Lees *et al.*, “Measurement of an Excess of $\bar{B} \rightarrow D^{(*)}\tau^-\bar{\nu}_\tau$ Decays and Implications for Charged Higgs Bosons,” *Phys. Rev.*, vol. D88, no. 7, p. 072012, 2013.

- [184] M. Huschle *et al.*, “Measurement of the branching ratio of $\bar{B} \rightarrow D^{(*)}\tau^-\bar{\nu}_\tau$ relative to $\bar{B} \rightarrow D^{(*)}\ell^-\bar{\nu}_\ell$ decays with hadronic tagging at Belle,” *Phys. Rev.*, vol. D92, no. 7, p. 072014, 2015.
- [185] A. Abdesselam *et al.*, “Measurement of the branching ratio of $\bar{B}^0 \rightarrow D^{*+}\tau^-\bar{\nu}_\tau$ relative to $\bar{B}^0 \rightarrow D^{*+}\ell^-\bar{\nu}_\ell$ decays with a semileptonic tagging method,” 2016.
- [186] R. Aaij *et al.*, “Measurement of the ratio of branching fractions $\mathcal{B}(\bar{B}^0 \rightarrow D^{*+}\tau^-\bar{\nu}_\tau)/\mathcal{B}(\bar{B}^0 \rightarrow D^{*+}\mu^-\bar{\nu}_\mu)$,” *Phys. Rev. Lett.*, vol. 115, no. 11, p. 111803, 2015. [Addendum: *Phys. Rev. Lett.*115,no.15,159901(2015)].
- [187] J. F. Kamenik and F. Mescia, “ $B \rightarrow D\tau\nu$ Branching Ratios: Opportunity for Lattice QCD and Hadron Colliders,” *Phys. Rev.*, vol. D78, p. 014003, 2008.
- [188] J. F. Kamenik and F. Mescia, “ $B \rightarrow D\tau\nu$ Branching Ratios: Opportunity for Lattice QCD and Hadron Colliders,” *Phys. Rev.*, vol. D78, p. 014003, 2008.
- [189] C. Bobeth, G. Hiller, and G. Piranishvili, “Angular distributions of $\bar{B} \rightarrow \bar{K}\ell^+\ell^-$ decays,” *JHEP*, vol. 12, p. 040, 2007.
- [190] R. Aaij *et al.*, “Test of lepton universality using $B^+ \rightarrow K^+\ell^+\ell^-$ decays,” *Phys. Rev. Lett.*, vol. 113, p. 151601, 2014.

- [191] S. Descotes-Genon, J. Matias, and J. Virto, “Understanding the $B \rightarrow K^* \mu^+ \mu^-$ Anomaly,” *Phys. Rev.*, vol. D88, p. 074002, 2013.
- [192] W. Altmannshofer and D. M. Straub, “New physics in $b \rightarrow s$ transitions after LHC run 1,” *Eur. Phys. J.*, vol. C75, no. 8, p. 382, 2015.
- [193] R. Aaij *et al.*, “Angular analysis of the $B^0 \rightarrow K^{*0} \mu^+ \mu^-$ decay using 3 fb^{-1} of integrated luminosity,” *JHEP*, vol. 02, p. 104, 2016.
- [194] R. Aaij *et al.*, “Angular analysis and differential branching fraction of the decay $B_s^0 \rightarrow \phi \mu^+ \mu^-$,” *JHEP*, vol. 09, p. 179, 2015.